The background image shows a mountainous landscape with green hills and a clear blue sky. In the foreground, several white cylindrical radiometers are mounted on a metal structure, with various cables connected to them. The radiometers have blue domes on top and are arranged in rows.

## Report of the PMOD/WRC-COST Calibration and Intercomparison of Erythemal Radiometers

**Authors:** Julian Gröbner, Gregor Hülsen, Laurent Vuilleumier,  
Mario Blumthaler, Jose M. Vilaplana, Daniel Walker,  
Jaime E. Gill

Report of the PMOD/WRC-COST Calibration and  
Intercomparison of Erythemat radiometers

Davos, Switzerland 28 July – 23 August 2006

J. Gröbner, G. Hülsen, L. Vuilleumier, M. Blumthaler,  
J. M. Vilaplana, D. Walker, and J. E. Gil

© COST Office, 2009

No permission to reproduce or utilise the contents of this book by any means is necessary, other than in the case of images, diagrammes, or other material from other copyright holders. In such cases, permission of the copyright holders is required. This book may be cited as: COST 726 – Report of the PMOD/WRC-COST Calibration and Intercomparison of erythema Radiometers.

Neither the COST Office nor any person acting on its behalf is responsible for the use which might be made of the information contained in this publication. The COST Office is not responsible for the external websites referred to in this publication.

## Table of contents

<b>Summary</b> .....	<b>5</b>
<b>1. Introduction</b> .....	<b>6</b>
<b>2. Setup and Measurements</b> .....	<b>6</b>
2.1 Location and measurement conditions .....	6
<b>3. Instrumentation</b> .....	<b>7</b>
<b>4. Laboratory Characterisation</b> .....	<b>9</b>
4.1 Relative spectral response Facility .....	10
4.2 Angular response Facility .....	11
4.3 Absolute Calibration .....	11
4.4 Horizon at PMOD/WRC .....	13
4.5 The effect of a finite scan time .....	14
4.6 The complete radiometer calibration equation .....	15
<b>5. Campaign Results</b> .....	<b>15</b>
5.1 Spectroradiometer intercomparison .....	15
5.2 Radiometer Absolute Calibration .....	17
<b>6. Radiometer comparison</b> .....	<b>18</b>
6.1 Comparison of broadband radiometer with the reference spectroradiometer QASUME .....	18
6.2 Comparisons using Taylor diagrams. ....	22
6.3 Instrument random (statistical) uncertainty .....	26
<b>References</b> .....	<b>30</b>
<b>Appendix: Taylor diagram comparison</b> .....	<b>31</b>
<b>Annex</b> .....	<b>33</b>



## Summary

Working group four of the COST Action 726 "Long term changes and climatology of UV radiation over Europe" is responsible for the Quality control of erythemally weighted solar irradiance radiometers. One major task of this activity was the organisation of a characterisation and calibration campaign of reference radiometers in use in regional and national UV networks in Europe. The campaign was organised at the PMOD/WRC from 28 July to 23 August 2006; it is located in the Swiss Alps at 1610 m a.s.l. A total of 36 radiometers from 16 countries participated at the campaign, including one radiometer from the Central UV Calibration Facility, NOAA, U.S.A. The radiometer types represented at the campaign were 9 Yankee UVB-1, 5 Kipp & Zonen, 2 Scintec, 11 analog and 8 digital Solar light V. 501, 1 Eldonet and 1 SRMS (modified Solarlight V501). A second spectroradiometer from the Medical University of Innsbruck, Austria participated as well to provide redundant global spectral solar UV irradiance measurements; this spectroradiometer agreed with the QASUME spectroradiometer to within  $\pm 2\%$  over the two week measurement campaign. The atmospheric conditions during the campaign varied between fully overcast to clear skies and allowed a reliable calibration for the majority of instruments. A novel calibration methodology using the spectral as well as the angular response functions measured in the laboratory provided remarkable agreement with the reference spectroradiometer, with expanded uncertainties ( $k=2$ ) of 7% for the most stable instruments. The measurements of the broadband radiometers were analysed both with the PMOD/WRC provided calibration as well as the prior calibration from the home institutes. The relative differences between the measurements using the prior calibration and the reference spectroradiometer varied between excellent agreement to differences larger than 50% for specific instruments.

# 1. Introduction

The calibration and intercomparison campaign of radiometers measuring erythemally weighted solar irradiance was held at the Physikalisch-Meteorologisches Observatorium Davos, World Radiation Center from 28 July to 23 August 2006. The campaign was organised by working group four of COST Action 726 “Long Term changes and Climatology of UV radiation over Europe”. The objective of the campaign was to provide a uniform calibration to all participating radiometers traceable to the QASUME reference, in view of homogenising UV measurements in Europe. The specific tasks of the campaign were to individually characterise each radiometer with respect to the relative spectral and angular responsivity in the laboratory immediately prior to the absolute calibration of the instrument. The absolute calibration was then obtained by direct comparison of solar irradiance measurements with the traveling reference spectroradiometer QASUME on the roof platform of PMOD/WRC.

This intercomparison campaign followed two similar campaigns held in 1995 in Helsinki, Finland [1] and in September 1999 in Thessaloniki, Greece [2]. 36 broadband radiometers from 31 Institutions participated at the intercomparison, including one radiometer from the Central UV Calibration Facility (CUCF) from NOAA, Boulder, US. The radiometers were for the most part reference instruments within their respective regional or national networks. The measurement campaign at PMOD/WRC allowed comparing the original calibration with the QASUME-based calibration on the one hand, and to estimate the variability between the UV radiometer measurements based on calibrations originating from different sources (manufacturer or national calibration laboratory) on the other hand. The final result of the campaign was the release of calibration certificates to all participating institutes traceable to the QASUME reference.

This publication is supported by COST.

## 2. Setup and Measurements

### 2.1 Location and measurement conditions

The calibration and intercomparison campaign took place at the PMOD/WRC, Switzerland, from 28 July to 23 August 2006. The laboratory facilities and the QASUME reference spectroradiometer were provided to PMOD/WRC by the Physical and Chemical Exposure Unit of the Joint Research Centre of the European Union in Ispra, Italy through collaboration agreement 2004-SOCP-22187. The measurement platform is located on the roof of PMOD/WRC at 1610 m.a.s.l., latitude 46.8 N, Longitude 9.83 E. The measurement site is located in the Swiss Alps and its horizon (see Figure 4) is limited by mountains; a valley runs NE to SW.

The laboratory characterisations of most radiometers were accomplished in the first week of the campaign, from 28 July to 4 August 2006. A few radiometers arrived at PMOD/WRC too late to participate at this initial laboratory characterisation. These radiometers were characterised at the end of the outdoor campaign, i.e. in the week of 21 to 25 August 2006.

The radiometers were installed on the roof platform of PMOD/WRC on 4 August (Friday); The QASUME and UIIMP spectroradiometers were installed on August 7 (Monday). The measurement data used for the calibration were obtained in the period 8 to 23 August, totaling 15 ½ measurement days.

The measurement conditions were very variable, with periods of sunshine, clouds and rain. Three clear-sky days occurred on August 15, 18, and 23. The other days were characterised by totally overcast skies, rain, or rapidly changing cloud conditions.

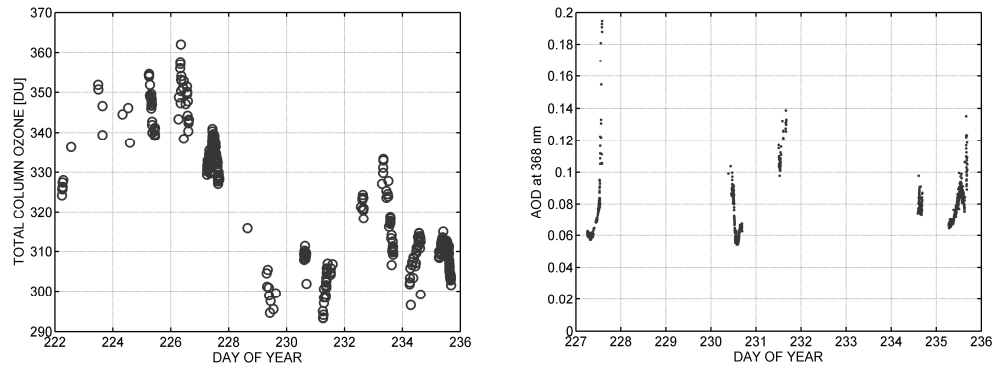


Figure 1 Left figure: Total column ozone values measured at KLI, Arosa by Brewer spectrophotometer #040. Right figure: Aerosol optical depth measurements at 368 nm from a Precision Filter radiometer at PMOD/WRC

The total column ozone is shown in the left graph of Figure 1 and was obtained from Brewer spectrophotometer #040 located at the Licht-Klimatisches Observatorium in Arosa, about 20 km horizontal distance from Davos at an altitude of 1800 m.a.s.l. The total column ozone varied between 293 and 362 DU with a mean value of 322 DU over the measurement period.

The aerosol optical depth (aod) at 368 nm, measured with PFR sunphotometers is shown in the right graph of Figure 1; the aod was between 0.05 and 0.1 on the clear sky days of August 15, 18 and 23. The afternoon of 15 August was perturbed by cirrus clouds.

### 3. Instrumentation

Thirty-six radiometers measuring erythemally weighted solar irradiance from 31 Institutions of 16 Countries took part in this campaign. A list of the participating radiometers is shown in Table 1. As can be seen from the table, the radiometers represented the most widely used instruments used for the measurement of erythemal weighted solar irradiance, namely 18 SL-501 radiometers from Solar Light Inc., 9 UVB-1 radiometer of Yankee Environmental Systems, Inc., and 7 radiometers from Scintec or Kipp&Zonen. One Eldonet radiometer and one SRMS system based on a SL-501 radiometer also participated at the campaign.

The analog voltages of the radiometers were acquired with an Agilent 34970A multiplexer unit with 60 channels and a repeat rate of 6 seconds. The Eldonet and SRSM systems used their own data acquisition system and stored measurements as one minute averages. The digital SL-501 radiometers were set to acquire one minute averages, and when possible their sensitivity factor was set to 10 to improve their resolution.

Table 1 List of participating radiometers

Country	Instrument	Manufacturer	Institution	ID
Spain	UVB-1 941204	YES	Instituto Nacional de Meteorología de España, Madrid (INM)	BB01
	SL-501 5782	Solar Light, Analog	MeteoGalicia, Santiago de Compostela (A Coruña), Spain	BB20
	UVB-1 030521	YES	Departamento de Física Aplicada, Univeristy of Granada, Spain	BB24
	UVB-1 990608	YES	Instituto Nacional de Técnica Aeroespacial – INTA, Huelva, Spain	BB29
	UVB-1 970839	YES	Izaña Atmospheric Observatory, INM, Spain	BB31
	K&Z 000518	Kipp & Zonen	Universidad de Extremadura, Badajoz, Spain	BB30
the Netherlands	UV-S-E-T 20599	Kipp & Zonen	Kipp & Zonen B.V., the Netherlands	BB02
Sweden	SL-501 0922	Solar Light, Digital	Sveriges meteorologiska och hydrologiska institut (SMHI), Sweden	BB03
	SL-501 8885	Solar Light, Analog	Abisko Scientific Research Station, Sweden	BB07
U.S.	UVB-1 000904	YES	Central UV Calibration Facility (CUCF), NOAA, US	BB04
France	UVB-1 920906	YES	Université des Sciences et Technologies de Lille, France	BB05
Finland	SL-501 635	Solar Light, Digital	Non-ionizing Radiation Laboratory, STUK, Finland	BB06
Switzerland	SL-501 8891	Solar Light, Analog	Federal Office of Meteorology and Climatology Meteoswiss, Switzerland	BB08
	SL-501 1903	Solar Light, Analog	Federal Office of Meteorology and Climatology Meteoswiss, Switzerland	BB09
	SL-501 1904	Solar Light, Analog	Federal Office of Meteorology and Climatology Meteoswiss, Switzerland	BB10
	SL-501 1497	Solar Light, Analog	Federal Office of Meteorology and Climatology Meteoswiss, Switzerland	BB36
	SL-501 1492	Solar Light, Analog	PMOD/WRC	BB17
	SL-501 1493	Solar Light, Analog	PMOD/WRC	BB18
Italy	SL-501 5790	Solar Light, Analog	National Research Council, Sesto Fiorentino	BB11
	UVB-1 030528	YES	Agenzia Regionale per la Protezione dell'Ambiente della Valle d'Aosta (ARPA Aosta)	BB15
	UVB-1 970827	YES	University of Rome "La Sapienza"	BB26
Norway	SL-501 1450	Solar Light, Digital	Norwegian Polar Institute, Norway	BB12
	SL-501 0616	Solar Light, Digital	Norwegian Radiation Protection Authority, Norway	BB21
U.K.	K&Z 020614	Kipp & Zonen	School of Earth Atmospheric and Environmental Sciences, University of Manchester	BB13

	SRMS 26	Custom	Radiation Protection Division, Health Protection Agency, UK	BB25
Germany	Eldonet XP	Eldonet	Friedrich-Alexander Universität, Institut für Biologie, Germany	BB14
	010-A-00360	Scintec	Deutscher Wetterdienst, Richard-Assmann-Observatorium Lindenberg	BB16
	010-A-00407	Scintec	Meteorologisches Institut der Universität München, Germany	BB28
	SL-501 4818	Solar Light, Digital	Institut für Meteorologie und Klimatologie (IMUK), University of Hannover, Germany	BB33
Poland	SL-501 0935	Solar Light, Digital	Institute of Meteorology and Water Management, Legionowo, Poland	BB19
	K&Z 030616	Kipp & Zonen	Institute of Geophysics, Polish Academy of Sciences, Warsaw, Poland	BB27
Slovakia	SL-501 4811	Solar Light, Digital	Slovak Hydro-meteorological Institute, Poprad, Slovakia	BB22
	SL-501 5774	Solar Light, Analog	Meteorological Observatory of the Geophysical Institute, Slovakia	BB23
Hungary	SL-501 10403	Solar Light, Digital	Hungarian Meteorological Service, Budapest, Hungary	BB32
Greece	UVB-1 921116	YES	Laboratory of Atmospheric Physics, Aristotle University of Thessaloniki, Greece	BB34
Austria	010-A-00349	Scintec	Division for Biomedical Physics, Innsbruck Medical University, Austria	BB35

The traveling reference spectroradiometer QASUME provided the reference for the outdoor measurements; a second spectroradiometer from the Medical University of Innsbruck (UIIMP) participated at the outdoor measurements as secondary reference and backup solution in case of problems with the primary reference. In addition the presence of two spectroradiometers also allowed to ascertain the stability of the spectral solar irradiance measurements, as will be shown later. Both spectroradiometers were synchronised and measured solar irradiance spectra in the range 290 to 400 nm every 15 minutes.

## 4. Laboratory Characterisation

The UV Laboratory at PMOD/WRC is essentially composed of infrastructure previously at the European Reference Centre for UV radiation measurements (ECUV) at the JRC Ispra, Italy which was moved and set-up at PMOD/WRC in 2005 [3].

The radiometers were turned on and temperature stabilised for at least one hour prior to their laboratory characterisation. Before the measurement, the dark signal and the temperature were monitored for five to ten minutes in order to check the default operating parameters (dark signal and temperature) of the radiometer. The characterisation itself was done without temperature stabilisation since cross-talk on the signal and power lines increased the observed variability of the measured signal.

## 4.1 Relative spectral response Facility

The relative spectral response facility is described in Hülsen and Gröbner [3]. It consists of a Bentham double monochromator DM-150 with gratings of 2400 lines/mm. The wavelength can be selected within the range 250 to 500 nm and the slit width was chosen to yield a nearly triangular slit function with a full width at half maximum of 1.9 nm. A 300 W Xenon lamp positioned in front of the entrance slit acted as radiation source and was adjusted so as to maximise the radiation at the exit slit. Behind the exit slit a quartz plate mounted at 45° relative to the vertical transmitted about 92% of the radiation towards the test detector while about 8% were deflected towards a photodiode which was used to check the stability of the monochromator signal. An iris with a diameter of 6 mm was placed in the beam path in front of the test detector to define the beam spot size. Due to the large receiving surfaces of the radiometers only part of the detector could be illuminated by the monochromatic light source. Thus, spatial inhomogeneities of the receiving surface of the radiometer were not taken into account during the spectral response function (SRF) measurement. The relative spectral throughput of the monochromatic light source (MLS) was determined by measuring the spectral response of the MLS with the QASUME spectroradiometer between 260 and 400 nm, every 5 nm. Between 380 and 410 nm the rapidly changing spectral throughput of the MLS necessitated a step size of 1 and 2 nm. The wavelength scale of the MLS was determined by two methods which produced equivalent results:

- A mercury discharge lamp was placed at the entrance of the monochromator and the throughput measured with a photodiode to determine the slit function and thus the wavelength offset.
- The slit function measurements of the complete MLS (with Xe-Lamp source) with the QASUME spectroradiometer also allowed the determination of the wavelength offset from the slit function measurements.

The wavelength scale over the range 250 to 400 nm could be determined by both methods to within  $\pm 0.1$  nm.

The variability of the dark signal was monitored for five minutes prior to the SRF measurement as indicator for the minimum signal to noise ratio of the radiometer. The SRF measurement itself was obtained over the wavelength range 260 to 400 nm with a step size of 2 nm; the whole measurement required about 10 minutes. The overall relative expanded uncertainty of measurement ( $k=2$ ) of the SRF is estimated to be better than 10% for SRF values larger than  $5 \cdot 10^{-4}$ . Lower values have an estimated uncertainty of 30% due to the larger measurement variability.

The data-logger of the digital SL-501 radiometers were set to a sensitivity of 10 to increase the resolution of the stored measurement. To further increase the signal to noise, the output signal was sampled 10 times at each wavelength setting of the monochromatic light source. This increased the measurement time relative to the analog radiometers to about 30 minutes.

The SRF of the Eldonet radiometer could not be determined since the individual readings of the radiometer could not be accessed and synchronised with the wavelength setting of the MLS.

The SRF was obtained from the measurements by subtracting the dark signal measured before initiating the wavelength scan, and normalising it to the maximum signal.

## 4.2 Angular response Facility

The angular response function (ARF) of the radiometer was measured on a 3 m long optical bench. A 1000 W Xenon lamp was mounted at one end of the optical bench and served as radiation source. The detector was mounted on a goniometer at the other end with the vertical rotation axis passing through the plane of the receiving surface of the radiometer. The resolution of the rotation stage was 29642 steps per degree, or 0.12 arcseconds. The homogeneity of the radiation at the detector reference plane was measured and optimised to better than 1% over the receiving surface area of the detector. A baffle was placed in the beam path to reduce stray light within the dark room and a WG305 filter with a 50% cut off at 303 nm removed radiation below approx 300 nm. A mirror glued onto the rotation stage reflected some of radiation back on the Xe-lamp source which provided an adjustment precision of better than 0.1 degree. The expanded relative uncertainty ( $k=2$ ) of measurement is estimated to be less than 4% for zenith angles below 80%.

The measurements were performed in two orientations of the detector so that the angular response could be determined for the four quadrants N, S, E, W, with the N orientation defined by the connector of the radiometer.

The ARF of the Eldonet and the SRMS systems could not be measured because they could not be fitted on the goniometer.

The ARF for each quadrant was obtained by normalising the measurements at each angle to the reference measurement at normal incidence. The cosine error of each quadrant was calculated from the ARF by assuming an isotropic radiation distribution and integrating it over the whole hemisphere. The final ARF was obtained by averaging the measurements of the four quadrants.

## 4.3 Absolute Calibration

The absolute calibration was obtained by a comparison of solar UV radiation measured with the radiometer and the co-located QASUME spectroradiometer. The irradiance spectra were weighted with the detector spectral response to produce the absolute calibration factor for each radiometer. The conversion function  $f$  (see right side of Figure 2) to convert from detector weighted solar irradiance to erythemal weighted irradiance was calculated with the following equation,

$$f(\text{SZA}, \text{TO}_3) = \frac{\int \text{CIE}(\lambda) E_{\text{rad}}(\lambda) d\lambda}{\int \text{SRF}(\lambda) E_{\text{rad}}(\lambda) d\lambda}$$

where  $E_{\text{rad}}$  is a solar irradiance spectrum calculated with a radiative transfer model in dependence on solar zenith angle (SZA) and total column ozone  $\text{TO}_3$ ;  $\text{SRF}(\lambda)$  and  $\text{CIE}(\lambda)$  represent the detector and erythemal spectral responses respectively (see left side of Figure 2).

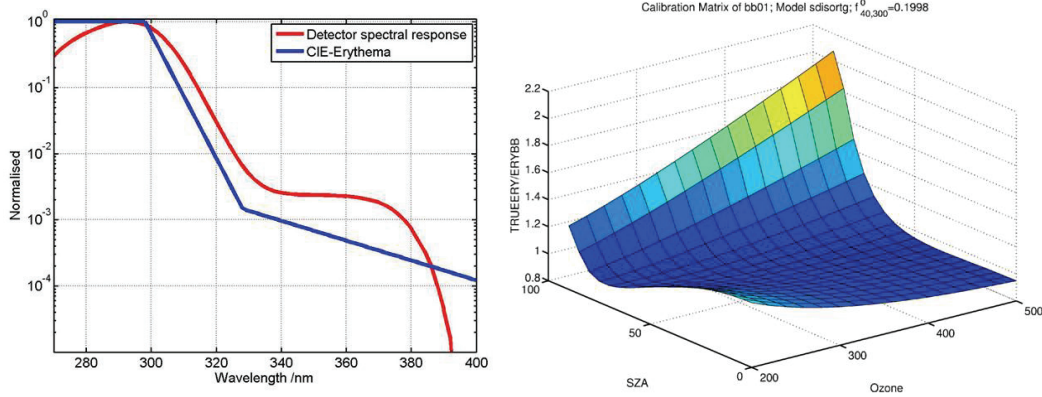
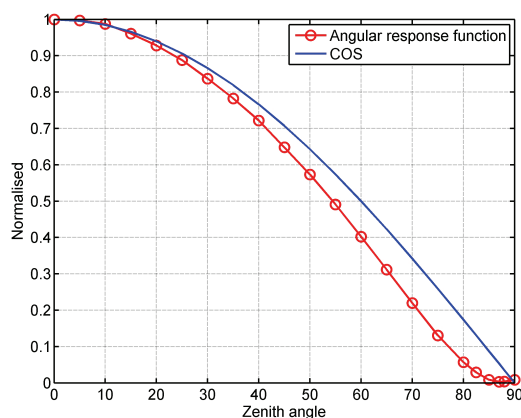


Figure 2 Left figure: radiometer spectral response function (red) and CIE-Erythema (blue). Right Figure: Conversion function  $f_r(SZA, TO_3)$  to convert from detector weighted to erythemally weighted solar irradiance.

For radiometers with a significant deviation of the angular response from the nominal cosine response, a cosine correction function has to be applied to the measurements. This correction depends on the atmospheric conditions and especially on the fraction of direct and diffuse radiation. The cosine correction applied for the data measured during the campaign used an isotropic diffuse radiation distribution; the fraction of direct and diffuse radiation was modeled by a radiative transfer model in dependence of the solar zenith angle (see Figure 3). For the determination of the calibration factor only two cases were distinguished:

1. clear sky: A cosine correction function  $1/f_{glo}(SZA)$  in dependence on the SZA was used.
2. diffuse sky: Only the diffuse cosine correction factor  $1/f_{dif}$  was applied to the calibration.

Depending on the radiometer type this simple approximation resulted in substantial variabilities especially during rapidly changing cloud conditions. In these cases, only the clear sky days were used for the calibration.



$$f_{dir} = \frac{ARF(\theta)}{\cos(\theta)}$$

$$f_{dif} = 2 \cdot \int_0^{\pi/2} ARF(\theta) \sin(\theta) d\theta$$

$$f_{glo} = f_{dir} \frac{E_{dir}}{E_{glo}} + f_{dif} \frac{E_{dif}}{E_{glo}}$$

Figure 3 Angular response function of a YES radiometer (circles) and the nominal cosine response function (blue curve).

$f_{dir}$  is the cosine error of the radiometer,  $f_{dif}$  represents the diffuse cosine error and  $f_{glo}$  the global cosine error of the radiometer. The radiometer shown in Figure 3 has a diffuse cosine error of 0.84, i.e. it underestimates the diffuse irradiance by 19%.

## 4.4 Horizon at PMOD/WRC

The horizon of the measuring site is limited by the surrounding mountains, as can be seen in Figure 4. The horizon actually obstructed the sun for SZA above 70°. For an isotropic diffuse radiation distribution the horizon would block about 5% of the total diffuse radiation.

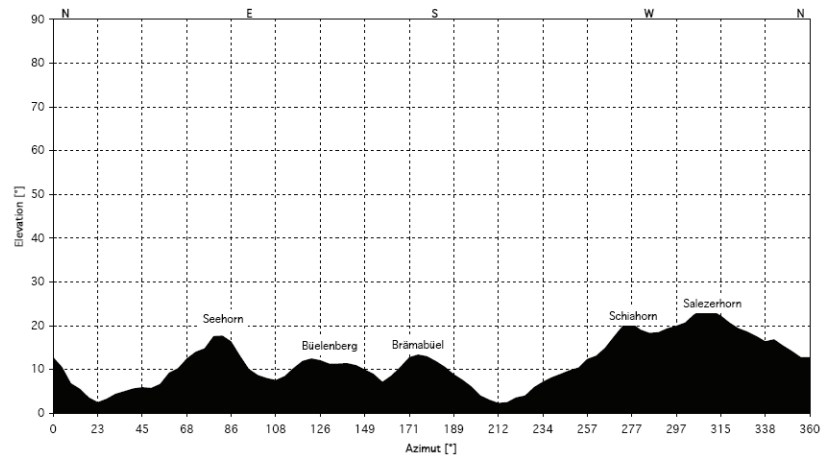


Figure 4 Horizon as observed from the roof platform of PMOD/WRC. North is Azimuth 0 and South is Azimuth 180.

We have estimated the effect of this horizon on the radiometers, taking into account their different angular responses. The resulting diffuse cosine error for each radiometer was calculated for either a full hemisphere or one with the horizon of PMOD/WRC.

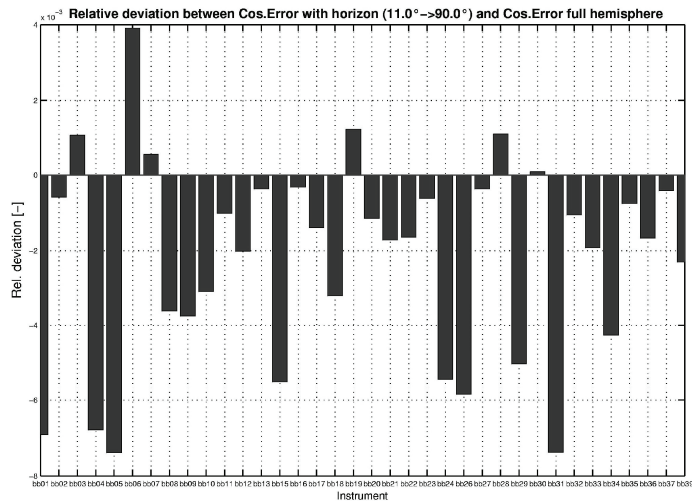


Figure 5 Relative deviation between the cosine error determined for a full hemisphere to the one of the PMOD/WRC horizon determined for each radiometer. The largest deviations are between +0.4% and -0.8%.

Figure 5 shows the ratio between these two values which represents the error made if a diffuse cosine correction is applied without taking into account the real horizon of the measurement site. As can be seen in the figure, the largest influence is of the order of 0.8% for a total overcast sky

and even less for a clear sky where this error would be reduced by the direct to diffuse radiation ratio. The calibrations at PMOD/WRC were calculated using the diffuse cosine correction factor calculated for the PMOD/WRC horizon.

#### 4.5 The effect of a finite scan time

The two spectroradiometers measured solar irradiance spectra by moving the diffraction gratings and measuring each wavelength sequentially. This resulted in a typical scan time of about 8 minutes for the wavelength range 290 to 400 nm. The following procedure was used to take into account the changing conditions during each scan, such as changing solar zenith angle or cloud variabilities:

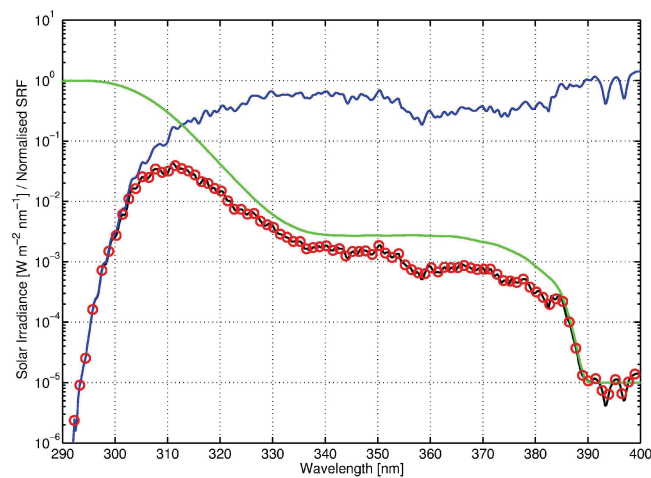


Figure 6 Solar spectrum measured with the QASUME spectroradiometer (blue curve), radiometer spectral response function (green curve), and detector weighted spectral irradiance (black curve). The red circles represent the radiometer readings during the scan time of the spectroradiometer.

At the core of the method is the availability of a large number of individual radiometer readings  $U(t)$  during a single solar spectrum measurement (see Figure 6). The solar spectrum, as measured by the spectroradiometer, is weighted with the detector spectral response to produce a spectral detector-weighted solar irradiance  $E_{\text{DET}}(\lambda)$

$$E_{\text{DET}}(\lambda) = \text{SRF}(\lambda) \cdot E(\lambda)$$

The detector weighted solar irradiance  $E_{\text{DET}}$  is further obtained by integrating  $E_{\text{DET}}(\lambda)$  over the whole wavelength interval and the representative time  $T_{\text{DET}}$  by integrating the weighted time of the solar spectrum with  $E_{\text{DET}}(\lambda)$

$$E_{\text{DET}} = \int E_{\text{DET}}(\lambda) d\lambda = \int \text{SRF}(\lambda) E(\lambda) d\lambda$$

$$T_{\text{DET}} = \int \text{SRF}(\lambda) E(\lambda) t_I(\lambda) d\lambda / E_{\text{DET}}$$

$$U_{\text{DET}} = \int \text{SRF}(\lambda) E(\lambda) U(t_{I(\lambda)}) d\lambda / E_{\text{DET}}$$

This effectively means that the radiation contribution of each wavelength weighted with the detector sensitivity is used as measure for the “relative importance” of each wavelength to the total measured irradiance. The radiometer readings during the time of the solar spectrum scan were weighted with  $E_{\text{DET}}(\lambda)$  to produce an average radiometer signal for each solar irradiance scan.

#### 4.6 The complete radiometer calibration equation

The calibration procedure used during this campaign to transform raw signals from a radiometer to erythemally weighted solar irradiance is based on the following equation:

$$E_{\text{CIE}} = (U - U_{\text{offset}}) \cdot C \cdot f_n(\text{SZA}, \text{TO}_3) \cdot \text{Coscor}$$

where  $E_{\text{CIE}}$  is the erythemal effective irradiance,  $U$  is the measured electrical signal from the radiometer and  $U_{\text{offset}}$  is the electrical offset for dark conditions [4, 5].  $C$  is the calibration coefficient, determined for a SZA of  $40^\circ$  and total column ozone of 300 DU.  $f_n(\text{SZA}, \text{TO}_3)$  is a function of SZA and total column ozone ( $\text{TO}_3$ ) to convert from detector based to erythemal based effective irradiance. By definition the function is normalised to unity for a total ozone column of 300 DU and a solar zenith angle of  $40^\circ$ .  $\text{Coscor}$  represents a cosine correction function which uses the ARF determined in the laboratory.

The dark offset  $U_{\text{offset}}$  was determined every day of the campaign during the night as the average over all measurements between 0 to 4 UT and 20 to 24 UT. The Cosine correction  $\text{Coscor}$  was calculated following the procedure described before and applied to the raw measurements  $U$ .

The calibration coefficient  $C$  at the time  $T_{\text{DET}}$  was then obtained by comparison with the solar spectrum measured by the spectroradiometer weighted with the SRF of the radiometer. Thus,

$$C = \frac{E_{\text{DET}}}{U_{\text{DET}} - U_{\text{offset}}} \cdot \frac{1}{\text{Coscor}} \cdot f(40^\circ, 300 \text{ DU})$$

## 5. Campaign Results

### 5.1 Spectroradiometer intercomparison

The reference spectroradiometer QASUME and the DM-300 spectroradiometer from the Medical University of Innsbruck measured synchronised solar irradiance spectra in the range 290 to 400 nm every 0.25 nm every 15 minutes. The instrument entrance optics were located within less than 50 cm from each other at the same height. Before installing the instruments on the roof, each spectroradiometer was calibrated with its own reference standard (portable lamps). Two of these lamps were also measured by the spectroradiometer of the other institute to determine the difference between the absolute reference of the respective laboratories. These measurements are shown in Figure 7 and demonstrate that the irradiance reference of the Medical University of Innsbruck is about 1% lower than the QASUME reference. This observed difference was not taken into account in the later analysis.

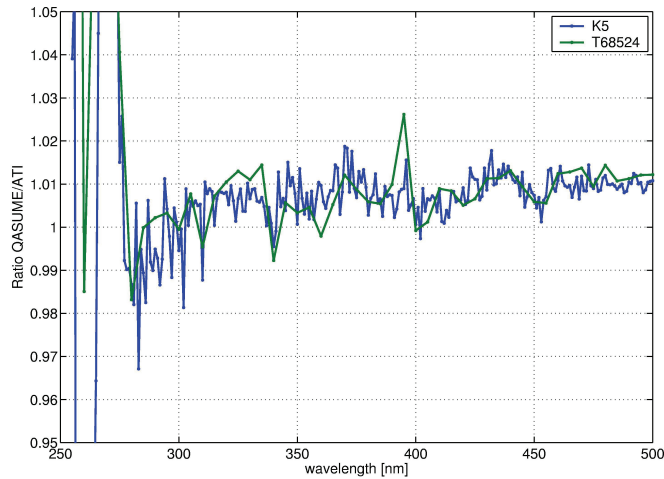


Figure 7 Comparison of two irradiance standards (portable lamps) of the Medical University of Innsbruck (K5) and of PMOD/WRC (T68524), measured respectively by the other institute.

The comparison of the solar irradiance spectra followed the standard operating procedure of a QASUME intercomparison, i.e. the spectra were convolved to a 1 nm slit width and wavelength adjusted to a common wavelength scale. The comparison of all measurements at selected wavelengths and the average over the measurement period is shown in Figure 8 .

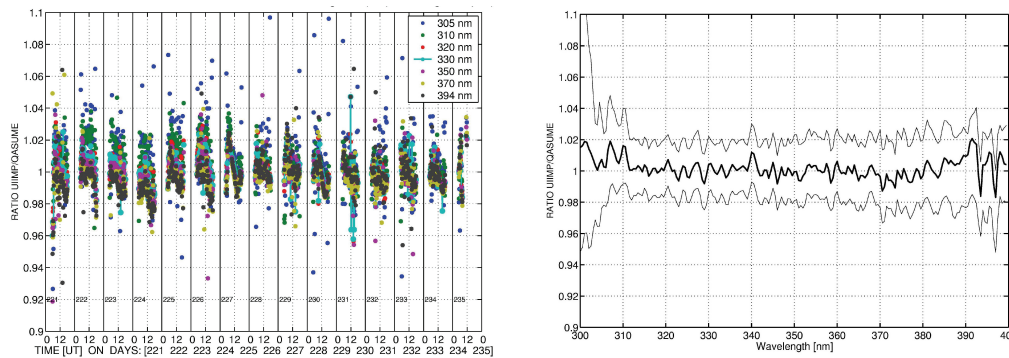


Figure 8 Comparison of spectral solar irradiance measurements between UIIMP and QASUME. The left figure shows the comparison over the whole measurement period for selected wavelength bands. The right figure shows the average spectral ratio between UIIMP and QASUME. The 90% variability is indicated by the two gray lines.

As can be seen in the figure the average difference between the two instruments is 0% with a variability of less than or equal to 2% for 90% of all measured spectra (658 out of 731). The observed diurnal variation was also below 2% for most days. For the clear sky days the diurnal variation was of the order of 5%; the pattern of this diurnal variation could be traced to an azimuth dependence of the angular response of the entrance optic used by UIIMP. This azimuth dependence was identified on August 23 by rotating the entrance optic of UIIMP by 180° and observing the expected change of 2 to 3% in the spectral ratio relative to the QASUME spectroradiometer, which was left unchanged.

## 5.2 Radiometer Absolute Calibration

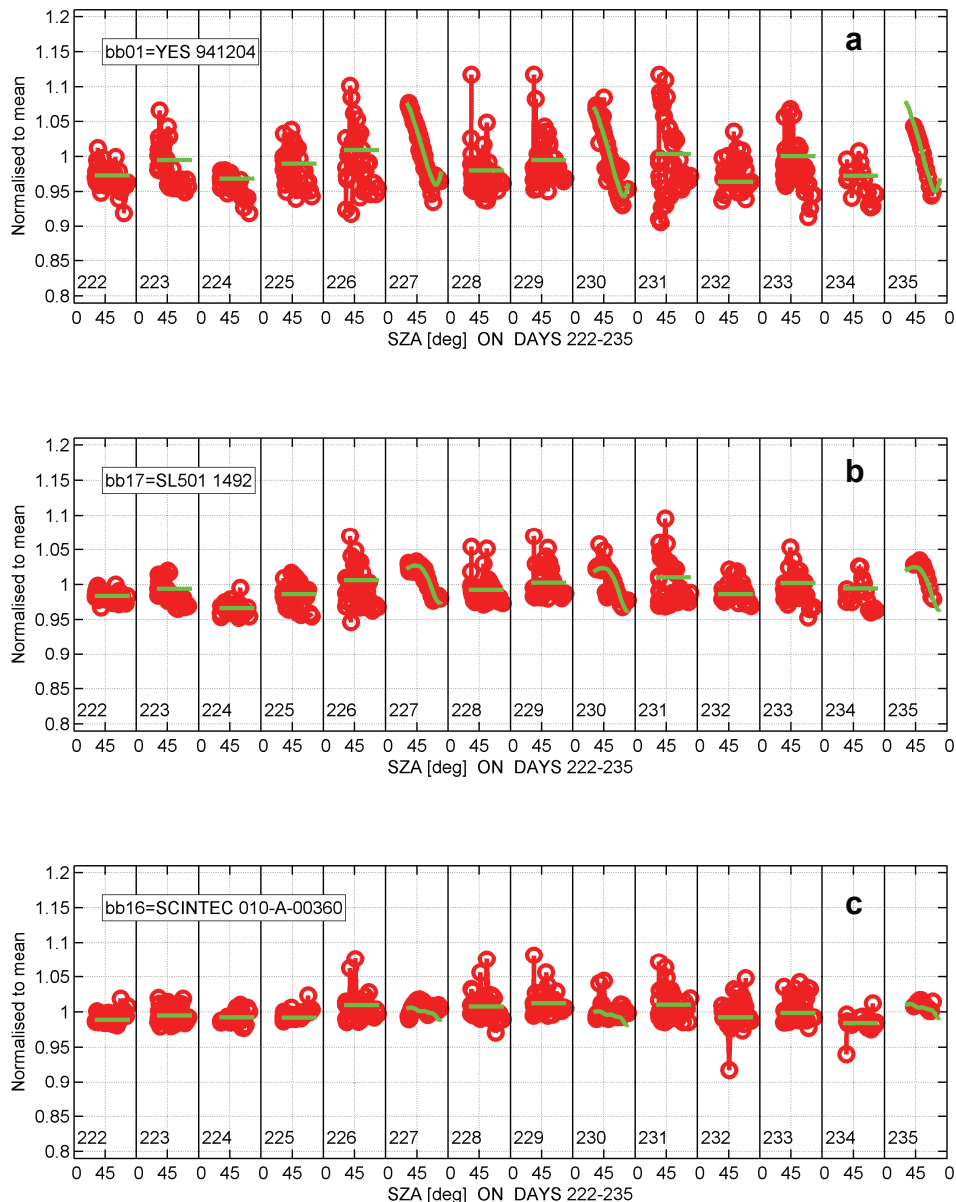


Figure 9 Calibration factors determined for the campaign period for three sample radiometers representing the three main types of radiometers present at the intercomparison, drawn against SZA; Figure 4a: YES (BB01), Figure 4b: SL-501 (BB17), and Figure 4c: Scintec (BB16). The plots actually show the inverse of C as defined in the equation above to facilitate the interpretation. A lower calibration factor means a lower signal measured with the radiometer. The green curves represent the cosine corrections calculated for each radiometer based on the ARF measured in the laboratory.

Figure 9a, 9b and 9c show the calibration coefficients of three sample radiometers from YES (BB01), Solar Light (BB17), and Scintec (BB16), for the whole campaign computed with the procedure described in the preceding paragraph but without applying the cosine correction to the calibration factor C. The cosine correction was added as a separate function (green curve) and normalised to one at 40 SZA. A clear sky cosine correction (function with SZA) was only applied on the clear sky days (15, 18, and 23 August); all other days used a diffuse cosine correction (constant factor). For days with rapidly

changing cloud conditions such as August 19 (day of year 231) for example, the increased variability of the calibration factor for instruments with a large cosine correction is apparent. This variability is explained with the inadequate cosine correction for these atmospheric conditions. These graphs also demonstrate that the observed diurnal variability of the calibration factor for the clear sky days can be almost completely explained with the cosine correction, i.e. the deviations of the ARF from the nominal cosine function. The cosine corrections for the three main types of radiometers in this campaign were:

- less than 3% for Kipp & Zonen or Scintec radiometers
- between 6% to 15% for Solar Light SL-501 radiometers
- between 14% and 25% for YES UVB-1 radiometers.

The expanded uncertainty of measurement ( $k=2$ ) of the calibration for all radiometers were of the order of 7%. The largest contribution came from the uncertainty of the reference spectroradiometer of about 5%. The variability of the radiometers during the calibration contributed only the remaining 2% of this uncertainty. Some instruments showed a higher variability which resulted in a larger uncertainty. The individual characterisation and calibration results for each radiometer are summarised in Table 2 and graphs are shown in the Annex. Two instruments were unstable during the campaign: The calibration factor determined for BB02 showed large diurnal variations which could be traced to a significant change in the spectral response of the instrument between the first measurement on August 1 and the second measurement on 24 August after the campaign. The Eldonet radiometer showed unexplained variations of about 10% during the measurement campaign, with even larger deviations of 60% on the morning of August 15.

## 6. Radiometer comparison

The comparison of broadband UV radiometers allows two types of analyses. In the first type, the results of the broadband radiometers are compared with the results of the spectroradiometer (the QASUME reference). In this case, the UV indices derived from the broadband radiometer measurements are compared with UV indices derived from QASUME. Such an analysis allows verifying how well the reference results can be reproduced with the broadband radiometers, i.e., it allows empirically estimating the uncertainty of the calibration procedure.

In the second type of analysis, the broadband UV radiometers are compared to each other. Since the goal in this case is to estimate the short-term statistical random uncertainty, the broadband radiometers are not anymore compared to QASUME, because of its longer integration time.

### 6.1 Comparison of broadband radiometer with the reference spectroradiometer QASUME

UV indices derived from the broadband UV radiometers were compared to concurrent UV indices derived from the reference QASUME spectroradiometers. The reference UV indices from the reference spectroradiometer QASUME were derived by integrating each solar

spectrum by the CIE action spectrum and calculating the reference time of the calculated UV index by weighting the time stamp at each wavelength with the CIE-weighted irradiance at this wavelength and integrating over all time stamps of the spectrum (see description in section 4.5).

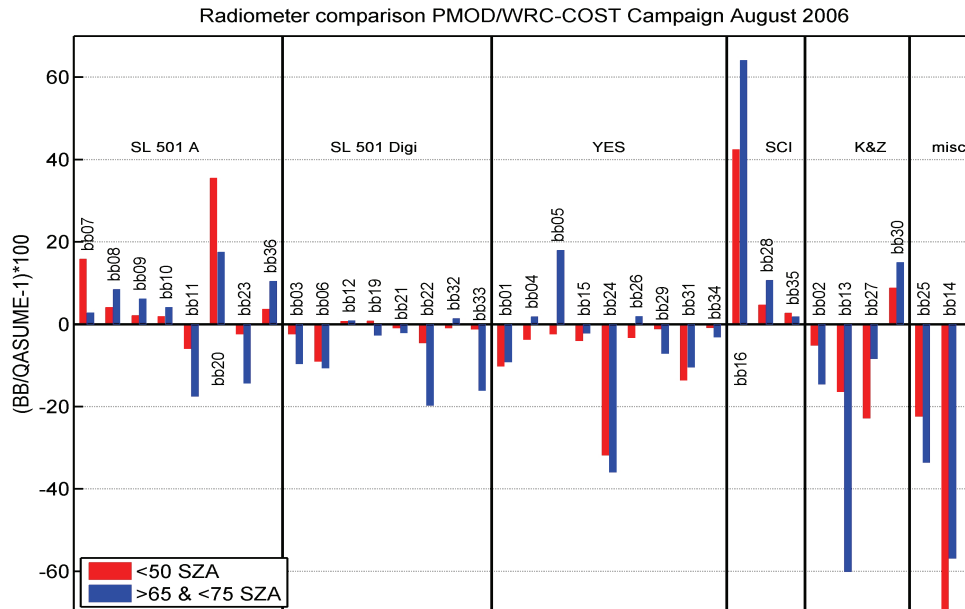


Figure 10 Average relative differences between the radiometers and the QASUME reference spectroradiometer for the two solar zenith angle ranges 1) smaller than 50° and 2) higher than 65° and lower than 75°.

Two sets of UV indices from the broadband radiometers were compared to the reference. For the first set, the raw signal measured by the radiometers during the campaign were communicated to the instrument owners who were asked to derive UV indices applying the procedures and calibration values they used prior to the campaign (thereafter described as *prior (or owner)* calibration). For the second set, UV indices were derived by PMOD/WRC using procedures and calibration values determined during the campaign (thereafter described as *campaign* calibration). The comparison between the UV indices derived for each radiometer and the QASUME spectroradiometer are shown in the Annex for each instrument. In addition the average relative differences between each radiometer and the QASUME reference for two SZA ranges (SZA below 50° and for SZA between 65° and 75°) are listed in Table 2 and shown in Figure 10.

Table 2 Summary of the calibration performed at the PMOD/WRC-COST726 calibration and intercomparison campaign of broadband radiometers measuring erythemally weighted solar irradiance, 28 July to 23 August 2006. The fifth column shows the relative difference in UV indices calculated by the instrument owners using their home calibration relative to the QASUME derived UV indices for low and high SZA ranges.

Radiometer type	Serial Number	Days used for the calibration (August 06)	Calibration Factor at 40° and 300 DU	Ratio $E_{ERY}$ , Owner calib. to QASUME SZA		ID
				<50°	65-75°	
SL-501A	8885	9-11, 13,15,18,22-23	0.2060 W m <sup>-2</sup> nm <sup>-1</sup> V <sup>-1</sup>	1.16	1.03	BB07
	8891	9-11, 13,15,18,22-23	0.1787 W m <sup>-2</sup> nm <sup>-1</sup> V <sup>-1</sup>	1.04	1.09	BB08
	1903	13,15,18,22-23	0.2203 W m <sup>-2</sup> nm <sup>-1</sup> V <sup>-1</sup>	1.02	1.06	BB09
	1904	13,15,18,22-23	0.2204 W m <sup>-2</sup> nm <sup>-1</sup> V <sup>-1</sup>	1.02	1.04	BB10
	5790	10,11,13,15,18,23	0.2440 W m <sup>-2</sup> nm <sup>-1</sup> V <sup>-1</sup>	0.94	0.83	BB11
	1492	9-11,13,15,18,22-23	0.2452 W m <sup>-2</sup> nm <sup>-1</sup> V <sup>-1</sup>	–	–	BB17
	1493	9-11,13,15,18,22-23	0.2200 W m <sup>-2</sup> nm <sup>-1</sup> V <sup>-1</sup>	–	–	BB18
	5782	9-11,13,15,18,22-23	0.1687 W m <sup>-2</sup> nm <sup>-1</sup> V <sup>-1</sup>	1.35	1.17	BB20
	5774	9-11,13,15,18,22-23	0.2356 W m <sup>-2</sup> nm <sup>-1</sup> V <sup>-1</sup>	0.98	0.85	BB23
	1497	15,23	0.2407 W m <sup>-2</sup> nm <sup>-1</sup> V <sup>-1</sup>	1.04	1.11	BB36
SL-501	922	15,18	1.0433	0.98	0.91	BB03
	635	15,18	0.9817	0.91	0.89	BB06
	1450	15,18	1.0996	1.01	1.01	BB12
	935	15,18	1.1026	1.01	0.98	BB19
	616	10,11,13,15,18	0.9621	0.99	0.98	BB21
	4811	15,18	1.0014	0.96	0.80	BB22
	10403	10,11,13,15,18	0.8963	0.99	1.01	BB32
	4818	10,11,13,15,18	0.9793	0.99	0.84	BB33
SRMS	26	10,13,15,18,23	1.2567	0.78	0.67	BB25
YES UVB-1	941204	15,18,23	0.1216 W m <sup>-2</sup> nm <sup>-1</sup> V <sup>-1</sup>	0.90	0.91	BB01
	000904	15,18,23	0.1150 W m <sup>-2</sup> nm <sup>-1</sup> V <sup>-1</sup>	0.96	1.02	BB04
	92906	15,18,23	0.1412 W m <sup>-2</sup> nm <sup>-1</sup> V <sup>-1</sup>	0.96	1.18	BB05
	030528	15,18,23	0.1161 W m <sup>-2</sup> nm <sup>-1</sup> V <sup>-1</sup>	0.96	0.98	BB15
	030521	15,18,23	0.1172 W m <sup>-2</sup> nm <sup>-1</sup> V <sup>-1</sup>	0.68	0.64	BB24

	970827	15,18,23	$0.1104 \text{ W m}^{-2} \text{ nm}^{-1} \text{ V}^{-1}$	0.97	1.02	BB26
	990608	15,18,23	$0.1199 \text{ W m}^{-2} \text{ nm}^{-1} \text{ V}^{-1}$	0.99	0.93	BB29
	970839	15,18,23	$0.1178 \text{ W m}^{-2} \text{ nm}^{-1} \text{ V}^{-1}$	0.86	0.90	BB31
	921116	15,18,23	$0.1506 \text{ W m}^{-2} \text{ nm}^{-1} \text{ V}^{-1}$	0.99	0.97	BB34
Scintec 010-A	00360	9-11,13,15,18,22-23	$0.2143 \text{ W m}^{-2} \text{ nm}^{-1} \text{ V}^{-1}$	1.42	1.64	BB16
	00407	9-11,13,15,18,22-23	$0.1295 \text{ W m}^{-2} \text{ nm}^{-1} \text{ V}^{-1}$	1.05	1.11	BB28
	00349	9-11,13,15,18	$0.1474 \text{ W m}^{-2} \text{ nm}^{-1} \text{ V}^{-1}$	1.03	1.02	BB35
Kipp & Zonen	020599	9-11,13,15,18,22-23	N/A unstable inst.	0.95	0.85	BB02
	020614	10,11,13,15,18,22-23	$0.1113 \text{ W m}^{-2} \text{ nm}^{-1} \text{ V}^{-1}$	0.84	0.40	BB13
	030616	10,11,13,15,18,23	$0.2339 \text{ W m}^{-2} \text{ nm}^{-1} \text{ V}^{-1}$	0.77	0.92	BB27
	000518	9-11,13,15,18,22-23	$0.1062 \text{ W m}^{-2} \text{ nm}^{-1} \text{ V}^{-1}$	1.09	1.15	BB30
Eldonet XP	084	10-13,15	N/A unstable inst.	0.27	0.43	BB14

## 6.2 Comparisons using Taylor diagrams.

The broadband and spectroradiometer measurements were performed at different frequencies. The spectroradiometer needed an integration time of about 8 min. Most of the broadband radiometers were measuring with time steps of about 7 sec, but some of them, typically the SolarLight radiometers with digital read-out, measured at 1 Hz, but only recorded the 1-min average. In order to accommodate all different repeat rates, times were defined for each QASUME measurement by using a weighted average, then a two minute window was defined around each of these time points (QASUME measurement time  $\pm 1$  min). Finally, for each broadband radiometer bbXX, QASUME-concurrent UV indices were determined by averaging the bbXX UV indices in each two minute window. For each bbXX, this procedure was repeated for UV indices determined using the prior and the campaign calibration, leading to two time series of QASUME concurrent UV indices for each bbXX (see Figure 11).

The agreement between UV indices determined by the QASUME reference and by the broadband UV radiometer (bbXX) is evaluated using Taylor diagrams ([6], see Appendix). In addition, each comparison was carried out using two time selections. In the first selection, all times when the solar zenith angle was less than  $70^\circ$  were selected, and in the second selection an additional criterion was used based on the smoothness of the UV index as a function of cosine solar zenith angle in order to select clear-sky times. Figure 11 (right panel) shows the data that satisfy only the solar zenith angle criterion in red and data satisfying both criteria in blue. Thereafter, the data set including all times with solar zenith angle less than  $70^\circ$  will be referred as all-sky, while the subset satisfying the additional criterion will be referred as clear-sky. In addition, a further subdivision was introduced for the analysis between times when the solar elevation was low (solar zenith angle between  $50$  and  $70^\circ$ ) and times when the solar elevation was high (solar zenith angle between  $30$  and  $50^\circ$ , the minimum solar zenith angle reachable during the inter-comparison was slightly higher than  $30^\circ$ ).

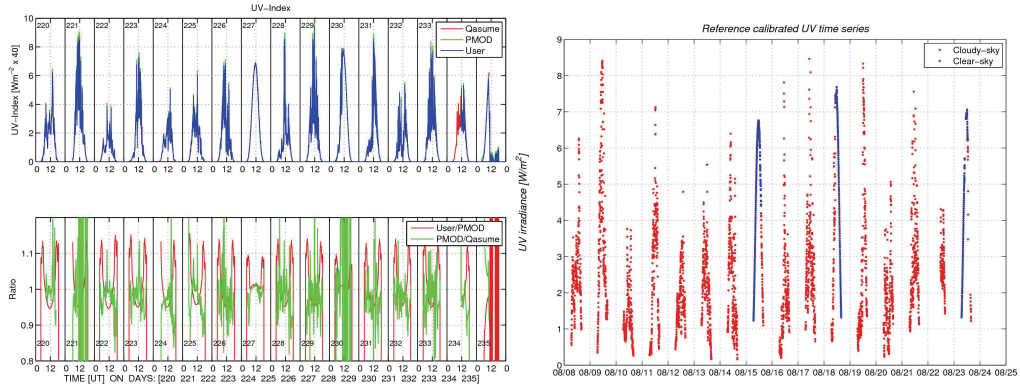


Figure 11 UV indices measured during the inter-comparison. *Left top panel:* UV indices measured by the QASUME reference and the broadband UV erythral radiometer YES UVB-1 000904 (bb04). The red curve is the QASUME measurement, the blue curve is the bb04 determination using the prior calibration, and the green curve is the bb04 determination using the campaign calibration. *Left down panel:* Ratio between the bb04 UV index using prior calibration and using campaign calibration (red curve), and ratio between bb04 UV index (campaign calibration) and QASUME UV index. *Right panel:* UV indices of times selected for the comparison between broadband radiometers and the QASUME reference. Times satisfying the UV index vs. cosine solar zenith angle smoothness criterion are shown in blue (clear-sky), and times not satisfying this criterion are shown in red.

Taylor diagrams summarising the agreement of the UV indices measured by the broadband radiometers with the UV indices measured by the QASUME reference are shown in Figure 12. On the panels on the left, the agreement is evaluated using times for all sky with different selections on the solar zenith angle, while the panels on the right use only times corresponding to the clear-sky selection. The panels on the first row show the comparison using all solar zenith angles below the  $70^\circ$  limit, the second row corresponds to solar zenith angles below  $50^\circ$  (high solar elevation), while the third row corresponds to solar zenith angles between  $50$  and  $70^\circ$  (low solar elevation). On all panels, the crosses correspond to the UV indices determined with the prior calibration, while the dots correspond to the campaign calibration. The black cross on the horizontal axis corresponds to the reference.

Because the different diagrams apply to different data sets with a relatively wide range of standard deviation (the standard deviation of the reference data set is shown by the position of the black cross on the horizontal axis), the Taylor diagrams are given in absolute unit (UVI), rather than relatively to the standard deviation of the reference. For example, the black cross on panel (a) shows that the standard deviation of the whole reference UVI data set is about 1.75 (all-sky and all solar zenith angles below  $70^\circ$ ). Data points at the same radius than the reference indicate that the UVI data set measured by the corresponding radiometer has a standard deviation equal to the data set measured by the reference, and consequently gives the same result than the reference in average. The angle between the radius to the data point and the horizontal axis indicate how well the data set of the corresponding radiometer is correlated with the reference data set. The distance between the black cross and the data points indicates the centered RMSE between the data set of the corresponding radiometer and the reference data set in UVI units. Finally, the orientation of the segment between the data points and the black cross indicates whether the RMSE is mainly due to a bad normalisation (segment almost parallel to the horizontal axes, corresponding to high correlation) or to a lack of correlation (segment close to the perpendicular to the horizontal axes).

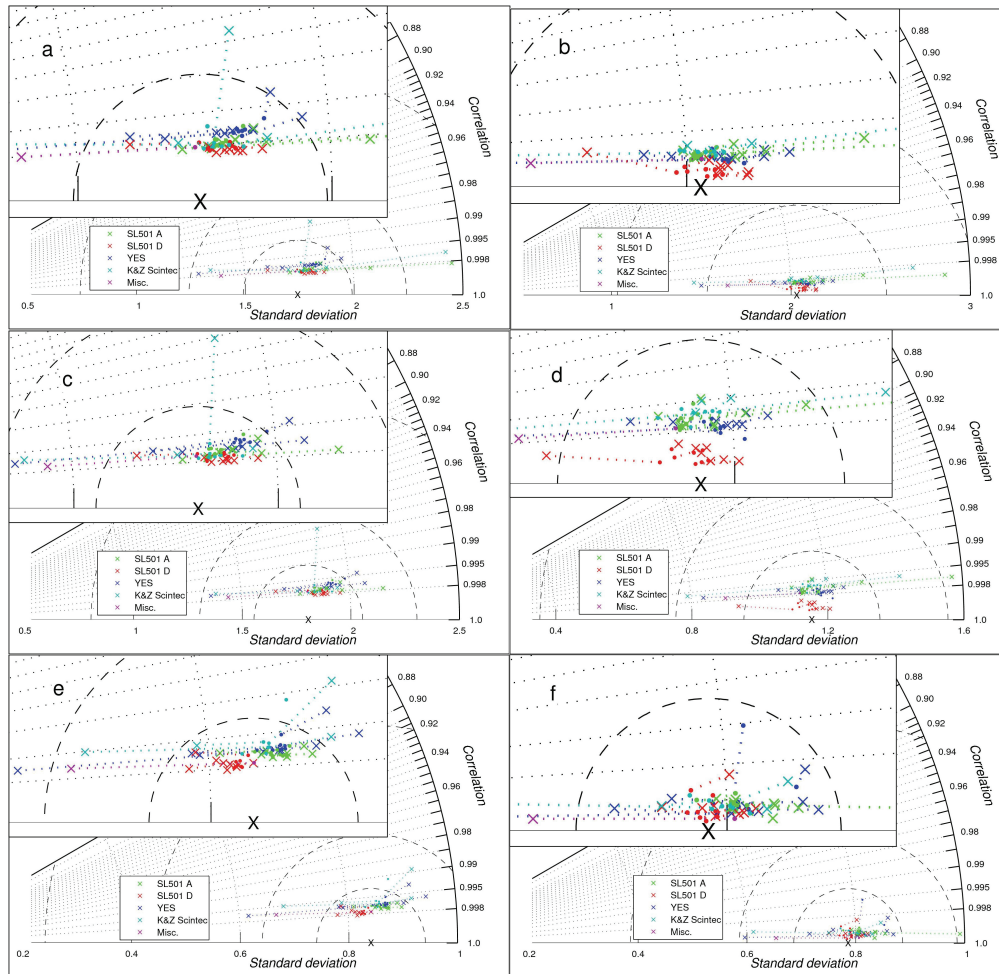


Figure 12 Taylor comparison of broadband radiometer-measured UV indices with UV indices measured by the QASUME reference. The crosses illustrate the agreement with the reference when using the original calibration from the instrument owner and the dots show the agreement when using the calibrations determined during the inter-comparison. The different panels show the comparisons for different selections based on solar zenith angles and clear sky times or all-sky times (both clear-sky and cloudy-sky times – see figure 11).

- Panel a) all-sky, SZA 30 to 70°,  
 b) clear-sky, SZA 30 to 70°,  
 c) all-sky, SZA 30 to 50°,  
 d) clear-sky, SZA 30 to 50°,  
 e) all-sky, SZA 50 to 70°,  
 f) clear-sky, SZA 50 to 70°.

In all cases, Taylor diagrams demonstrate a high correlation between broadband radiometers and the QASUME UV indices. It is only when comparing data for all-sky times at high solar elevation (panel c), that one instrument is shown to have a correlation below 0.98. On the other hand when comparing clear-sky UV indices for all solar zenith angles (panel b), the correlation is higher than 99.8% for all instruments. Such a high correlation is expected because the variations of UV indices are mostly driven by external factors such as solar zenith angle or cloudiness to which all the broadband radiometers respond similarly, whether they are correctly calibrated or not. Consequently, very large RMSE between the reference and the broadband radiometers are only found for some instruments, when using prior calibration, and in case of large normalisation error. In such case, the influence of the correlation is negligible. For a few instruments, normalisation errors larger than 25% are found.

Comparisons using all-sky situations are more difficult to interpret. In such situations lower correlations can be due to a multiplicity of factors. In some cases, differences in measurement frequency can play a role, because rapid changes occur for broken cloud coverage. Correlation for instruments having large cosine correction can also suffer from the fact that the cosine error was applied only for clearly identified clear-sky situations. In case of broken cloud with direct sunshine on the instrument, the direct beam cosine correction should also be applied, but was not. However, the instrument showing the most important lack of correlation in panels a, c and e is a Scintec radiometer when applying prior calibration. Thus, the effect of cosine error should probably be ruled out in this case. The clearest pattern for all-sky cases is that SL501 radiometers with digital readout and, to a lesser degree, SL501 radiometers with analog readout seem to group in clusters with nearly identical correlation with the reference. Instruments in each group (SL501D and SL501A) measured with a particular frequency pattern. SL501D radiometers used 1Hz measurement frequency and recorded 1-min averages, while SL501A measured about every 7s and recorded all measurements. (Except one SL501A that used a measurement frequency similar to the SL501D). Thus, the observed pattern for SL501D, and to a lesser degree for SL501A, may be due to difference in measurement frequency between the broadband radiometers and the spectro-radiometer.

In clear-sky cases, panel b of Figure 12 shows that most instruments have an RMSE with the reference of less than 0.25 UVI (the first equal-RMSE circle is at 0.5 UVI), with a very high correlation. As mentioned earlier this high correlation reflects only a similar response to external factors. Restricting the analysis to a given solar zenith angle domain allows diminishing the influence of such external factors, especially for clear-sky cases since the solar elevation is then the dominant factor. Panel d shows that when restricting to high solar elevation, the RMSE does not diminish as much as the standard deviation of the reference data set: Most instruments have an RMSE of less than 0.2 (first equal-RMSE circle is at 0.2 UVI), but the standard deviation of the reference data diminishes from about 2 UVI when considering all solar zenith angles to slightly less than 1.2 when considering only high solar elevation. In this case, for many instruments, the correlation with the reference is reduced and contributes significantly to the RMSE, when the analysis is restricted to high solar zenith angles. When restricting to low solar elevation, most instruments have an RMSE below 0.1, while the reference data set standard deviation is about 0.8. Here, the correlation is high (similar to considering all solar zenith angle) and not contributing much to the RMSE. The difference in the influence of correlation on the RMSE between high and low solar elevation data set can be explained by the fact that solar elevation influence UV radiation proportionally to the air mass, which changes much more rapidly at low than at high solar elevation. Thus, this external dominating factor has more influence for the low solar elevation data set, which leads to higher correlation.

In Figure 12, the agreement between the UV indices measured by the broadband radiometers and the reference are illustrated for both prior and campaign calibration. A light dotted line joins the cross to the dot for each instrument. The new calibration brings an improvement when the dot is closer to the reference point (black cross). Both for clear-sky cases and all-sky cases most instruments show a marked improvement, and for some instruments there is no significant change. For clear-sky cases, the improvement is mainly occurring in the direction of better normalisation (overall calibration factor). However, when all-sky cases are considered,

some instruments show a significant improvement in the correlation, which is likely to be due to a better consideration of zenith angle and ozone effects.

Finally, considering only clear-sky cases and using the calibration determined during the intercomparison, the relative RMSE between the broadband radiometer and the QASUME reference is on the order of 0.1 UVI or less for all instruments when restricting to high solar elevation and even lower on the order of 0.04 UVI when restricting to low solar elevation (see Figure 13). This is better than 10% for high solar elevation and on the order of 5% for low solar elevation. This indicates that for clear-sky cases, broadband UV radiometers that are recently and properly calibrated can reproduce the reference measurements with an uncertainty of about 5–10%. This reproducibility was achieved for more than 30 instruments including all major manufacturers of such instruments.

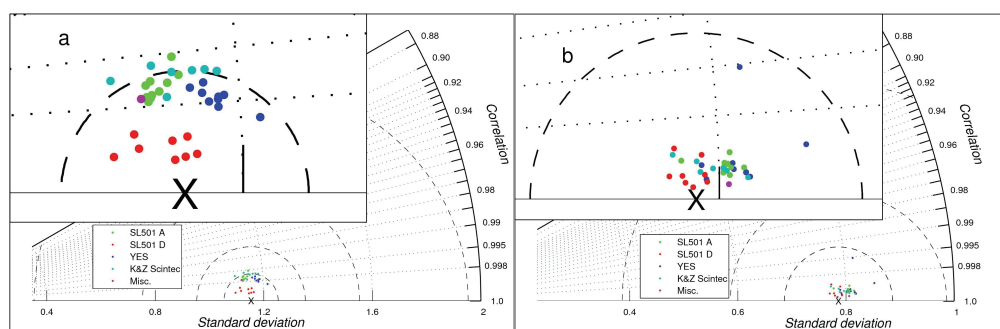


**Figure 13 Taylor comparisons of broadband radiometer-measured UV indices with UV indices measured by the QASUME reference. Selected clear-sky cases and UV indices using PMOD/WRC calibrations. The inner circle indicates a centered RMSE of 0.1 UVI. Panel a) clear-sky, solar zenith angle 30 to 50°, b) clear-sky, solar zenith angle 50 to 70°.**

### 6.3 Instrument random (statistical) uncertainty

The short-term random variability of the broadband UV radiometers was estimated by inter-comparing their measurements. Because of integration time issues, the QASUME was not chosen as reference. The average of all valid UV-indices measurements from all broadband UV radiometers for each two-minute window were taken as reference, under the assumption that short-term statistical variability will cancel out between instruments<sup>1</sup>. For each instrument, the ratio of the average UV index to the UV index measured by the given instrument using campaign calibration is fitted with a quadratic response surface to empirically express systematic solar zenith angle and ozone dependences (see Figure 14) that would not have been captured by the campaign calibration procedure.

<sup>1</sup> Other combinations were tried such as all broadband radiometers except the 5 instruments with largest residuals to the average, or three instruments of each manufacturer having the smallest RMSE with the QASUME reference, but results were similar to results obtained with average of all instruments taken as reference.

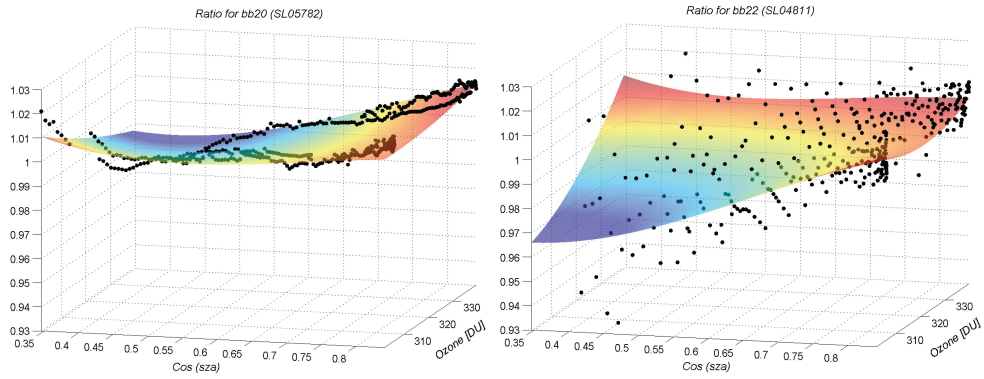


Figure 14 Ratio of average UV index to single instrument-measured UV index as a function of ozone total column and cosine solar zenith angle. The black dots are the individual measurement ratios, and the colored surface show the quadratic response surface fit. The left panel shows an example with small residuals, while the right panel shows an example with large residuals.

This method is chosen for isolating the random uncertainty as much as possible, and not including the systematic effects that could be linked to the known influential parameters mentioned above. Thus, the residuals between the measurement ratios and the fit surface are analysed for estimating the random variability of the instruments. Similarly to the Taylor diagram analysis, this analysis was repeated considering first only cases considered as clear-sky, then considering both clear- and cloudy-sky (see Figure 11).

Analysis of the residuals in clear-sky cases shows that the random statistical variability is below  $\pm 2\%$  (for many instruments, it is more of the order of  $\pm 1\%$ ). It also seem that most SolarLight radiometers with analog read-out (SL501 A) have a small random variability, while many SolarLight radiometers with digital read-out have larger than average random variability (see Figure 15). Analysis of residuals for all-sky cases shows much larger random variability, which is most likely due to quick variations of UV radiation level when partial cloud coverage is occurring. In all-sky cases, the short-term random variability is on the order or below  $\pm 5\%$  (see Figure 16). As was the case in the clear-sky analysis, SolarLight radiometers with analog read-out have smaller than average random variability. On the other hand, instruments with larger than average variability seem not to be of a specific type. As was the case in the Taylor diagram analysis, subsets including only solar zenith angles between 30 and 50°, and between 50 and 70° were analysed separately. However, there were no significant differences in the analysis results when the subsets were analysed separately or together.

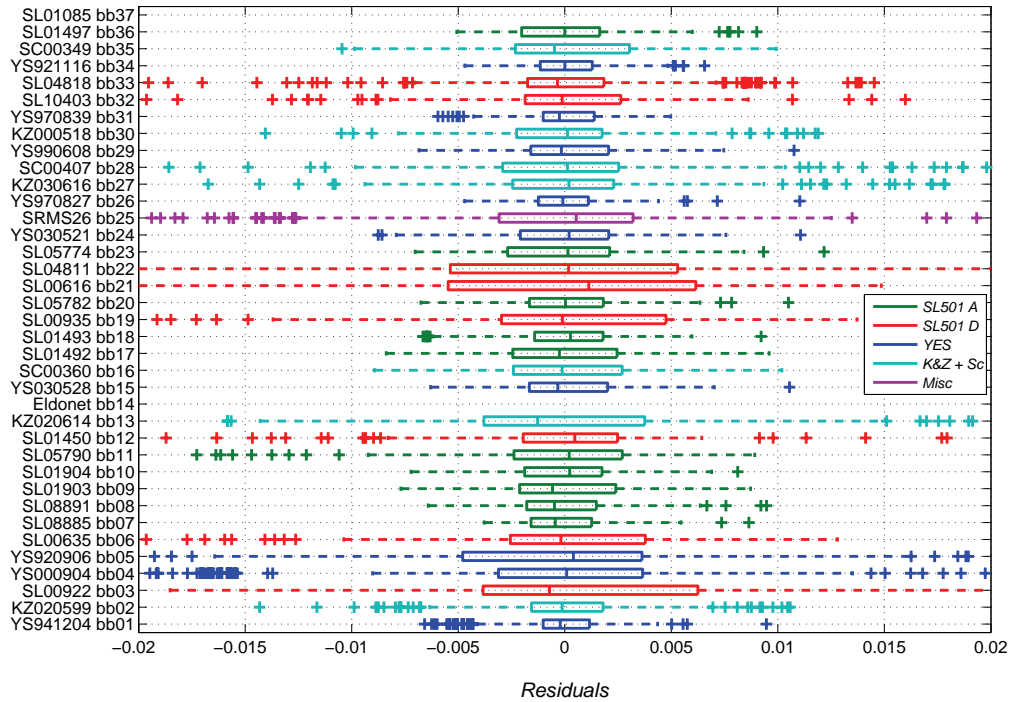


Figure 15 Distribution of residuals for selected clear-sky situations. Boxes represent the inter-quartile range of the distribution. The dashed lines show the extent of the rest of the distribution, *except if there are outliers*, that are defined as values that are more than 1.5 times the inter-quartile range away from the extremities of the boxes. In some cases large groups of outliers are present. It is due to the high auto-correlation of the data, which leads to clusters of outliers.

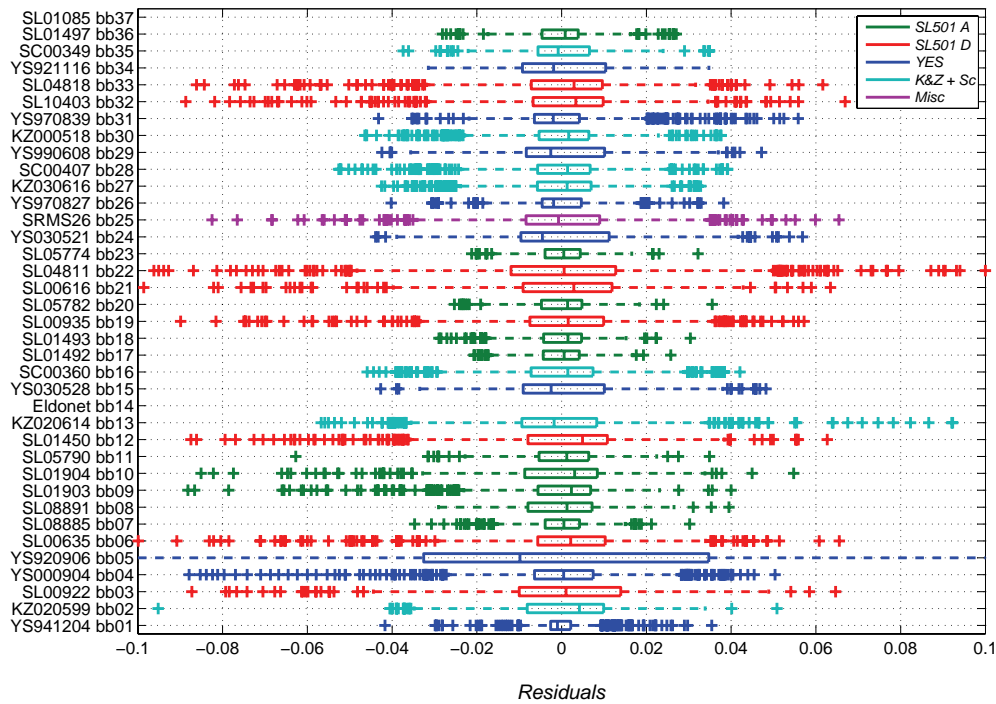


Figure 16 Same as Figure 15, but for all-sky situations. (Note that the horizontal scale is 5 times larger than in Figure 15).

## **Acknowledgments**

We would like to acknowledge the active support of the PMOD/WRC staff in the preparation and organisation of the intercomparison campaign. The instrument owners provided the calibrated data for the intercomparison period using their home calibration. The total ozone column measurements from Arosa were provided by Meteoswiss. The instrumentation of the UV Calibration Section of the PMOD/WRC is made available by the Joint Research Centre of the European Commission in Ispra under cooperation agreement 2004-SOCP-22187. G. Hülsen is supported by the Swiss COST Office under contract C05.0068. D. Walker is supported by the Swiss State Secretariat for Education and Research, COST Office, under contract C04.0242. Financial support of the stay of J.E. Gil from the Ministerio de Educación y Ciencia and FEDER funds from CGL2004-05984-C07-03, REN2003-03175 projects are gratefully acknowledged. The participation of M. Blumthaler and J. M. Vilaplana at the campaign was partly financed by COST 726 (STSM-COST726-03 and STSM-COST726-04).

## References

- [1] K. Leszczynski, K. Jokela, L. Ylianttila, R. Visuri and M. Blumthaler. Erythemally weighted radiometers in solar UV monitoring: Results from the WMO/STUK Intercomparison. *Photochem. Photobiol.*, 67:212–221, 1998.
- [2] WMO/GAW Report No. 141: Report of the LAP/COST/WMO Intercomparison of Erythemal radiometers, Thessaloniki, Greece, 1999. WMO TD{No. 1051}.
- [3] Hülsen, G., and J. Gröbner, Characterisation and Calibration of UV Broadband radiometers Measuring Erythemally Weighted Irradiance, *Applied Optics*, 46, 5877-5886, 2007.
- [4] A. Webb, J. Gröbner, and M. Blumthaler. A Practical Guide to Operating Broadband Instruments Measuring ErythemallyWeighted Irradiance, 2007. EUR 22595, ISBN 92-898-0032-1.
- [5] G. Seckmeyer, A. F. Bais, G. Bernhard, M. Blumthaler, C. R. Booth, R.L. Lantz, R.L. McKenzie, P. Disterhoft, and A. Webb. Instruments to measure solar ultraviolet radiation. Part 2: Broadband Instruments Measuring Erythemally Weighted Solar Irradiance. WMO/GAW No. 164 World Meteorological Organization, Geneva, 2007.
- [6] Taylor, K. E. (2001), Summarizing multiple aspects of model performance in a single diagram, *J. Geophys. Res.*, **106**(D7), 7183–7192.

## Appendix: Taylor diagram comparison

Taylor diagrams (Taylor, 2001) are a tool for evaluating the agreement between a tested data set and a reference data set (with one-to-one correspondence between the tested data points and the reference data points). The evaluation of the agreement between a given data set and the reference data set is illustrated by a single point on the Taylor diagram, which gives information about the relative normalisation between the tested and reference data set, their correlation and the root mean square error (RMSE) between the two sets. Since the information on the agreement of a given data set with the reference is given by a single point, many tested data sets can be compared to a single reference in a given Taylor diagram.

Taylor diagrams are based on the recognition that the relative standard deviation (the ratio of the tested data set standard deviation over the reference data set standard deviation), the centered root mean square error (see Taylor, 2001 for definition), and the correlation can be seen as the different components of the law of cosines with the correlation being the cosine of the angle.

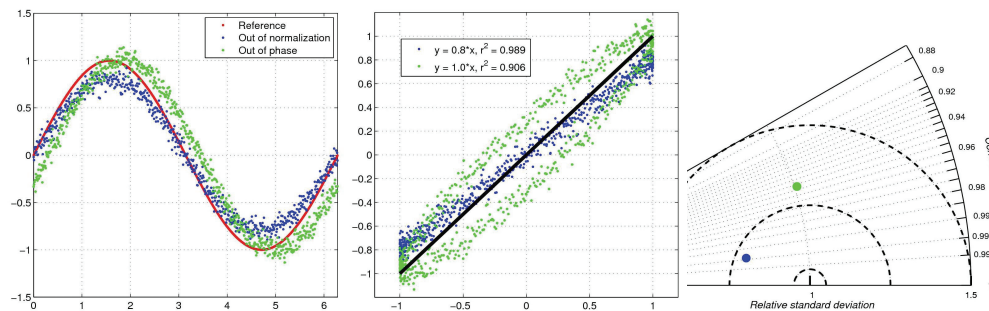


Figure A-1 Example of comparison for synthetic data sets. *Left panel:* tested data sets shown together with the reference data set. *Middle panel:* tested data sets shown as function of the reference data set. *Right panel:* Taylor diagram comparison of tested data sets with reference.

Figure A1 shows an example of Taylor diagram comparison between two synthetic tested data sets and a corresponding reference. On the left panel, the reference data set is shown in red, while the first tested data set has a different overall normalization (in blue), and the second has a phase shift (in green). On the middle panel, the two tested data sets are shown as function of the reference data set. The first data set has a good correlation with the reference data set, but the slope of the regression line is lower than 1. The second data set has a regression slope of 1, but a worse correlation than the other data set. The right panel shows the Taylor diagram comparison of the tested data sets with the reference. The Taylor diagram is a polar plot where the correlation is the cosine of the polar angle, and the relative standard deviation is the radius. On the Taylor diagram, one immediately sees that the first set has a better correlation than the second, but the overall normalization of the second set is almost identical to the overall normalization of the reference (relative standard deviation of 1). The concentric dashed circles are circles of constant RMSE (the first is at 5% RMSE, the second at 25% and the third at 50%). In this case, the second data set has a worse RMSE than the first data set.



## Annex

Individual results for each instrument participating at the calibration and intercomparison campaign at PMOD/WRC, Davos, Switzerland from 28 July to 23 August 2006.

Comments on the results obtained during the broadband UVB  
radiometers intercomparison and calibration campaign at the  
PMOD/WRC installations, Davos summer 2006  
*By Instituto Nacional de Meteorología, Madrid (INM)*

Davos Referente Documents

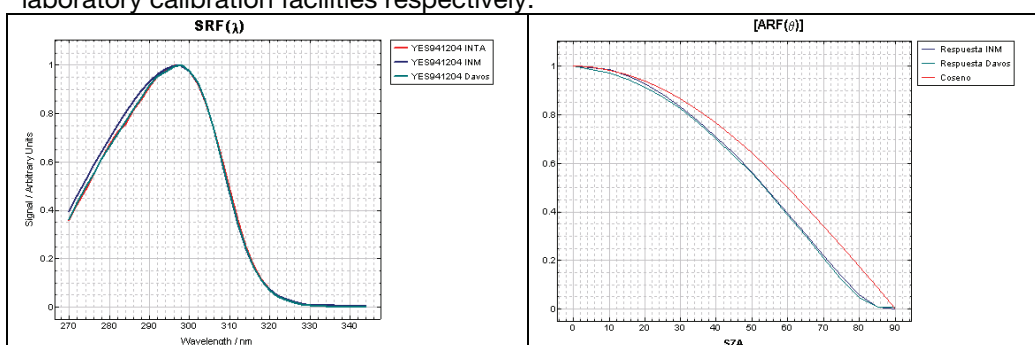
Calibration Certificate No 2006/BB01/1, No2006/BB01/2 and No 2006/BB01/3  
Report of the PMOD/WRC-COST Calibration and Intercomparison of Erythral Radiometers  
28 July-23 August 2006

Instrument

YES UVB-1 No 941204 owned by INM (labelled as BB01 during the campaign)

Characterisation at the laboratory

The calibration certificate and the report PMOD/WRC-COST are consistent with the calibration history of the instrument, both the relative spectral response function, [SRF( $\lambda$ )], as the angular response [ARF( $\theta$ )] .The figure shows the SRF( $\lambda$ ), as determined at Davos (green), at INTA in 2005 (red) and at INM in 2006 (blue) laboratory calibration facilities respectively.



The relative spectral response has been recently determined at INM using its double monochromator Bentham (DMc 150) with 2400 l/mm, in the range 280-400 nm at 1 nm wavelength step. The next table shows the wavelength at the maximum and the FWHM in nm. Although the behaviour of SRF( $\lambda$ ) determined by INM in the range 270-290 has still to be completely understood, both INTA and Davos spectral responses seem to be very similar between them and to that obtained at INM from 290nm onwards.

YES 941204	Máximo (nm)	Anchura a media altura (nm)
SRF( $\lambda$ ) Davos	298.307	35.3
SRF( $\lambda$ ) INM	296.961	36.3
SRF( $\lambda$ ) INTA	297.734	35.3

Next figure shows the angular response as obtained at the INM (blue) and Davos (green) laboratories. They show to be rather similar, although that determined at INM presents smaller cosine error at low solar zenith angles.

Differences in UVI as calculated by INM and by PMOD/WRC

The results obtained during the Davos campaign have shown a general underestimation of UVI (its magnitude depending on sza) calculated by the INM with respect to that calculated by PMOD/WRC and from the solar spectral irradiance measured by the QASUME spectroradiometer. The UVI calculated by INM using the raw data provided by PMOD/WRC is based on the calibration matrix determined by INTA for the instrument in 2005, taking into account the total column ozone and the solar zenith angle, but without subtracting the offset (with a minor contribution to the total UVI). Provided the SRF as determined by INTA and PMOD seems to be very similar, we think that the observed discrepancies in UVI between the values calculated by us and using PMOD calibration, or against QASUME measurements, are mainly due to the differences between both PMOD and INTA to obtain the calibration matrix and/or the angular correction factor (Brewer vs QASUME spectral irradiance).

YES UVB-1 s/n 941294 (BB01)

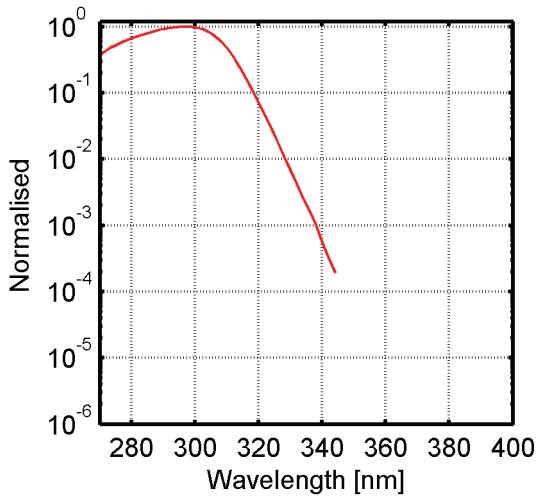


Figure 1 Relative spectral response function

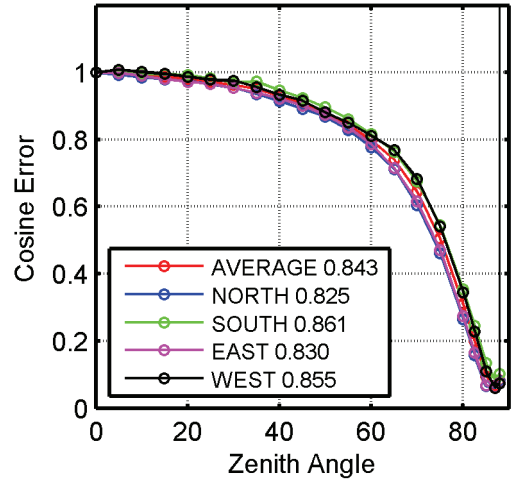


Figure 2 Cosine Error

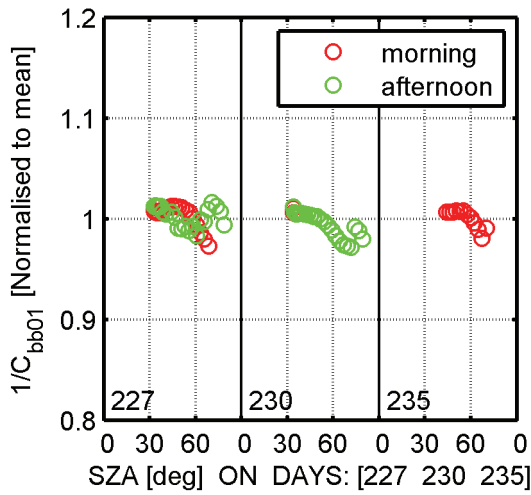


Figure 3 Calibration factor normalised to the average

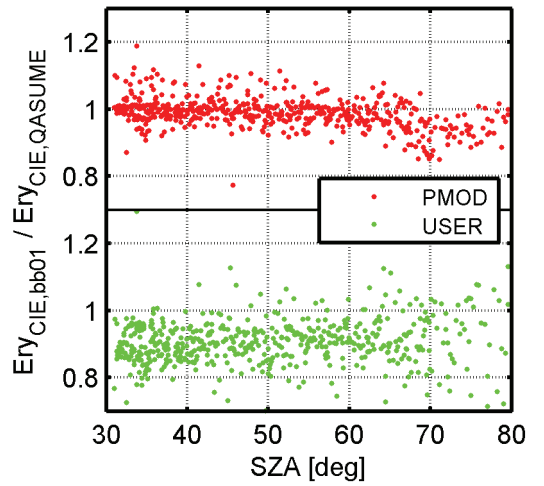


Figure 4 Erythemal weighted irradiance from Radiometer relative to QASUME

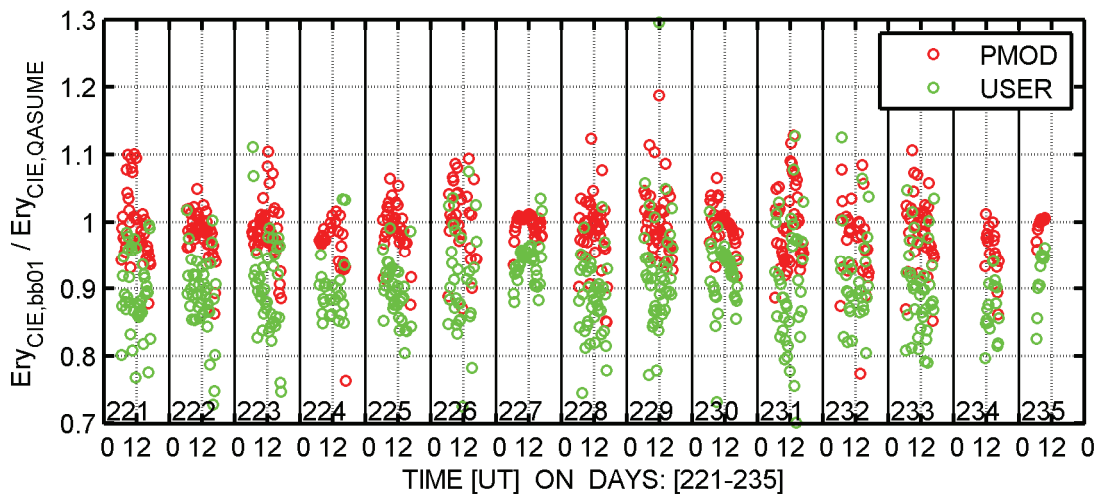


Figure 5 Erythemal weighted irradiance from Radiometer relative to QASUME spectroradiometer



Kipp & Zonen s/n 020599 (BB02)

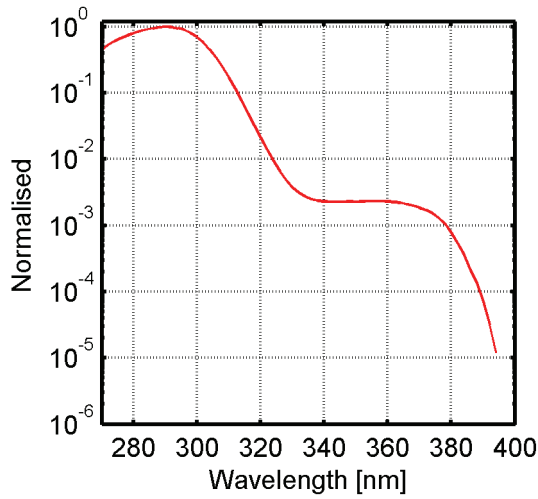


Figure 1 Relative spectral response function

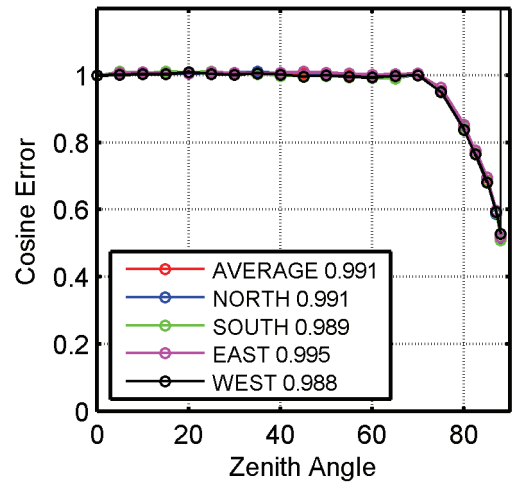


Figure 2 Cosine Error

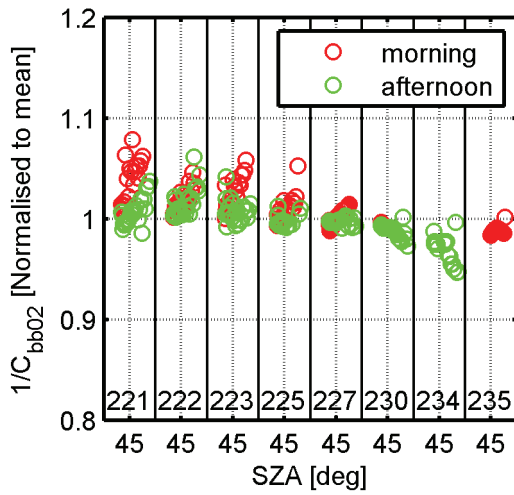


Figure 3 Calibration factor normalised to the average

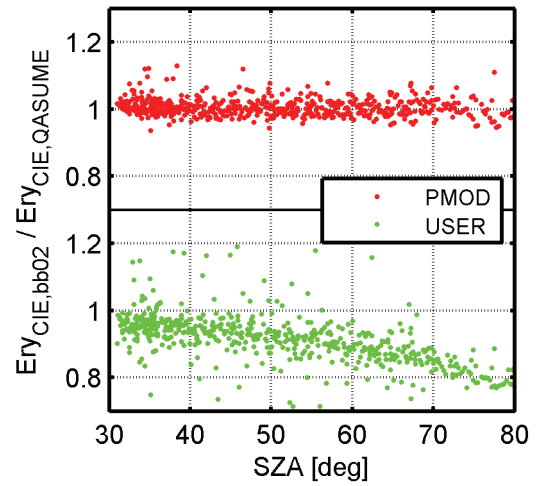


Figure 4 Erythemal weighted irradiance from Radiometer relative to QASUME

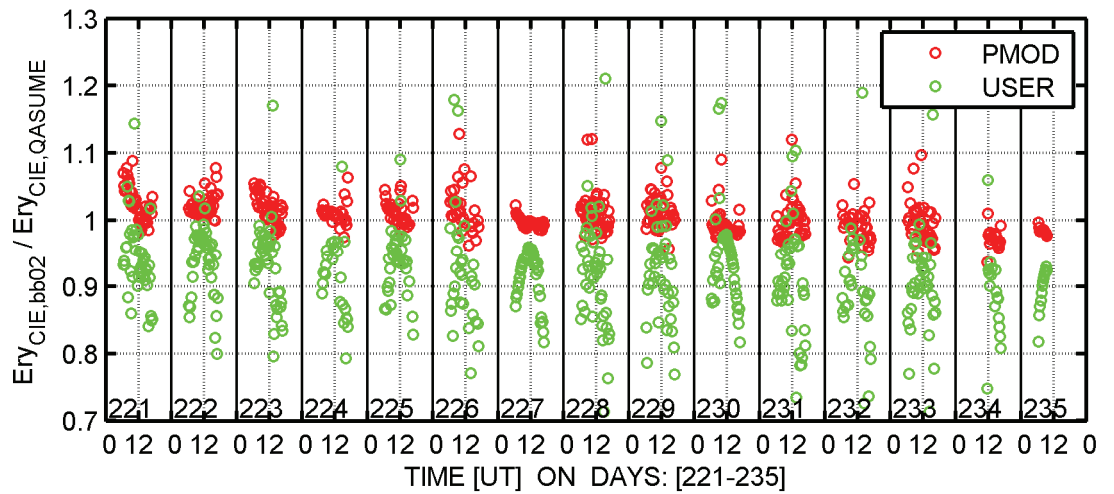


Figure 5 Erythemal weighted irradiance from Radiometer relative to QASUME spectroradiometer



Solar Light SL501 D s/n 0922 (BB03)

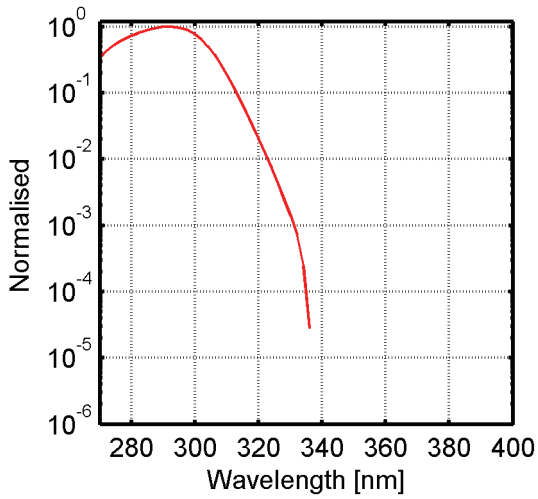


Figure 1 Relative spectral response function

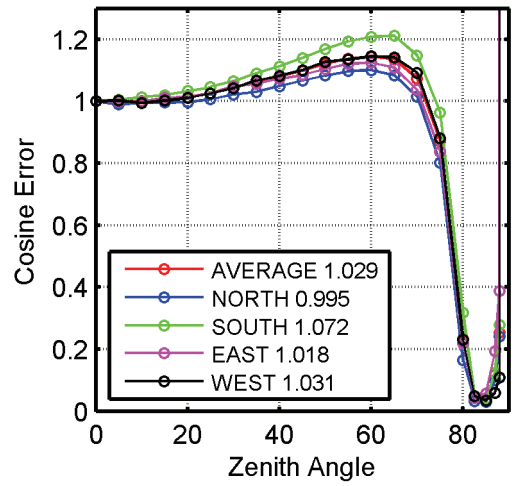


Figure 2 Cosine Error

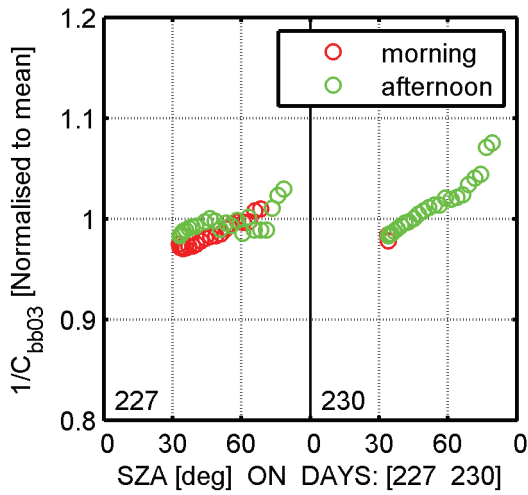


Figure 3 Calibration factor normalised to the average

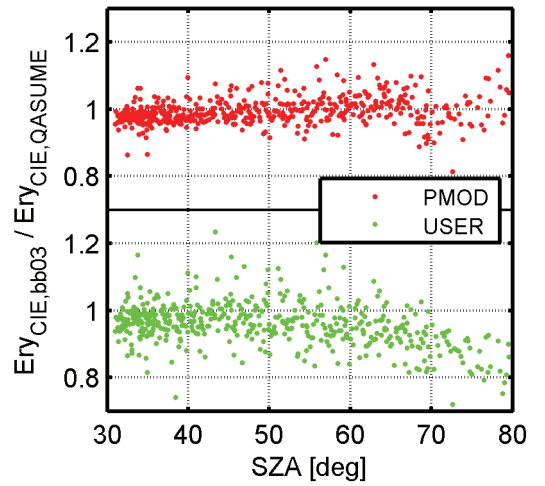


Figure 4 Erythemal weighted irradiance from Radiometer relative to QASUME

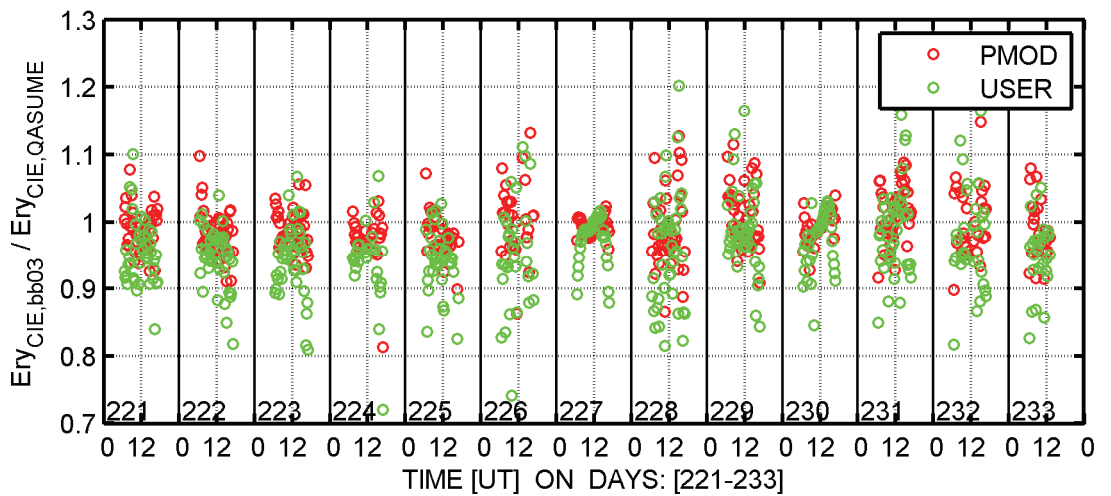


Figure 5 Erythemal weighted irradiance from Radiometer relative to QASUME spectroradiometer



YES s/n 000904 (BB04)

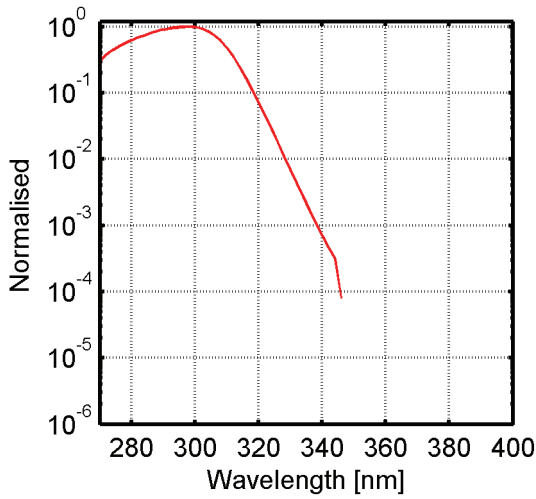


Figure 1 Relative spectral response function

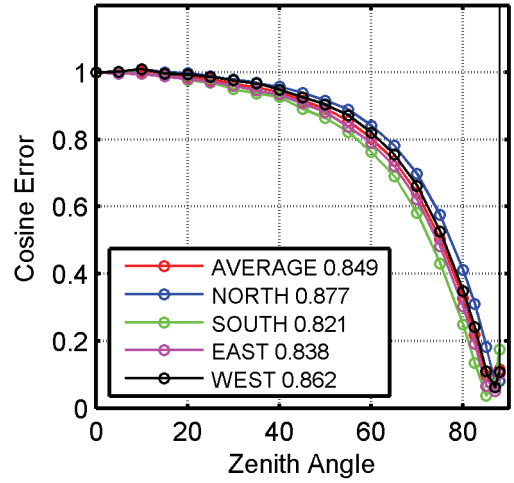


Figure 2 Cosine Error

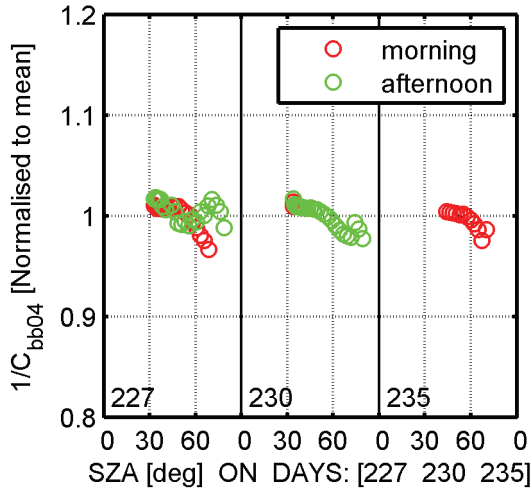


Figure 3 Calibration factor normalised to the average

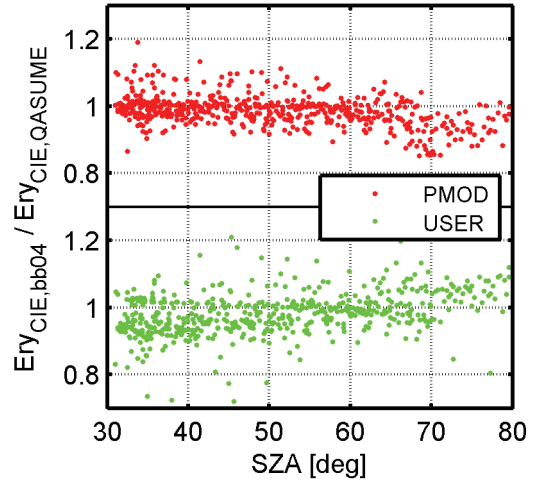


Figure 4 Erythemal weighted irradiance from Radiometer relative to QASUME

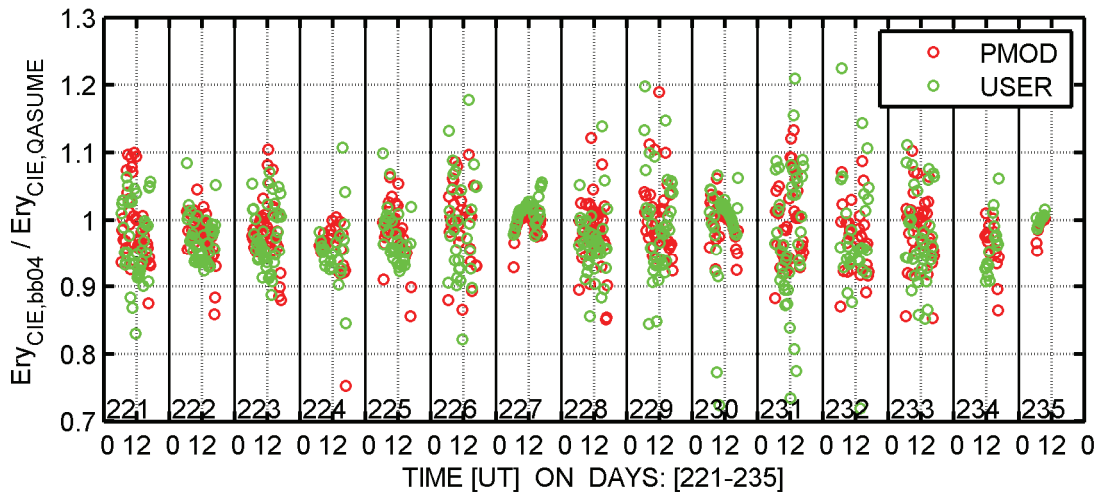


Figure 5 Erythemal weighted irradiance from Radiometer relative to QASUME spectroradiometer

## Treatment of the YES broadband radiometer (LOA)

The erythemal dose rate is obtained as follows:

The spectral response which is provided by the manufacturer is normalized to 1 and is not function of SZA, so we use our Jobin-Yvon spectroradiometer (which is calibrated every 2-3 months) to determine a more appropriate response.

For cloudless days, we estimate a “good” spectral response by comparing for each SZA the erythemal dose computed from the spectroradiometer data with the radiometer raw measurements (that means that they are not multiplied by coefficients function of SZA given by the constructor).

Regression polynomials are obtained for several ranges of total ozone columns for periods covering one year. To perform the selection we take our own ozone value retrieved from each spectrum via a differential technique.

The temperature variations observed during the COST campaign are due to a bad electric connexion of the instrument during the outdoor measurements. We had provided an electric cable that did not allow monitoring the temperature. This problem did not occur during the indoor measurements since the cable used was not the same.

YES s/n 920906 (BB05)

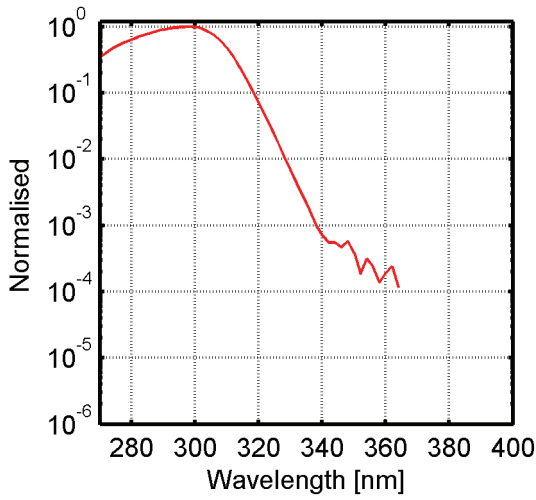


Figure 1 Relative spectral response function

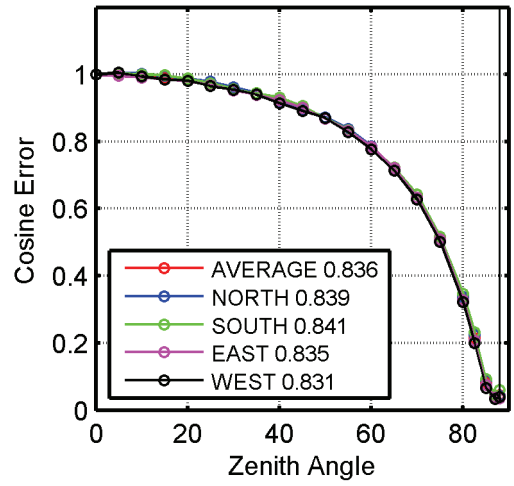


Figure 2 Cosine Error

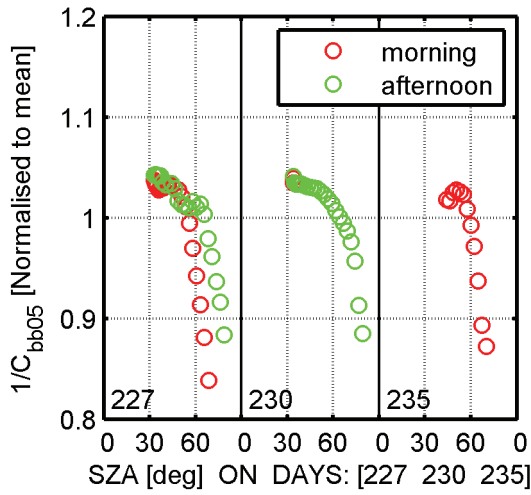


Figure 3 Calibration factor normalised to the average

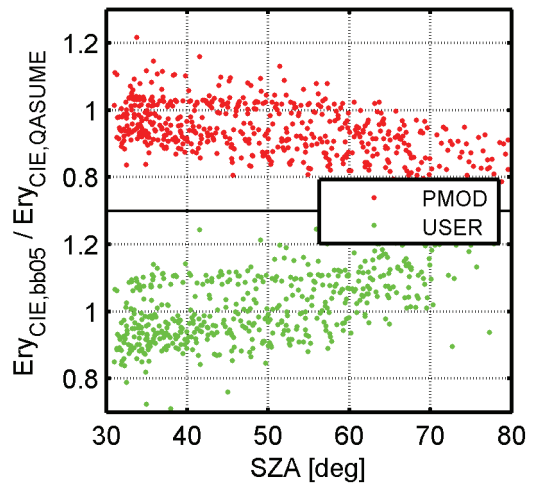


Figure 4 Erythemal weighted irradiance from Radiometer relative to QASUME

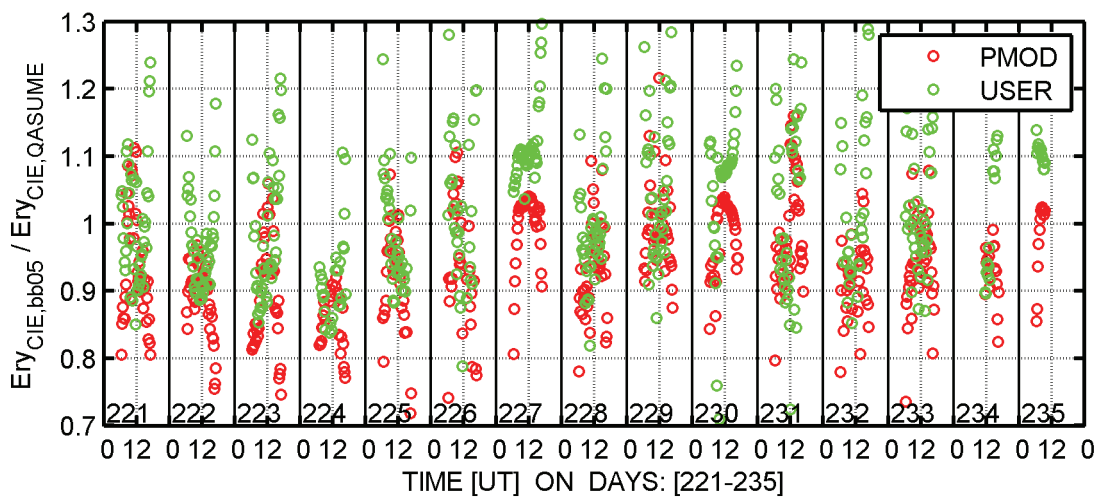


Figure 5 Erythemal weighted irradiance from Radiometer relative to QASUME spectroradiometer

## CALIBRATION HISTORY OF SL 501 #635 METER

Lasse Ylianttila  
STUK, P.O.Box 14, FI-00881 Helsinki, Finland

The SL 501 #635 meter has been in operation in STUK from 1992. The meter is used to measure UV-radiation on the top of STUK's office building in Helsinki. The measurement period is from the start of April to the end of September. The meter has been repaired twice, in 1993 after a thunderstorm and in the end of year 2000, when moisture had been condensed inside the meter. The phosphor of the meter has not been changed.

The meter is annually calibrated against STUK's spectroradiometer. Up to 1996 the reference spectroradiometer was Optronic 742 and after 1997 the reference spectroradiometer has been Bentham DM 150. At 1999 the Bentham's original D5 diffuser was changed to Schreder J1002 diffuser.

The calibration factors for #635 are presented in Figure 1. All the known systematic errors have been corrected and cosine correction on reference spectroradiometer has been used. The calibration factor is the average of the calibration measurements where the solar zenith angle (SZA) was smaller than 55°. In Helsinki this means that in the calibrations the SZA has been between 37° and 55° and the O<sub>3</sub>-column has varied between 300 DU and 400 DU. Current calibration uncertainty for SL 501 calibration is estimated to be 8.3 % (2 $\sigma$ ). With the Optronic 742 the calibration uncertainty of SL 501 meter was over 10 % (2 $\sigma$ ).

The #635 meter has participated in several intercomparisons. The calibration factors obtained from the intercomparisons are included in Figure 1. For the PMOD/WRC-COST intercomparison the calibration factor for SZA 40° and 300 DU was used.

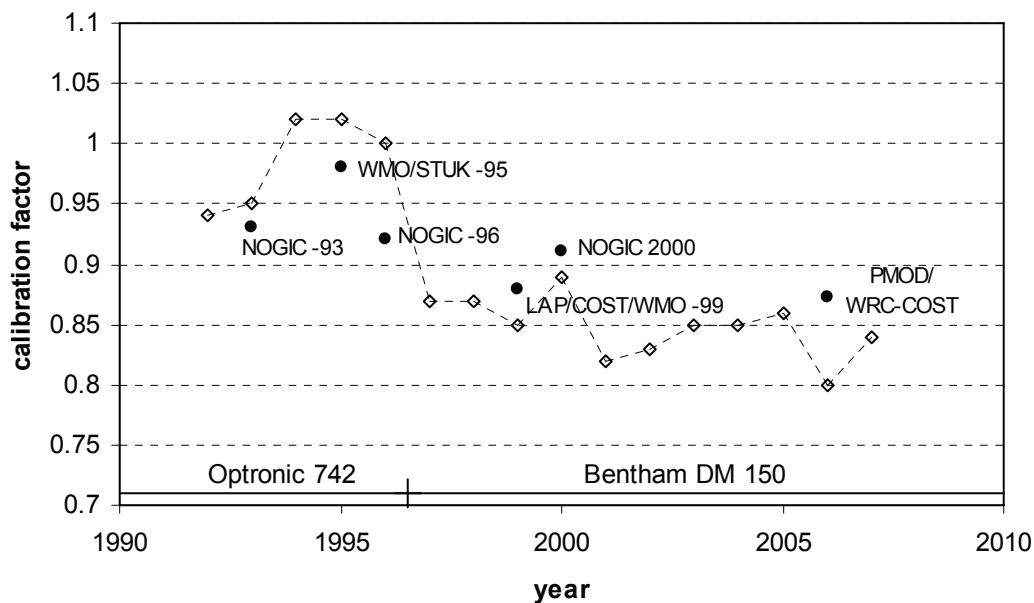


Figure 1. Calibration factors for SL 501 #635.

### Solar Light SL501 D s/n 635 (BB06)

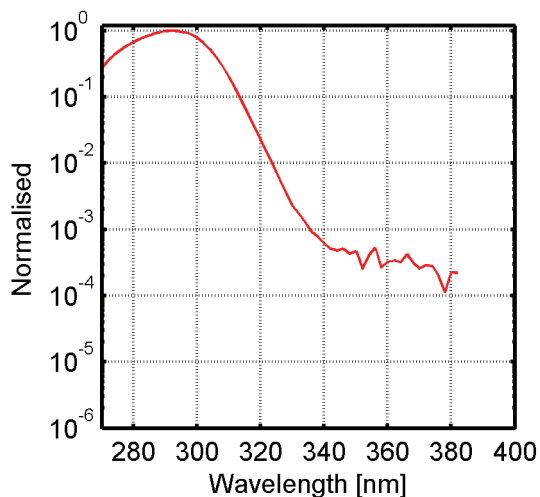


Figure 1 Relative spectral response function

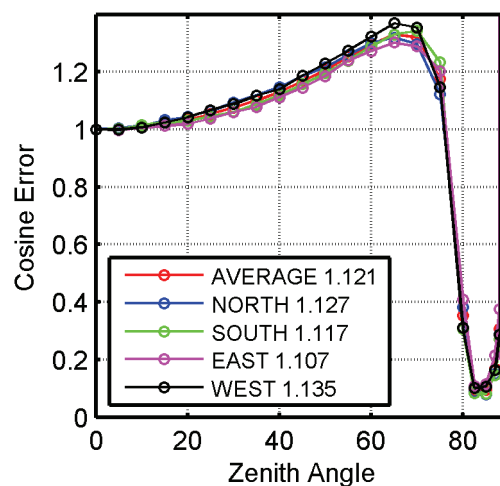


Figure 2 Cosine Error

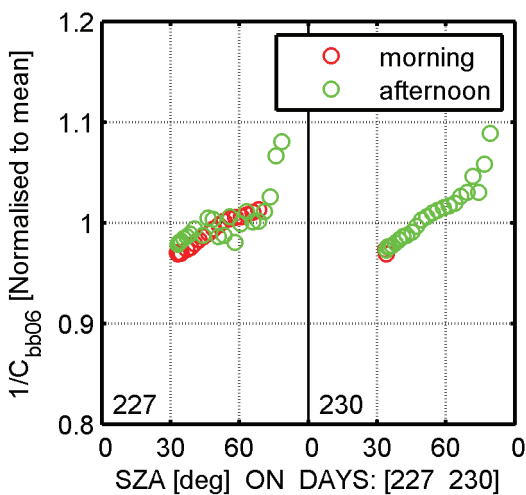


Figure 3 Calibration factor normalised to the average

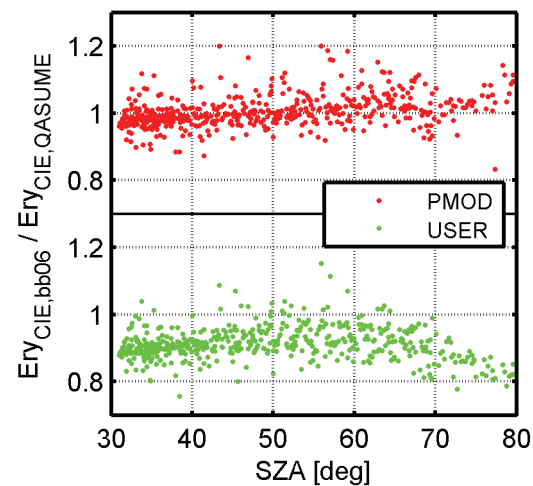


Figure 4 Erythemal weighted irradiance from Radiometer relative to QASUME

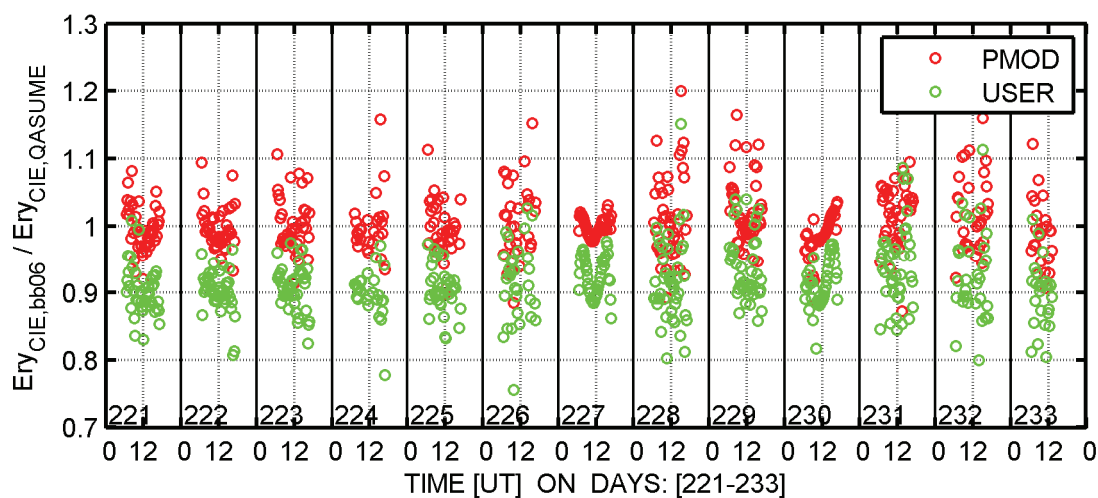


Figure 5 Erythemal weighted irradiance from Radiometer relative to QASUME spectroradiometer



Solar Light SL501 A s/n 8885 (BB07)

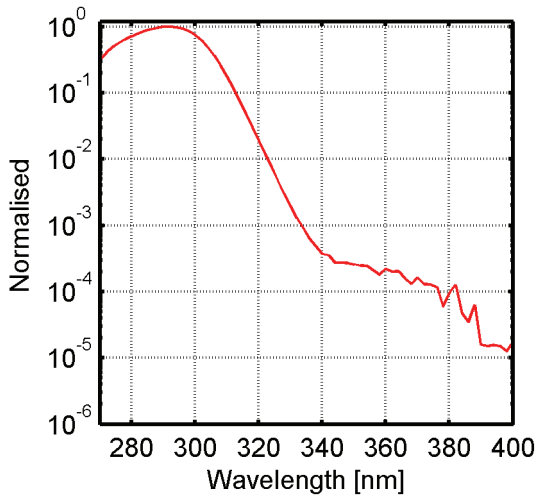


Figure 1 Relative spectral response function

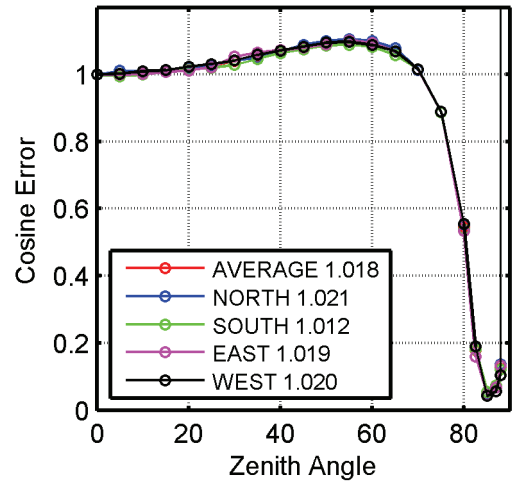


Figure 2 Cosine Error

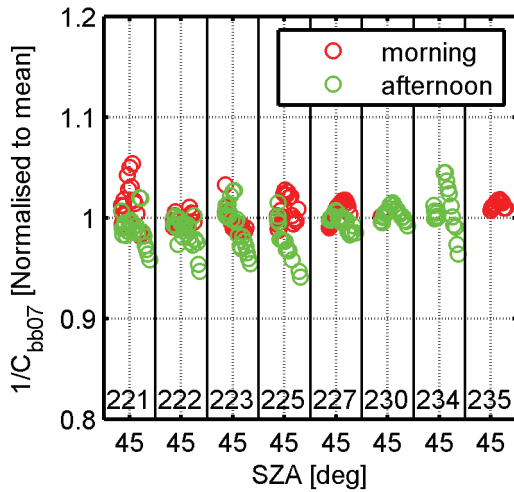


Figure 3 Calibration factor normalised to the average

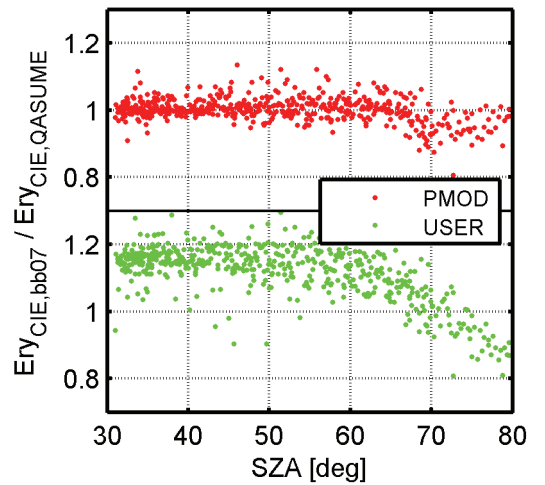


Figure 4 Erythemal weighted irradiance from Radiometer relative to QASUME

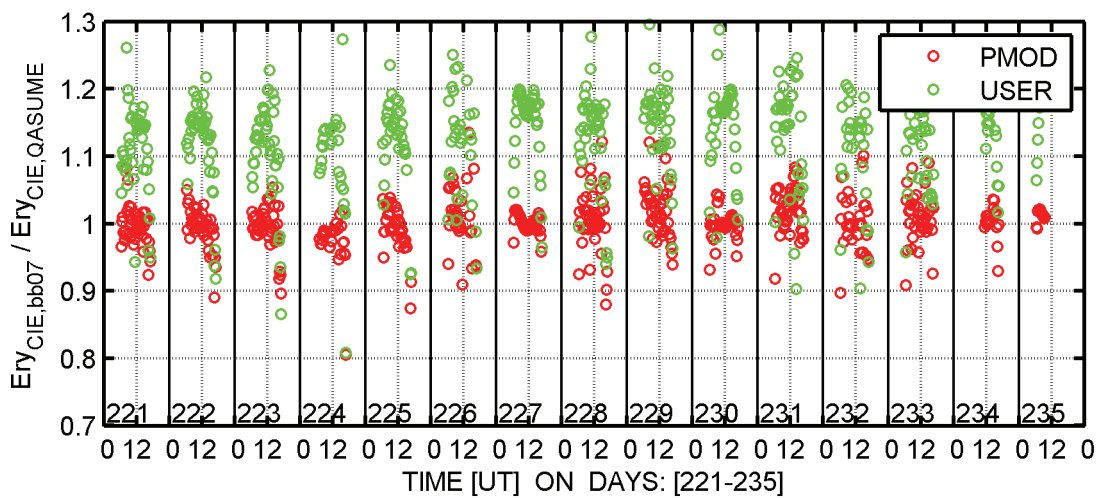


Figure 5 Erythemal weighted irradiance from Radiometer relative to QASUME spectroradiometer



Solar Light SL501 A s/n 8891 (BB08)

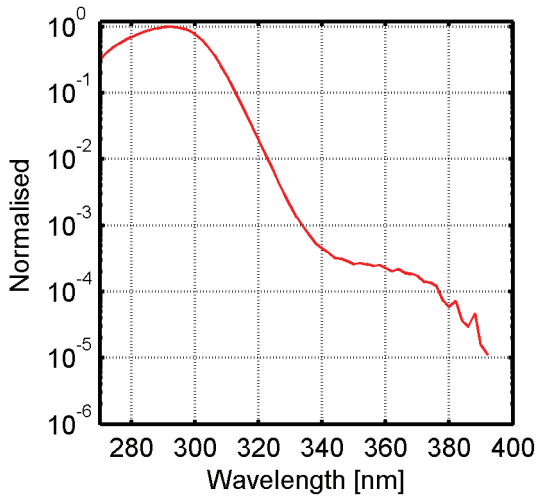


Figure 1 Relative spectral response function

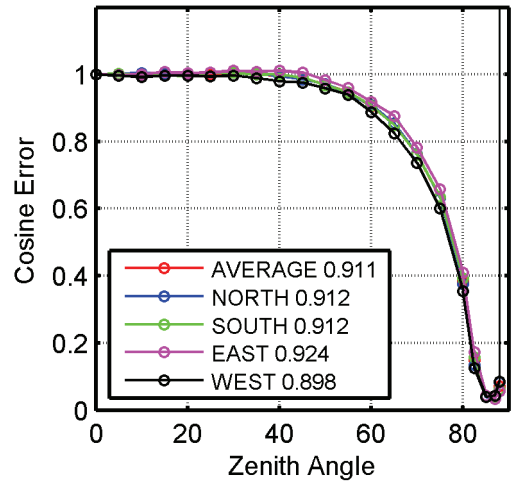


Figure 2 Cosine Error

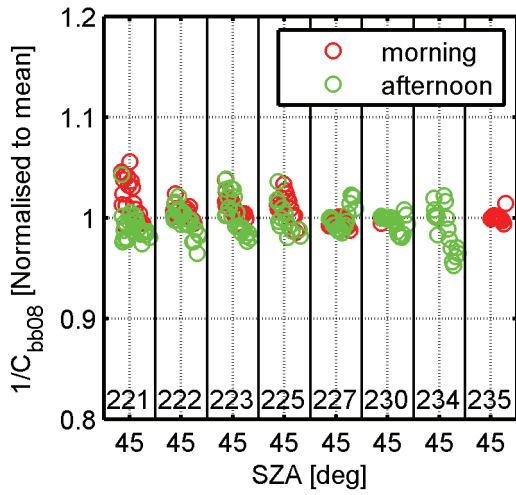


Figure 3 Calibration factor normalised to the average

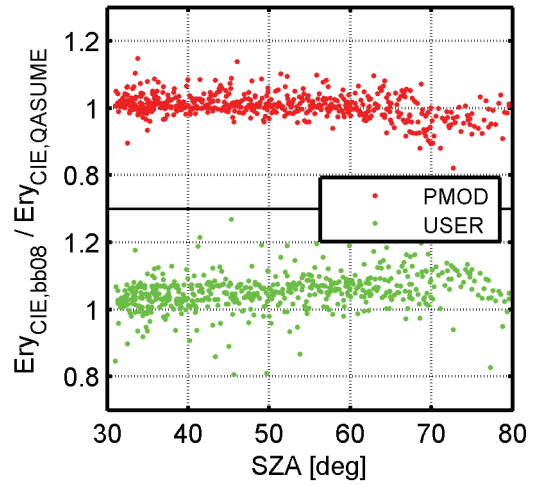


Figure 4 Erythemal weighted irradiance from Radiometer relative to QASUME

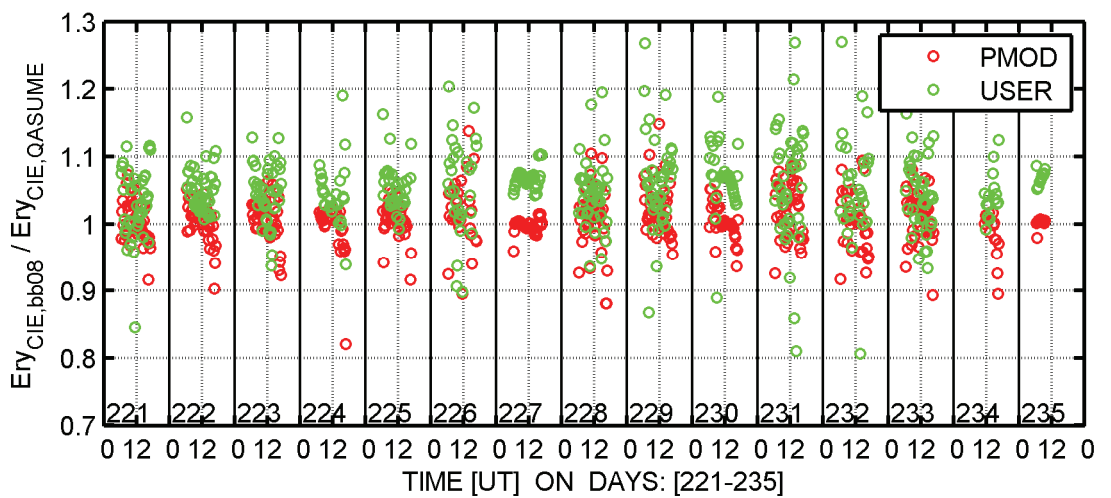


Figure 5 Erythemal weighted irradiance from Radiometer relative to QASUME spectroradiometer



Solar Light SL501 A s/n 1903 (BB09)

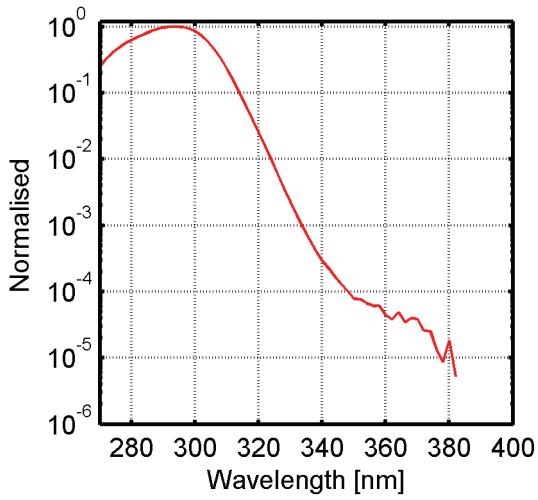


Figure 1 Relative spectral response function

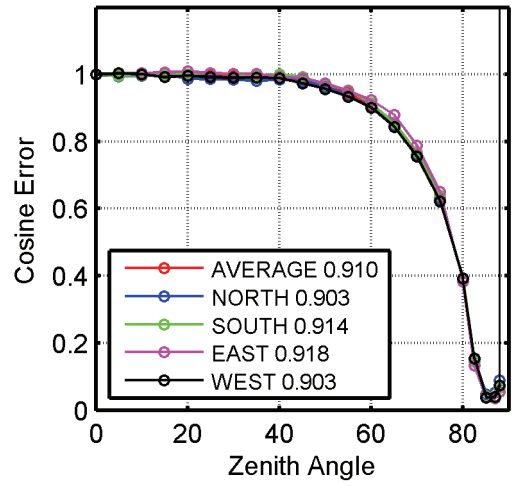


Figure 2 Cosine Error

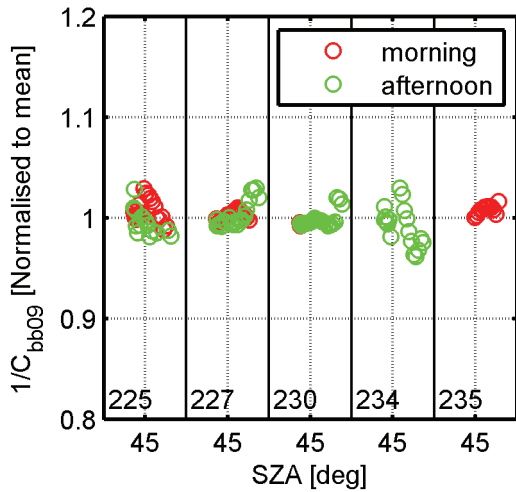


Figure 3 Calibration factor normalised to the average

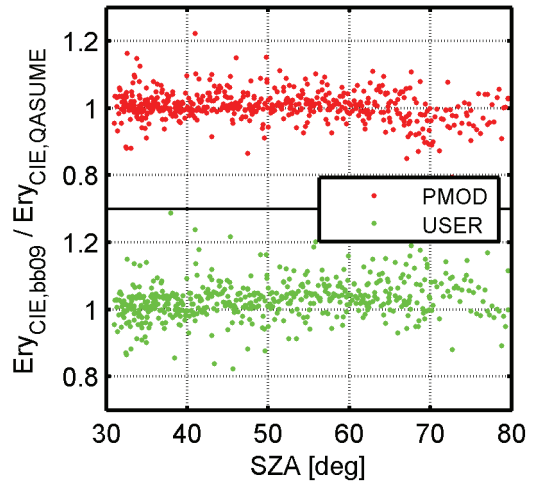


Figure 4 Erythemal weighted irradiance from Radiometer relative to QASUME

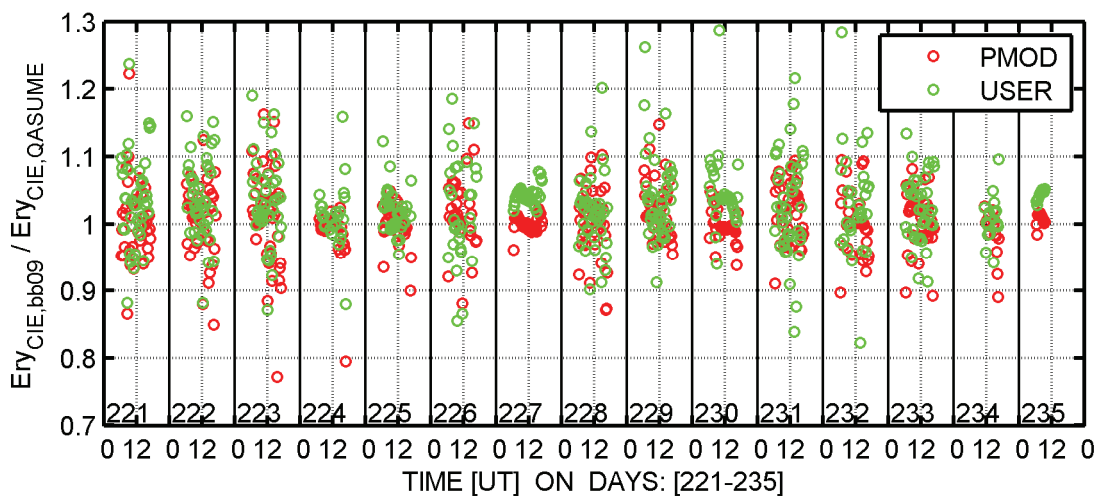


Figure 5 Erythemal weighted irradiance from Radiometer relative to QASUME spectroradiometer



Solar Light SL501 A s/n 1904 (BB10)

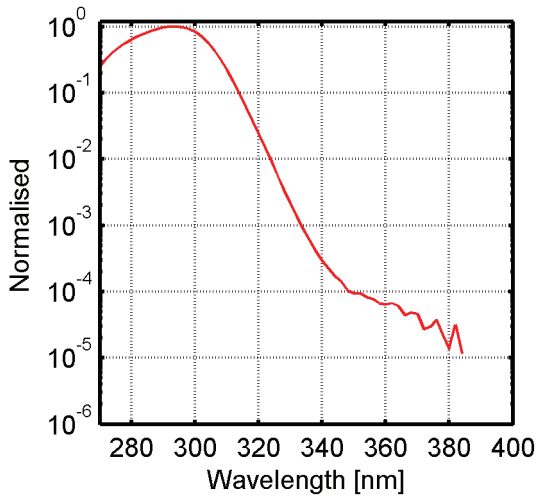


Figure 1 Relative spectral response function

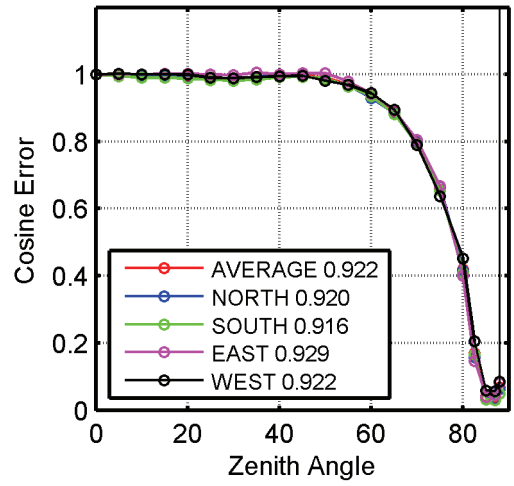


Figure 2 Cosine Error

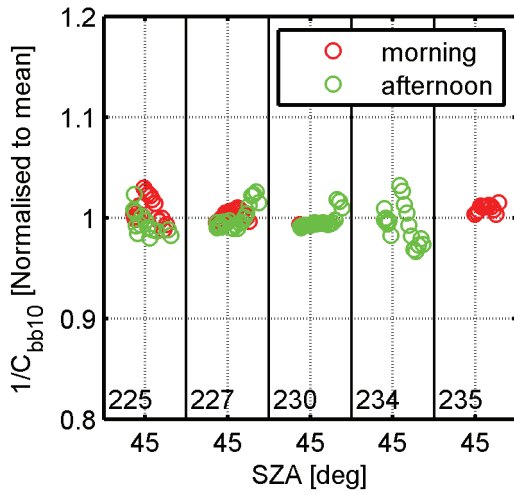


Figure 3 Calibration factor normalised to the average

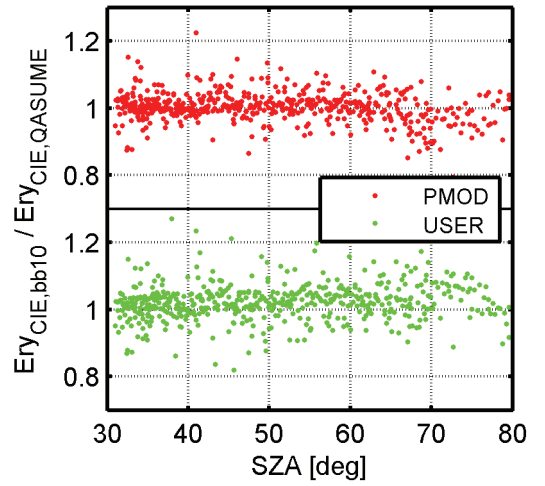


Figure 4 Erythemal weighted irradiance from Radiometer relative to QASUME

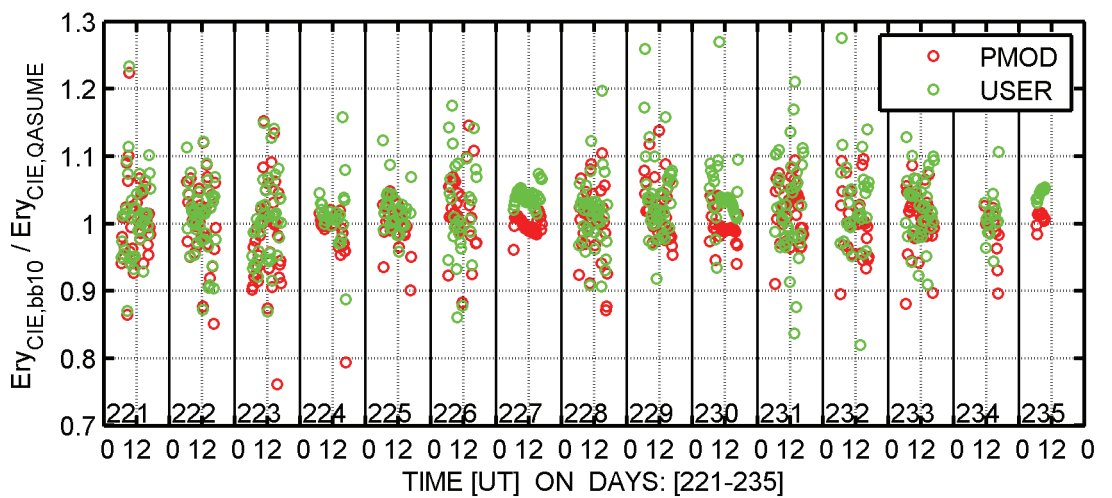


Figure 5 Erythemal weighted irradiance from Radiometer relative to QASUME spectroradiometer



Solar Light SL501 A s/n 5790 (BB11)

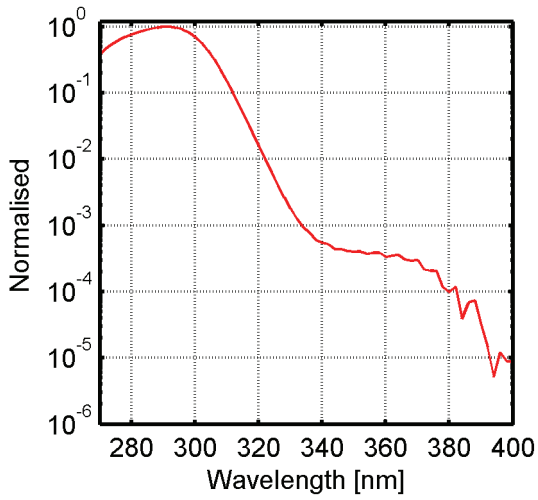


Figure 1 Relative spectral response function

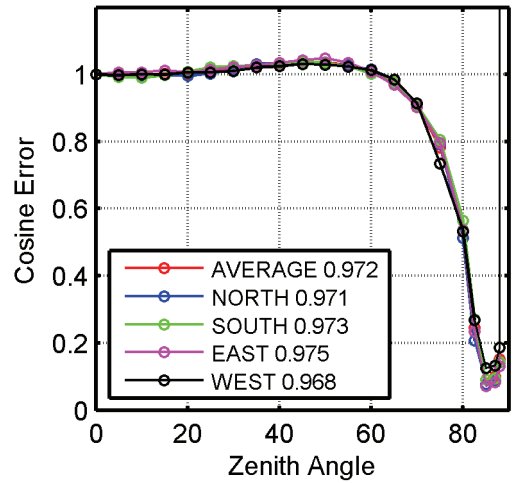


Figure 2 Cosine Error

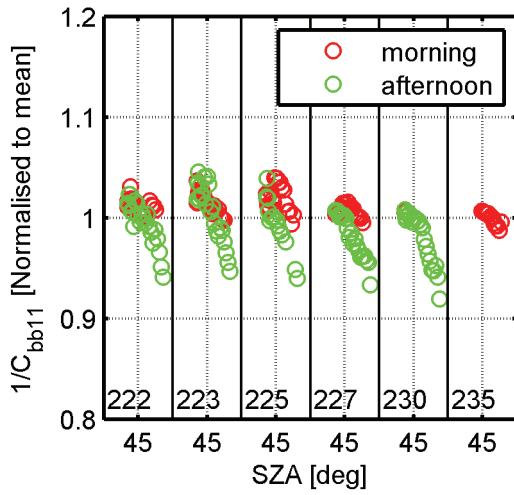


Figure 3 Calibration factor normalised to the average

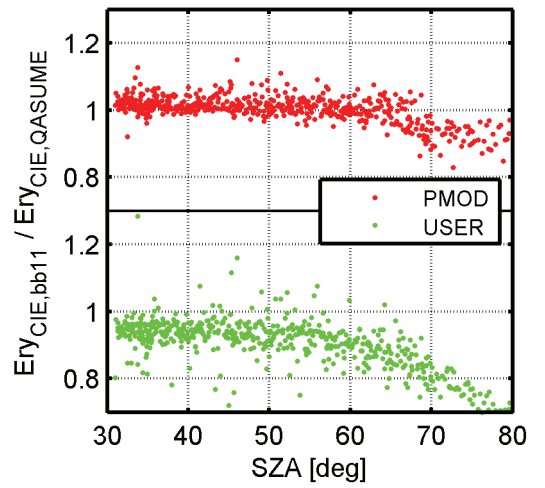


Figure 4 Erythemal weighted irradiance from Radiometer relative to QASUME

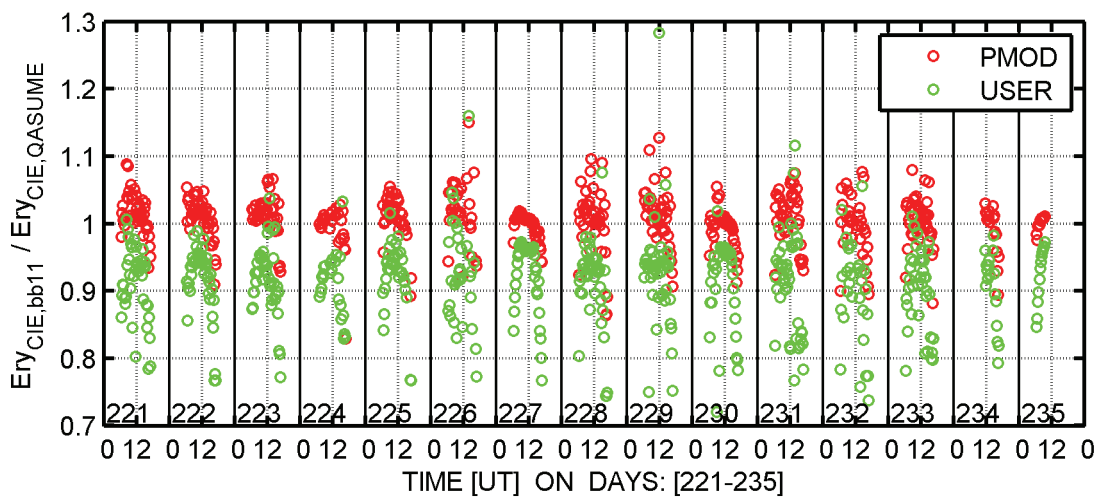


Figure 5 Erythemal weighted irradiance from Radiometer relative to QASUME spectroradiometer



### Solar Light SL501 D s/n 1450 (BB12)

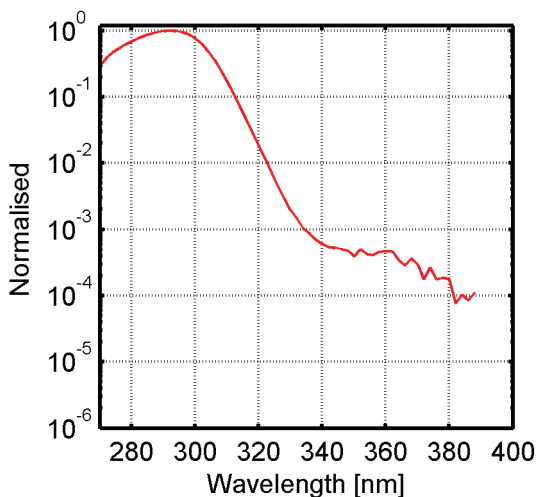


Figure 1 Relative spectral response function

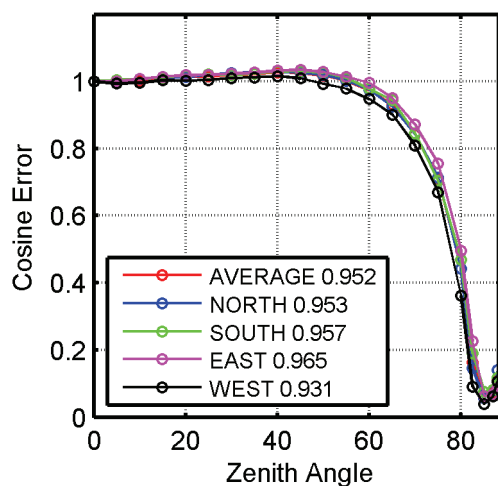


Figure 2 Cosine Error

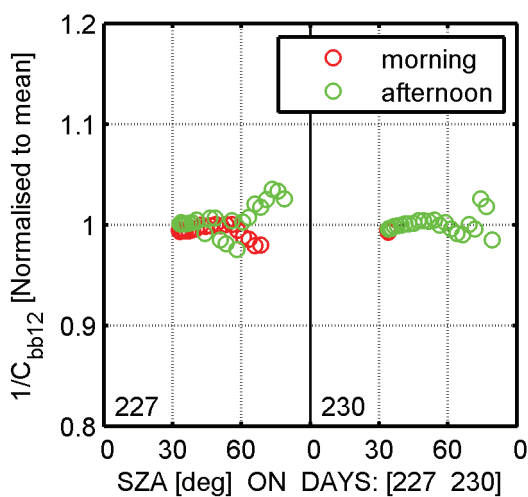


Figure 3 Calibration factor normalised to the average

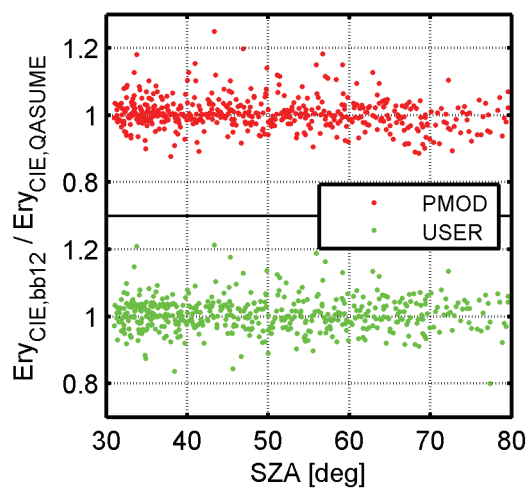


Figure 4 Erythemal weighted irradiance from Radiometer relative to QASUME

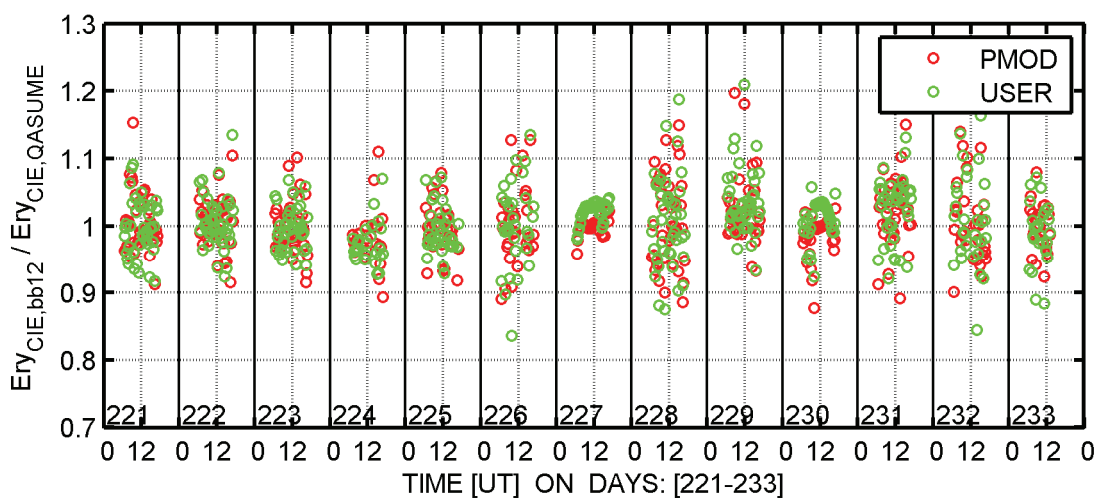


Figure 5 Erythemal weighted irradiance from Radiometer relative to QASUME spectroradiometer



Kipp & Zonen s/n 020614 (BB13)

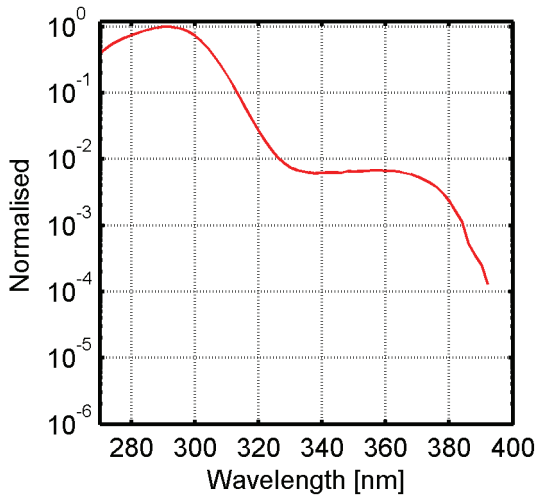


Figure 1 Relative spectral response function

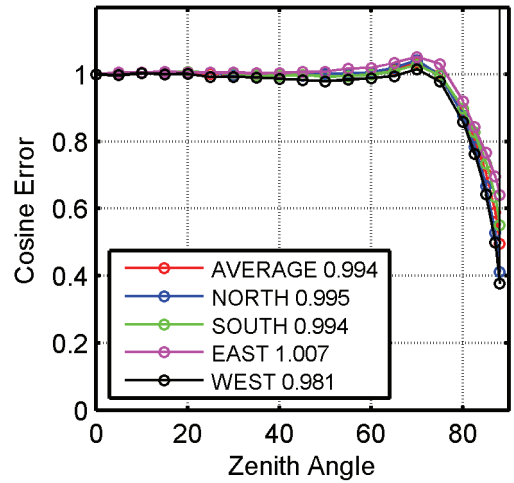


Figure 2 Cosine Error

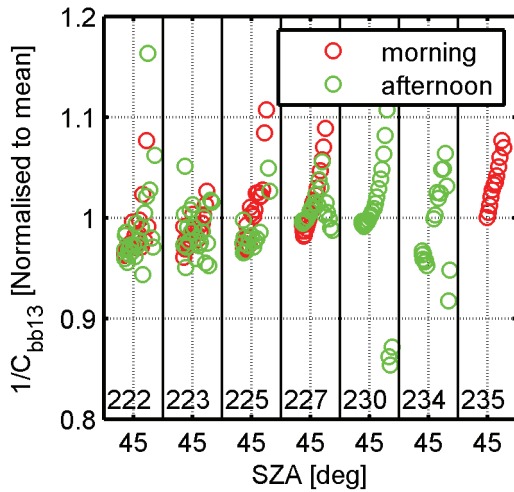


Figure 3 Calibration factor normalised to the average

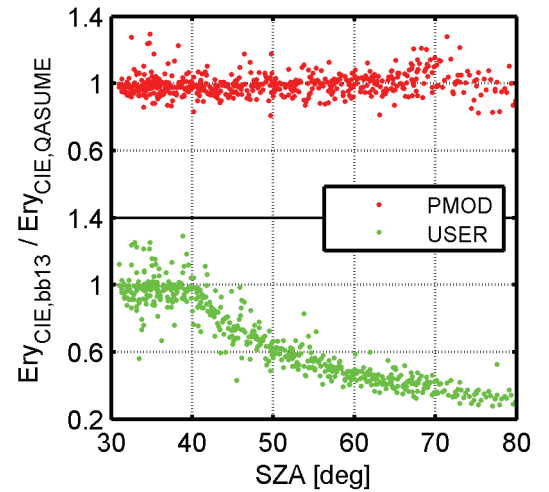


Figure 4 Erythemal weighted irradiance from Radiometer relative to QASUME

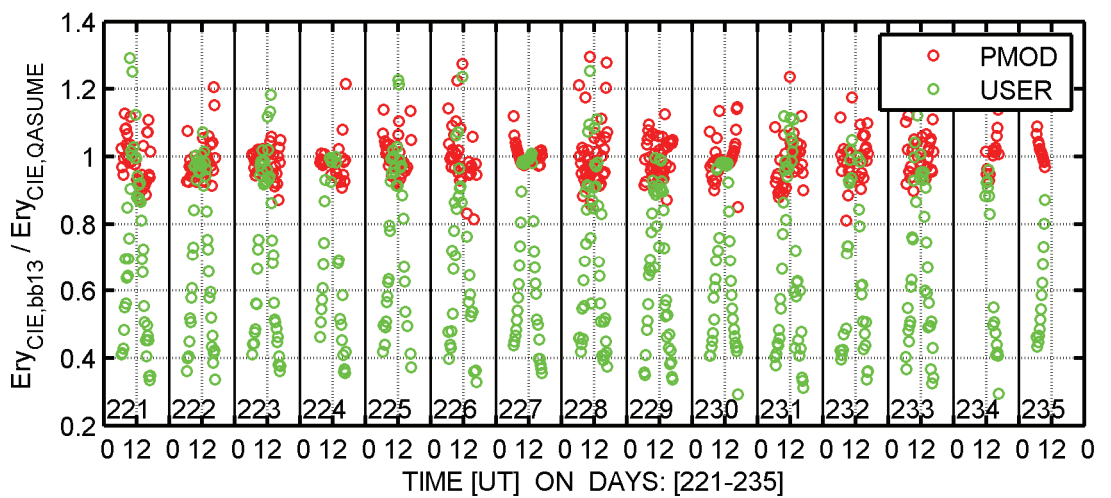


Figure 5 Erythemal weighted irradiance from Radiometer relative to QASUME spectroradiometer



Eldonet XP (BB14)

(not measured)

(not measured)

Figure 1 Relative spectral response function

Figure 2 Cosine Error

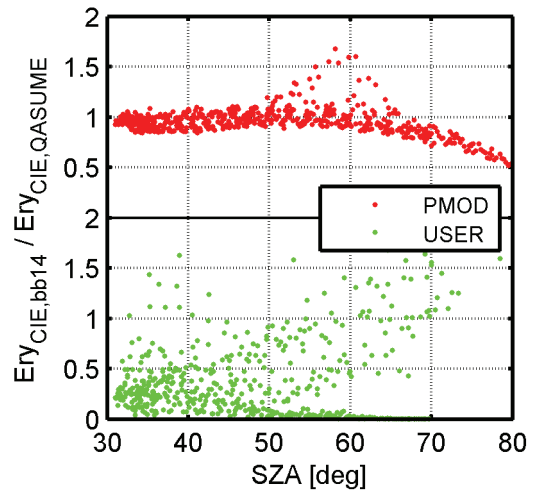
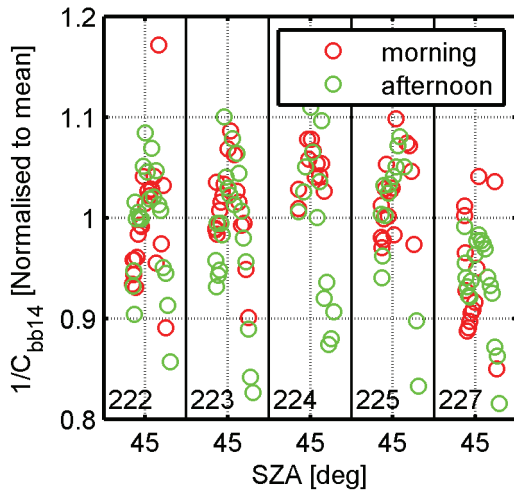


Figure 3 Calibration factor normalised to the average

Figure 4 Erythemal weighted irradiance from Radiometer relative to QASUME

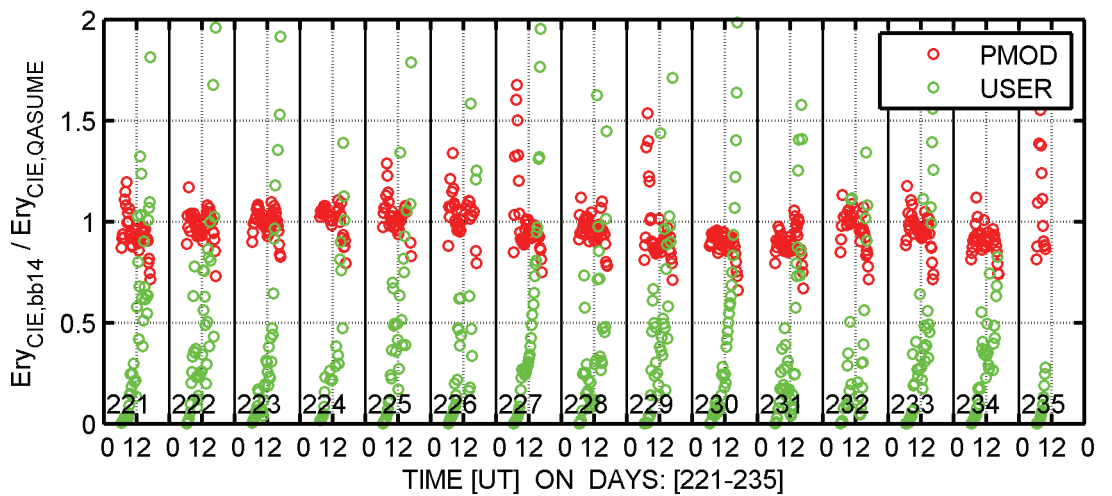


Figure 5 Erythemal weighted irradiance from Radiometer relative to QASUME spectroradiometer

BB15 radiometer - a YES UVB-1 Pyranometer – belongs to the regional UV network of ARPA Valle d'Aosta (the Environment Protection Agency of Aosta Valley, North of Italy). The network includes three broadband radiometers (1 YES and 2 Kipp&Zonen), a Bentham double monochromator spectroradiometer and a Brewer photometer. The BB radiometers are located at three different altitudes: 570 m (in the valley), 1640 m (mountain site) and 3500 m asl (top of the domain, glacier), allowing a measurement of the altitude effect. All the instruments are regularly calibrated, intercompared one with each other and with a RTM (libRadtran).

The BB15 instrument was sold together with a tabulation of conversion factors dependent on the solar zenith angle (no ozone dependence). It was therefore decided to use a more accurate matrix obtained from Schreder CMS. This matrix is defined as the product of the calibration coefficient  $C$ , the conversion function  $f_n$  and the cosine correction  $C_{\text{coscor}}$ , hence these three factors can't be treated separately (only  $f_{\text{glo}}$  is considered in the calculation of the matrix and the horizon obstruction is not taken into account). We routinely obtain the conversion factor from a double spline interpolation of the matrix, using the ozone measurements and the calculation of the solar zenith angle. The total ozone content, measured in the valley, is scaled depending on the altitude of the considered instrument.

The COST726 intercomparison was very helpful to know the potentiality and the limits of our reference BB instrument. A first remark is that the radiometer cosine response deviates very much from the ideal one, a common defect of the radiometers similar to ours. This triggers high deviations in the cloudy cases. Despite of this, we are very pleased with the results of the comparison: the systematic deviation from PMOD/WRC UV index estimate and the user's one is very low (few percents) compared to the variance introduced by the clouds and the wrong cosine response (up to  $\pm 10\%$ ).

COST726 Action suggested us some improvements in our processing procedure that are planned for the near future. First, we would like to consider the horizon obstruction in the calibration matrix (it is already taken into account in the forecasts of UVI, but not in the matrix). This is a quite interesting factor in a mountain region like ours. Second, we intend to distinguish two cases: clear sky (using  $f_{\text{glo}}$ ) and diffuse sky (using  $f_{\text{dif}}$ ).

The results of COST726 are very interesting and challenging. Once again, it came out that UV instrumentation needs attention and care, even if it looks very simple to use (as in the case of broadband radiometers). A reference method for the broadband calibration was established and the results highlight the need of homogenising UV measurements in Europe.

YES s/n 030528 (BB15)

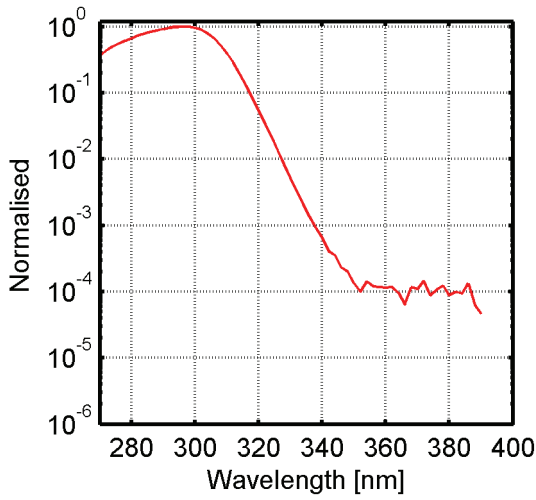


Figure 1 Relative spectral response function

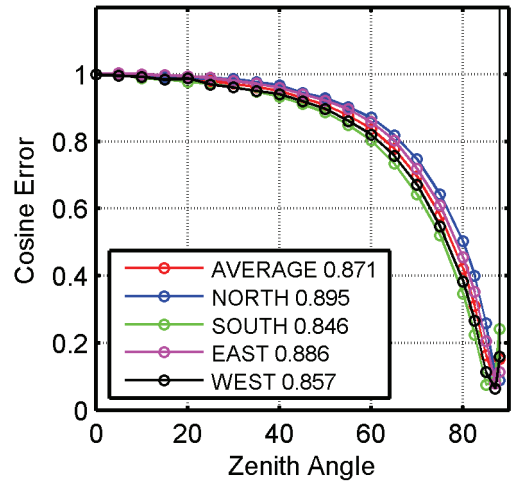


Figure 2 Cosine Error

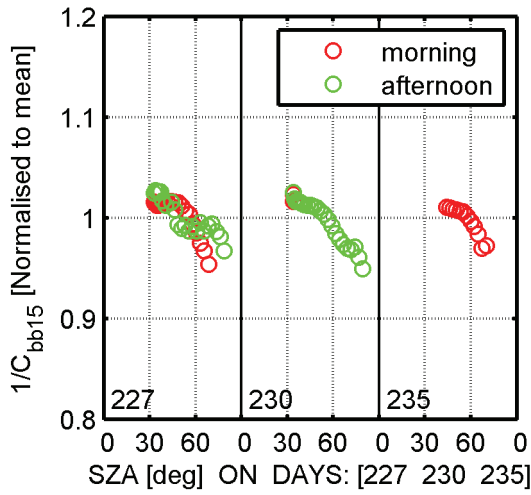


Figure 3 Calibration factor normalised to the average

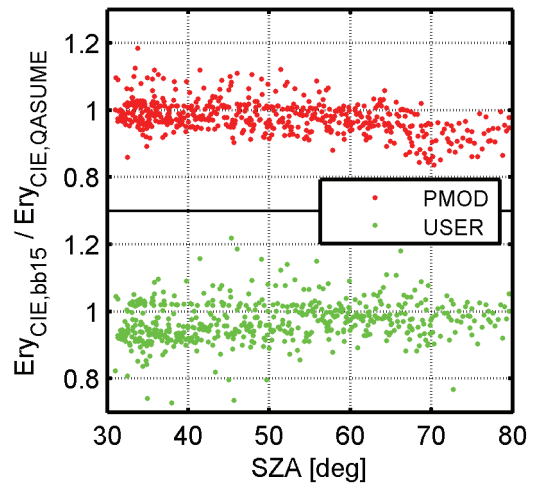


Figure 4 Erythemal weighted irradiance from Radiometer relative to QASUME

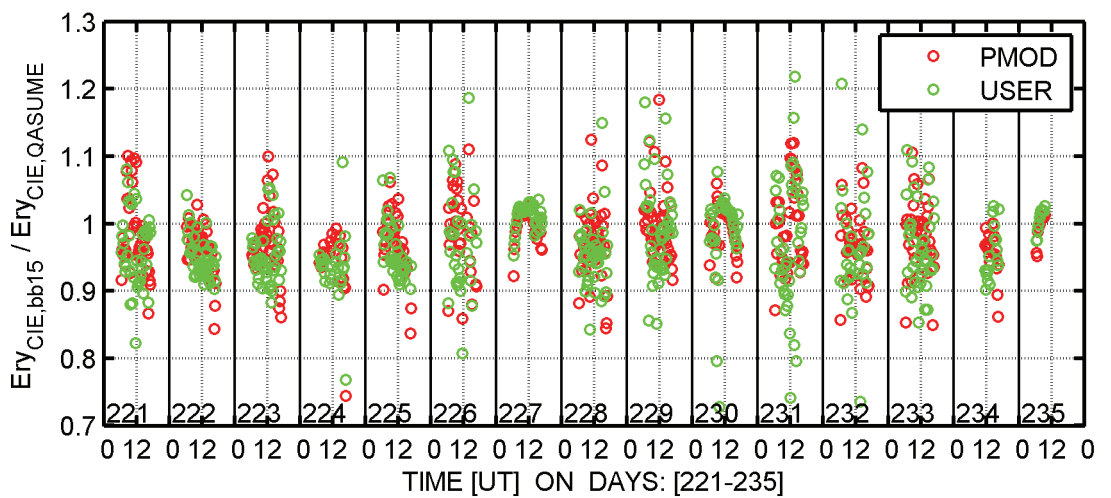


Figure 5 Erythemal weighted irradiance from Radiometer relative to QASUME spectroradiometer



Sintec s/n 010-A-00360 (BB16)

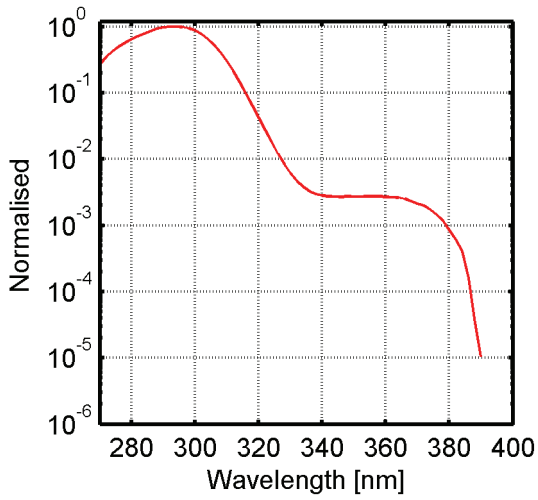


Figure 1 Relative spectral response function

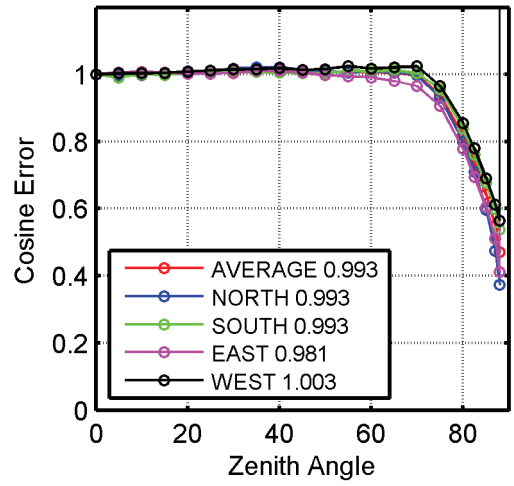


Figure 2 Cosine Error

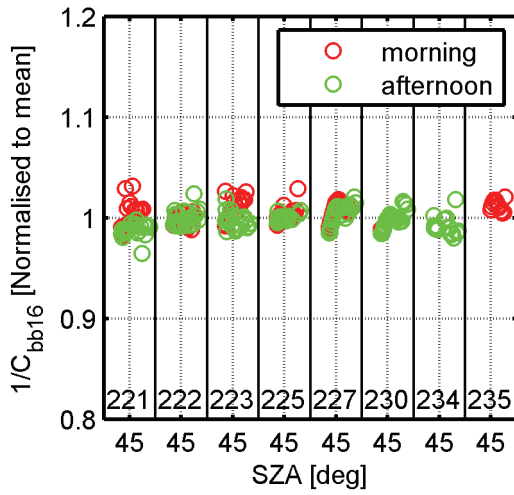


Figure 3 Calibration factor normalised to the average

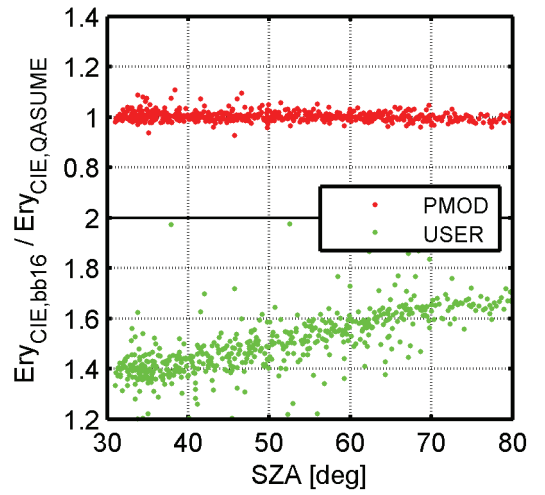


Figure 4 Erythemal weighted irradiance from Radiometer relative to QASUME

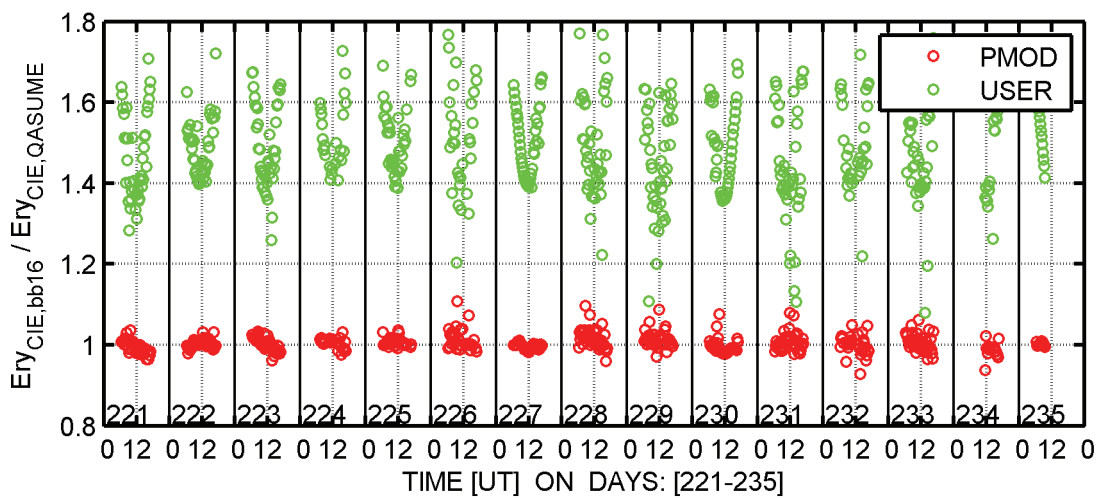


Figure 5 Erythemal weighted irradiance from Radiometer relative to QASUME spectroradiometer



Solar Light SL501 A s/n 1492 (BB17)

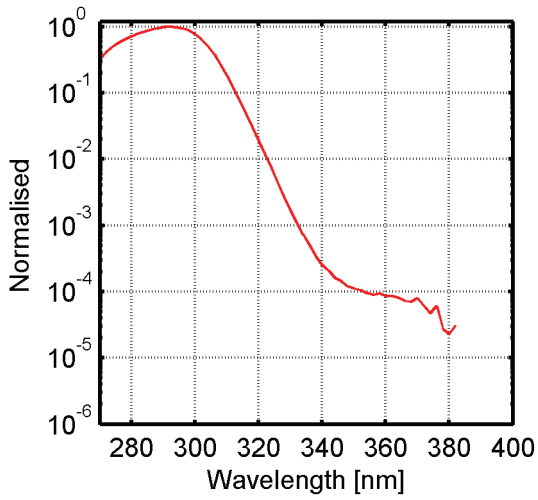


Figure 1 Relative spectral response function

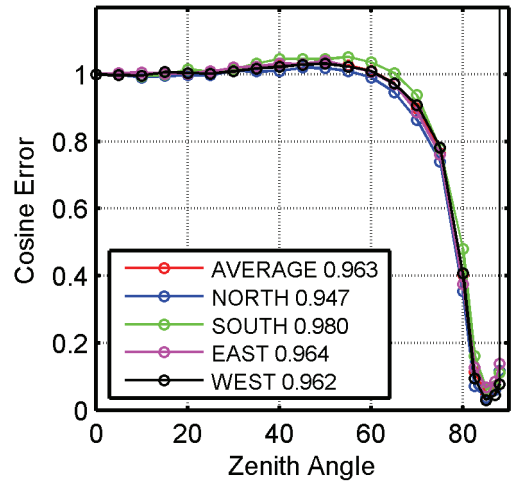


Figure 2 Cosine Error

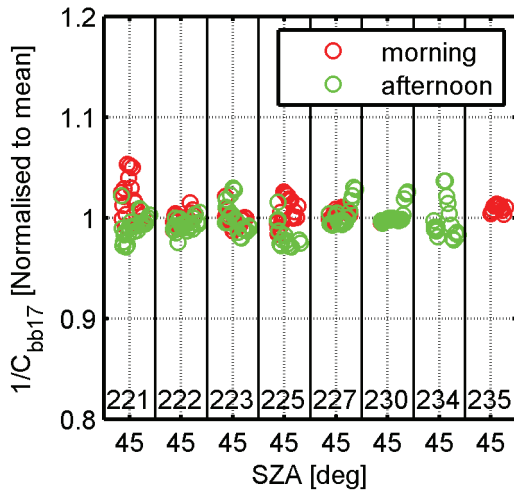


Figure 3 Calibration factor normalised to the average

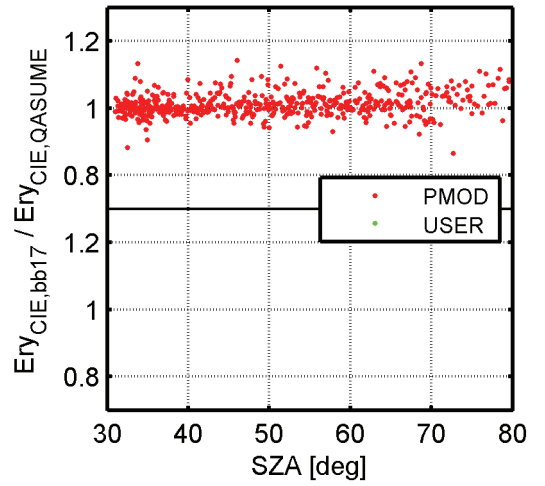


Figure 4 Erythemal weighted irradiance from Radiometer relative to QASUME

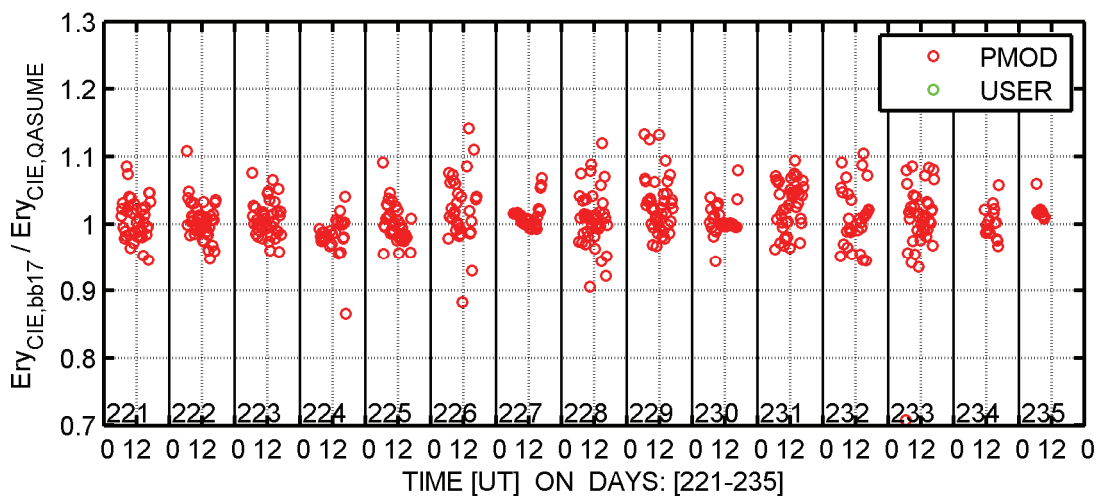


Figure 5 Erythemal weighted irradiance from Radiometer relative to QASUME spectroradiometer



Solar Light SL501 A s/n 1493 (BB18)

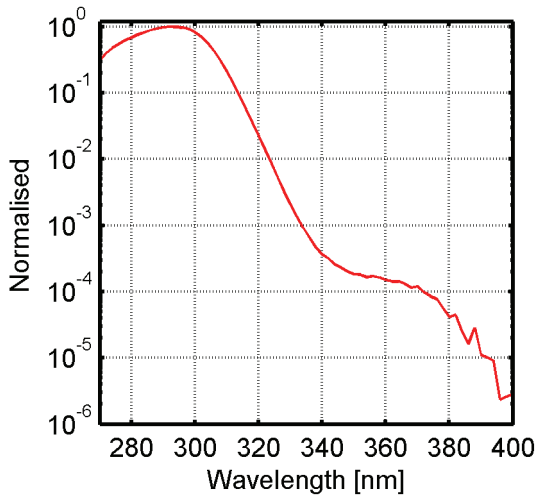


Figure 1 Relative spectral response function

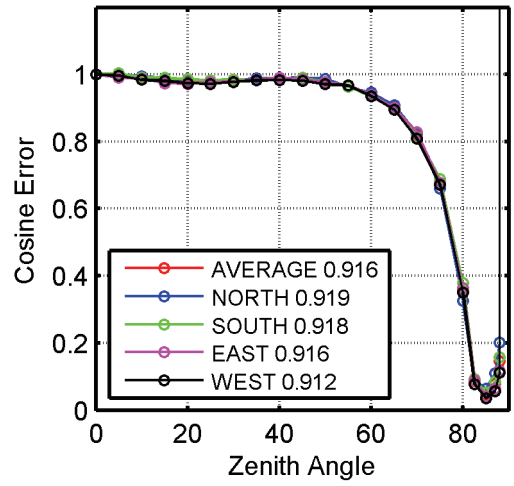


Figure 2 Cosine Error

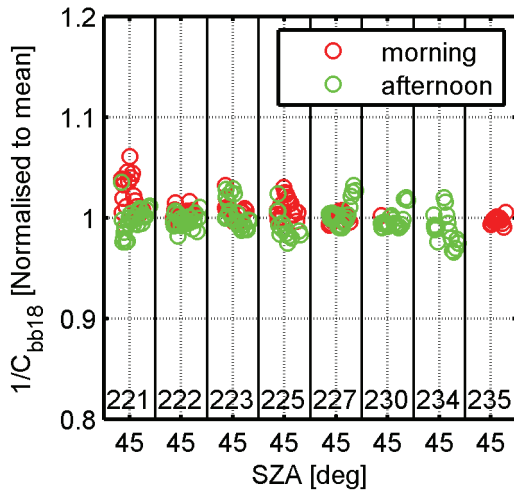


Figure 3 Calibration factor normalised to the average

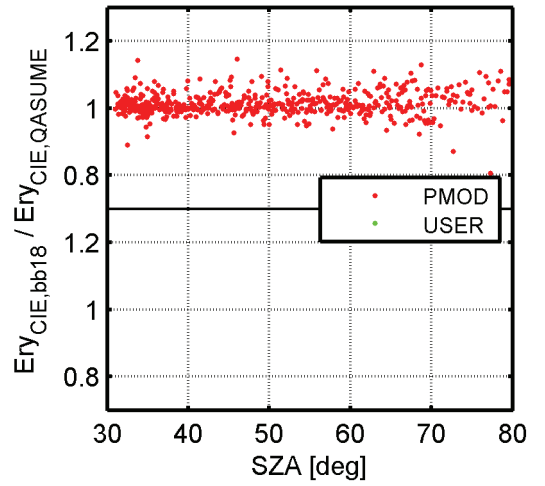


Figure 4 Erythemal weighted irradiance from Radiometer relative to QASUME

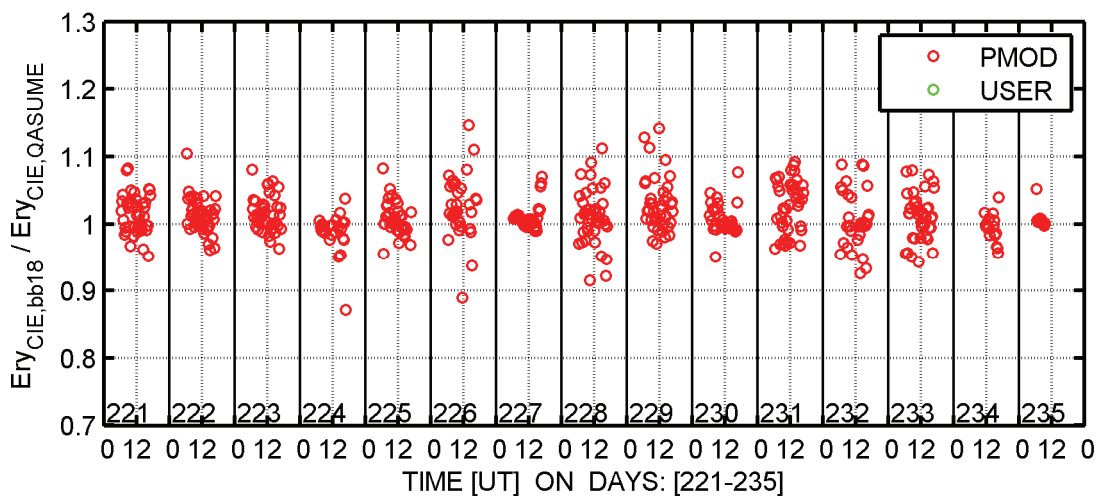


Figure 5 Erythemal weighted irradiance from Radiometer relative to QASUME spectroradiometer



Solar Light SL501 D s/n 0935 (BB19)

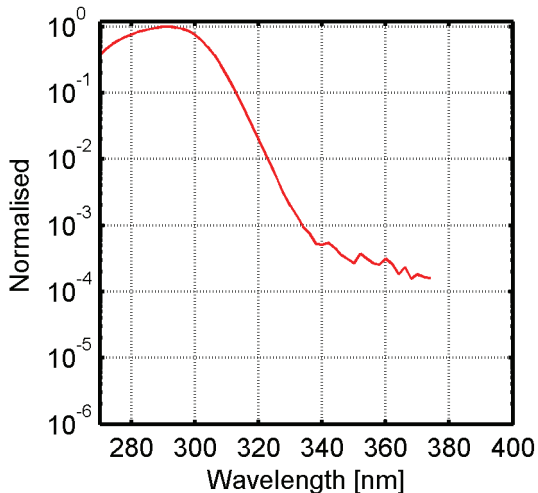


Figure 1 Relative spectral response function

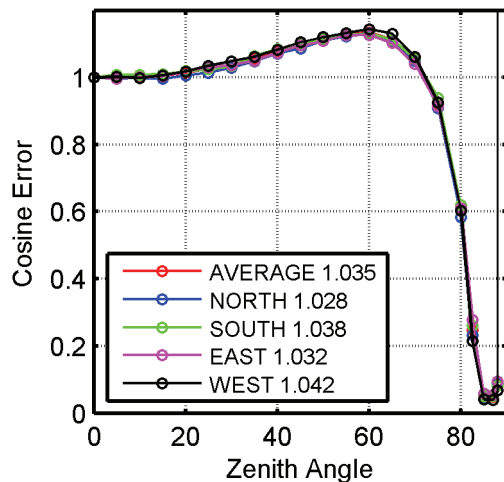


Figure 2 Cosine Error

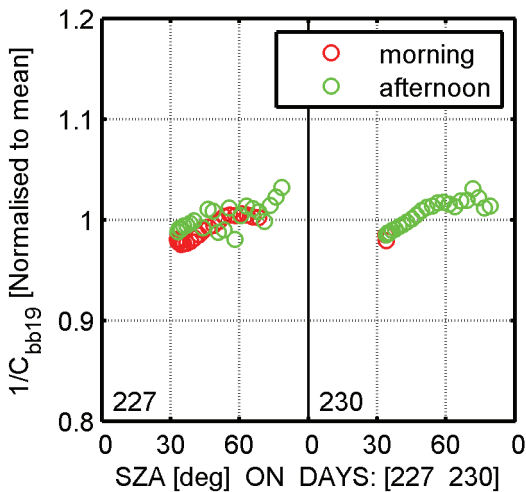


Figure 3 Calibration factor normalised to the average

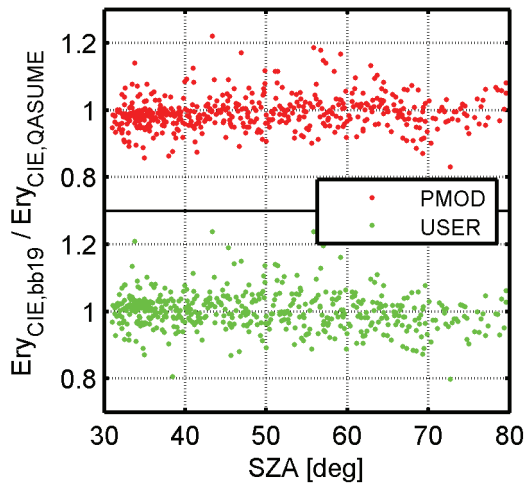


Figure 4 Erythemal weighted irradiance from Radiometer relative to QASUME

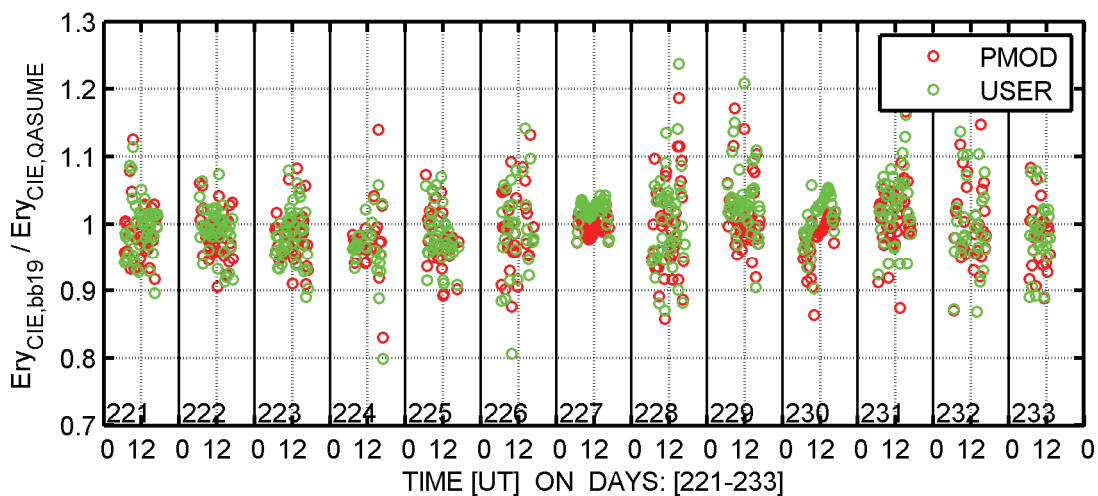


Figure 5 Erythemal weighted irradiance from Radiometer relative to QASUME spectroradiometer

Evaluation of the COST726 calibration of Solar Light 501A broadband radiometer at  
MeteoGalicia UV monitoring site

A. Pettazzi, J. A. Souto  
Department of Chemical Engineering  
University of Santiago de Compostela  
c/ Lope Gómez de Marzoa, s/n - Campus Sur, 15782 Santiago de Compostela  
e-mail: [mrtepax@usc.es](mailto:mrtepax@usc.es), [jasouto@usc.es](mailto:jasouto@usc.es)

After the COST 726 calibration campaign, the calibrated instrument broadband radiometer Solar Light 501A (namely SL-1) has been installed in the Shared Joint Atmospheric Observation Site of MeteoGalicia (namely EOAS) at Santiago de Compostela (NW Spain; 42.87° N, 8.57° E, 250 m a.s.l.), that belongs to the Galician UV Monitoring Network.

UV indexes (UVI) were operationally calculated using the calibration provided by the World Radiation Centre of Davos, from radiation measurements on ten-minute averages. Values of the calibration matrix  $f_n(\theta, TO_3)$  were calculated by means of a specific FORTRAN code. For this evaluation, cosine correction,  $Coscor(\theta)$ , was initially set to 1 and, after that, it was corrected depending on the sky conditions.

Another Solar Light 501A radiometer (namely, SL-2, with factory calibration) is already installed at the EOAS, providing operational measurements of UVI.

Fig. 1 shows time series of UV Index recorded by the SL-1 (black dots) and by the SL-2 (white squares). Comparison covers the period from 15<sup>th</sup> to 21<sup>st</sup> of May, 2007. It can be noticed the a good agreement between the two radiometers, except for a few of measurements on 16<sup>th</sup>, 17<sup>th</sup> and 18<sup>th</sup> of May that can be neglected as they appeared during occasional maintenance service at EOAS site.

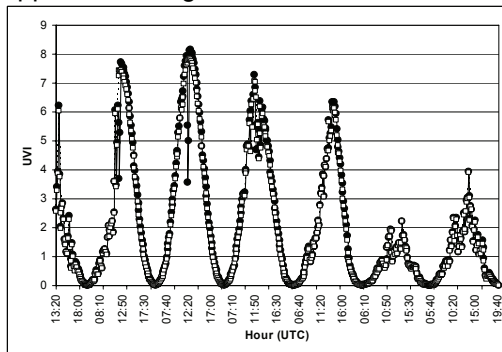


Fig.1: diurnal evolution of UV Indexes recorded by the SL 501 A radiometer calibrated in the COST 726 campaign (SL-1, black dots) and by the SL 501 A radiometer with factory calibration (SL-2, white squares).

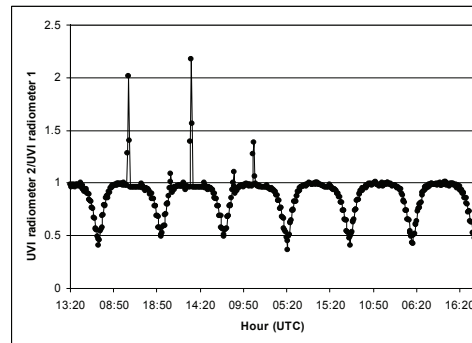


Fig. 2: diurnal evolution of the ratio of the UVI (SL-2 UVI/SL-1 UVI) recorded by both instruments.

Fig. 2 shows the evolution of the ratio between UVI recorded by both instruments. Apart from the spikes caused by the maintenance service above mentioned, the main differences appear with the highest values of solar zenith angle, SZA; this can be explained as factory calibration does not take into account the cosine correction, so that the highest values of the calibration matrix  $f_n(\theta, TO_3)$  and the cosine correction function  $Coscor(\theta)$  are associated to the highest values of SZA.

The broadband radiometer SL-1 calibrated in the COST 726 campaign will be installed in other sites of the Galician UV Monitoring Network in order to compare with measurements from other operational UV radiometers and to guarantee their reliability and data quality.

#### Acknowledgments

The helpful collaboration of S. Salsón and M. Rúa (MeteoGalicia) in the installation and management of Solar Light radiometers is acknowledged.

Solar Light SL501 A s/n 5782 (BB20)

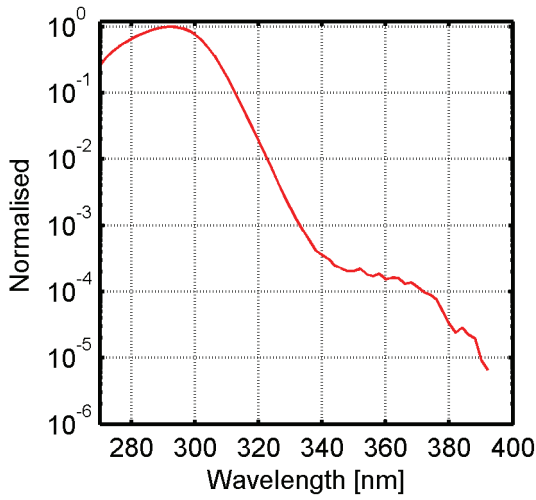


Figure 1 Relative spectral response function

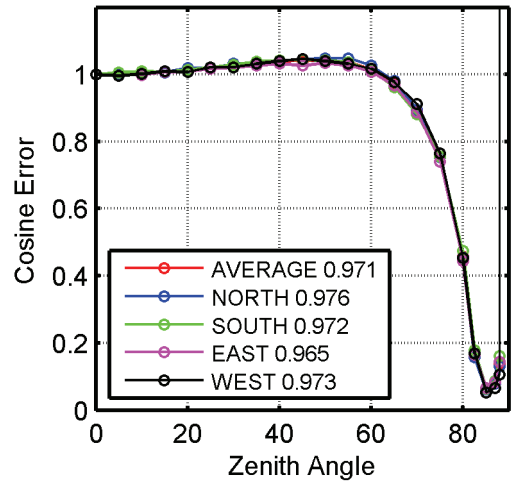


Figure 2 Cosine Error

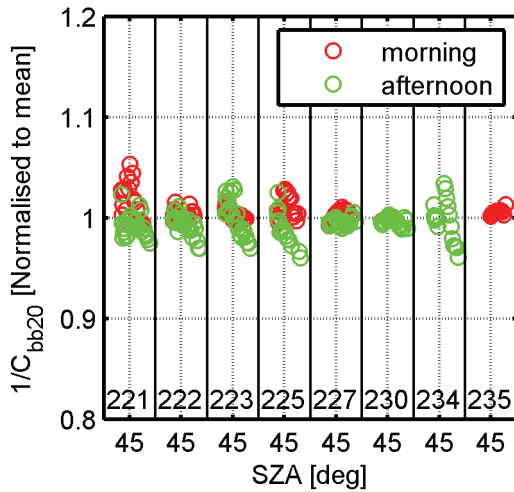


Figure 3 Calibration factor normalised to the average

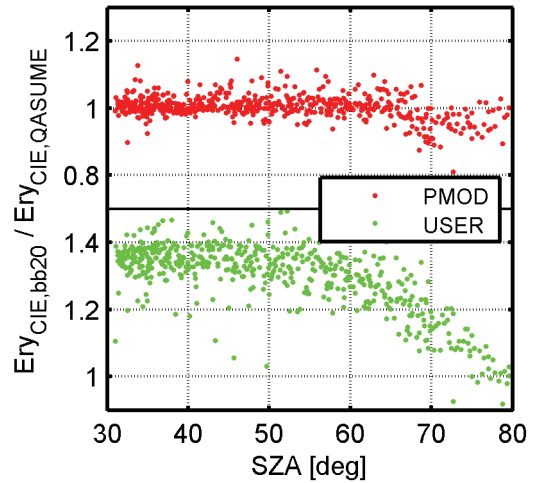


Figure 4 Erythemal weighted irradiance from Radiometer relative to QASUME

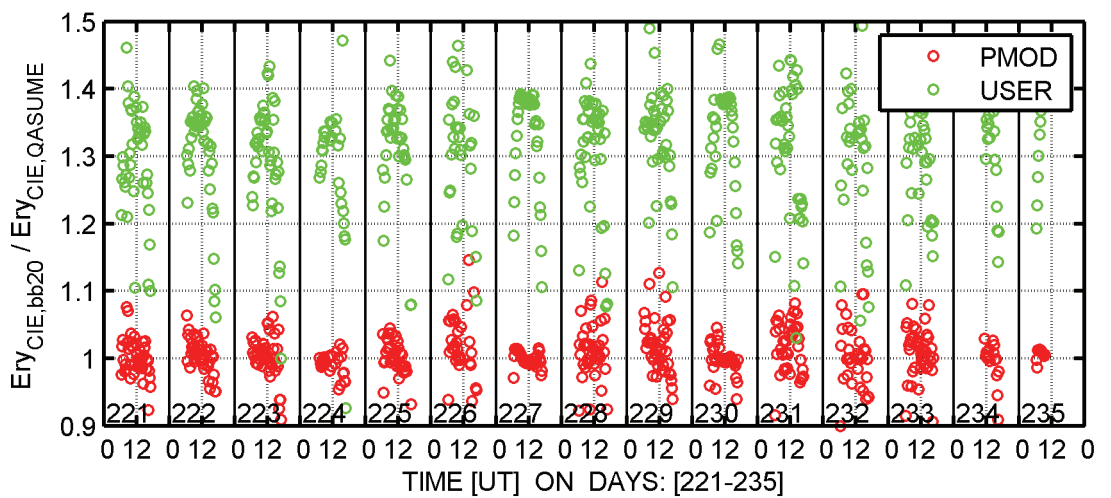


Figure 5 Erythemal weighted irradiance from Radiometer relative to QASUME spectroradiometer



Solar Light SL501 D s/n 0616 (BB21)

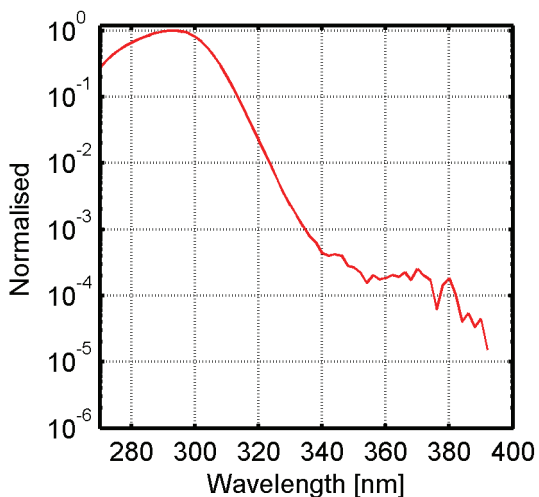


Figure 1 Relative spectral response function

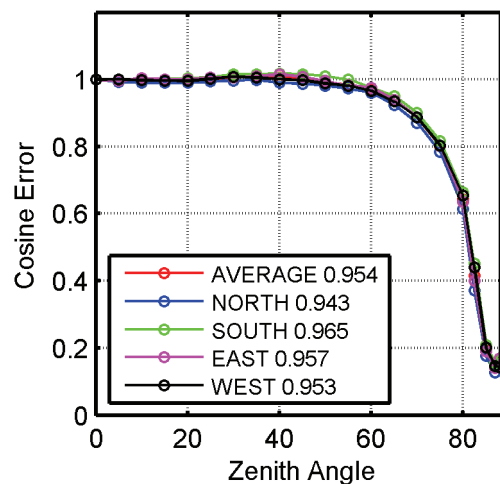


Figure 2 Cosine Error

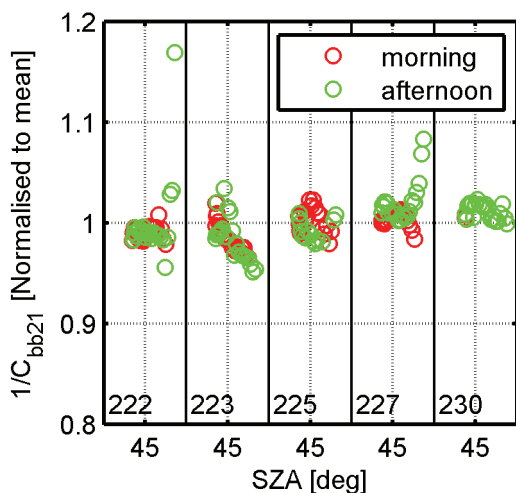


Figure 3 Calibration factor normalised to the average

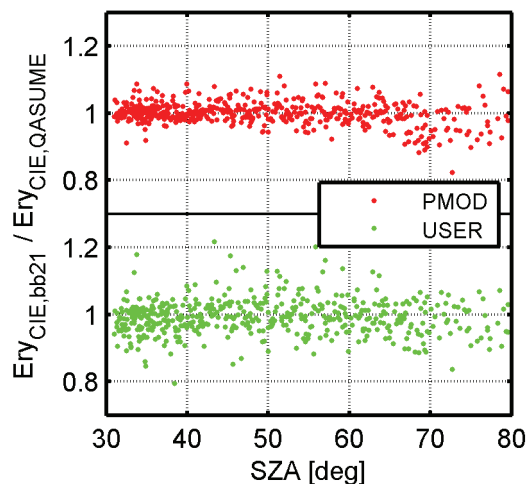


Figure 4 Erythemal weighted irradiance from Radiometer relative to QASUME

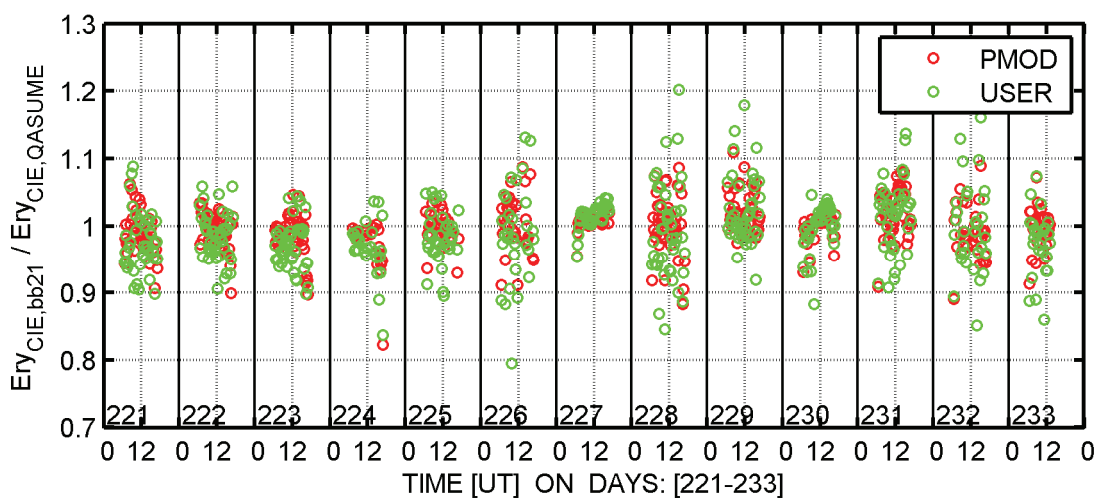


Figure 5 Erythemal weighted irradiance from Radiometer relative to QASUME spectroradiometer

Owner information about SL501 UV-Biometer Serial No. 4811 (bb22 in campaign)

SL501 UV-Biometer Serial No. 4811 is designated as the Slovak national reference instrument. It was purchased by Slovak Hydrometeorological Institute in November 2000 and is kept at Poprad-Ganovce station. In May 2001 during the Brewer calibration campaign in Budapest the instrument was compared with the Czech reference UV-Biometer No. 2733. Factory calibration scale did not require any adjustment.

Reference UV-Biometer is several times a year compared with Brewer ozone spectrophotometer MKIV No.097. Till May 2003 this comparison was only informative. In June 2003 during calibration campaign in Warsaw, Brewer No.097 was calibrated also for UV radiation. Since that date if an average difference of sufficient pairs of simultaneous measurements exceeds 5 % some additional calibration action should have been done in short time.

In May 2004 reference UV-Biometer was compared with Bentham instrument No.5503 in Warsaw but weather conditions did not enable radiometer comparison within sufficient range. UV-Biometer readings were 4 per-cent lower than Bentham data.

In May 2005 during the Brewer calibration campaign in Hradec Kralove the reference instrument was compared with the Czech reference UV-Biometer. New calibration coefficient of 1.041 for UV-Biometer No. 4811 was calculated and this value has been set as the instrument scaling factor. Scaling factor was confirmed in Davos where only slight adjustment of 1.0014 has been stated.

At present the Slovak UV-B network consists of four stations equipped with SOLAR Light 501 UV Biometers. Three of them belong to the Slovak Hydrometeorological Institute (Bratislava 48.17N, 17.12E, 287 m a.s.l., in operation since 1997, Kosice, 48.70N, 21.27E, 230 m a.s.l., since 1998, Poprad-Ganovce, 49.03N, 20.32E, 703 m a.s.l., since 1999) and one station situated in the High Tatras mountains belongs to the Geophysical Institute of the Slovak Academy of Sciences (Skalnate Pleso, 49.20N, 20.23E, 1778 m a.s.l., since 2001) which also measures the global ultraviolet radiation with Eppley UV-radiometer, model TUVR for the wavelength range 290-385 nm at Stara Lesna (49.15N, 20.29E, 808 m a.s.l.).

Each network instrument is once a year compared and calibrated with reference instrument. In situ calibration lasts 2-5 days. A simple calibration procedure will be gradually improved. Between calibrations the reference UV-Biometer is stored in the box. Upon latter recommendations it is more frequently exposed alongside the network instruments at Poprad-Ganovce.

### Solar Light SL501 D s/n 4811 (BB22)

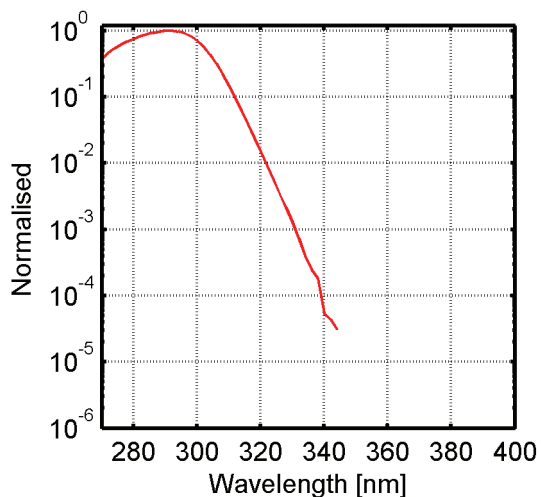


Figure 1 Relative spectral response function

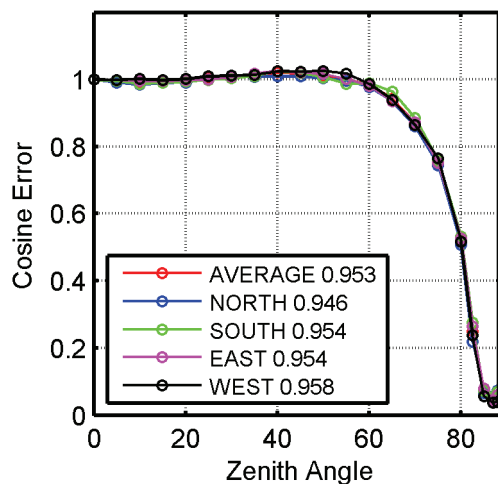


Figure 2 Cosine Error

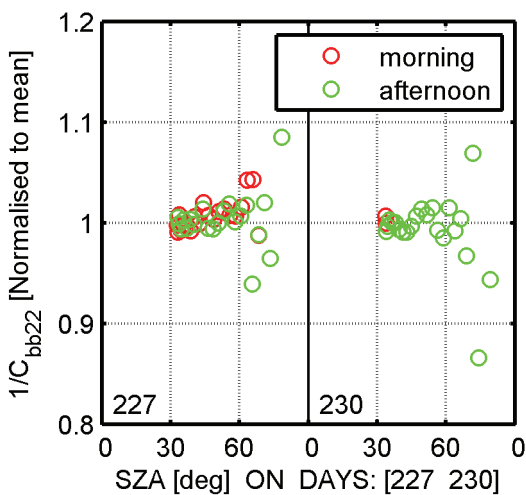


Figure 3 Calibration factor normalised to the average

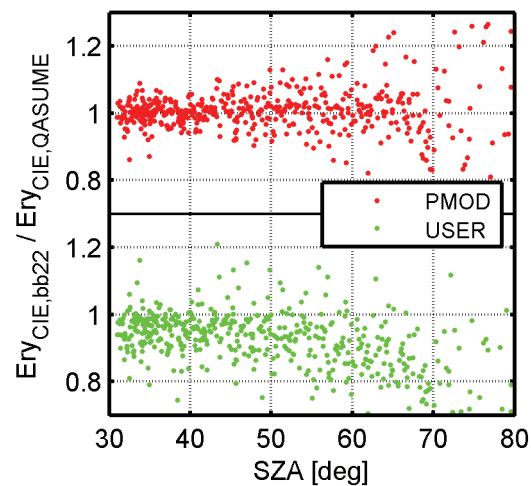


Figure 4 Erythemal weighted irradiance from Radiometer relative to QASUME

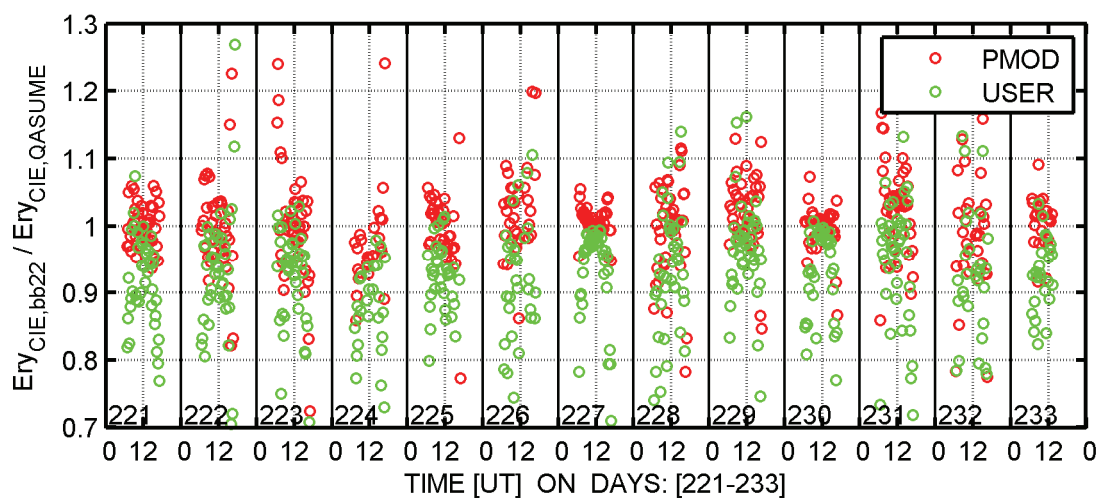


Figure 5 Erythemal weighted irradiance from Radiometer relative to QASUME spectroradiometer



Solar Light SL501 A s/n 5774 (BB23)

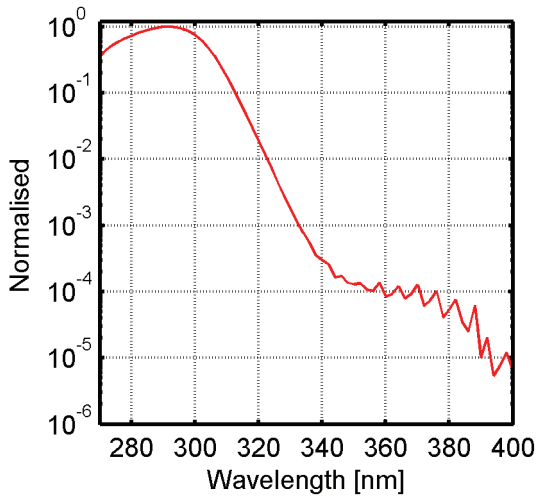


Figure 1 Relative spectral response function

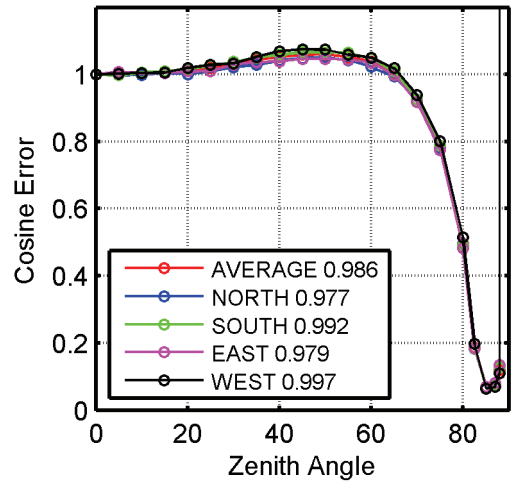


Figure 2 Cosine Error

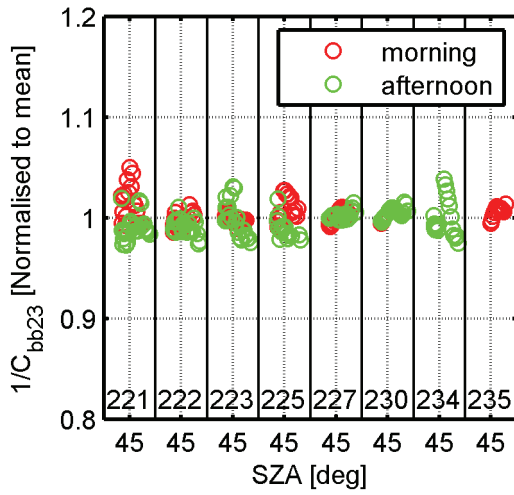


Figure 3 Calibration factor normalised to the average

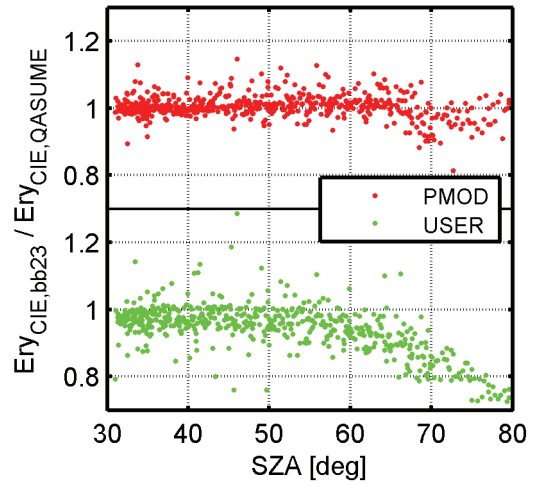


Figure 4 Erythemal weighted irradiance from Radiometer relative to QASUME

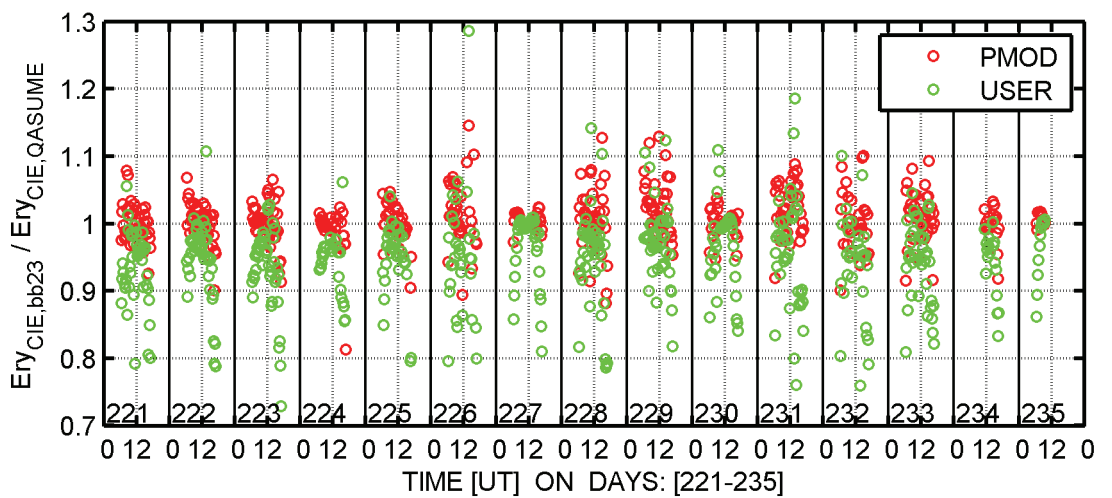


Figure 5 Erythemal weighted irradiance from Radiometer relative to QASUME spectroradiometer



YES s/n 030521 (BB24)

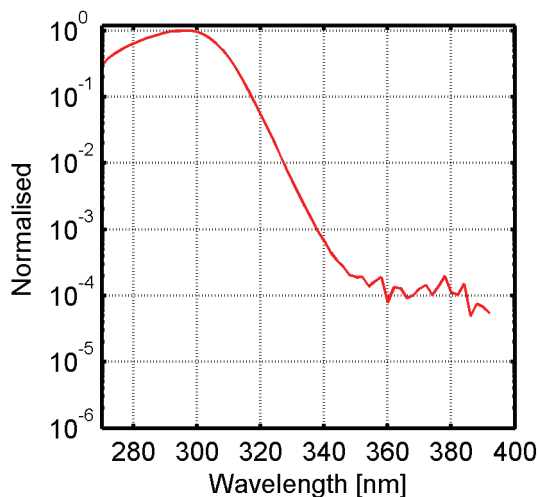


Figure 1 Relative spectral response function

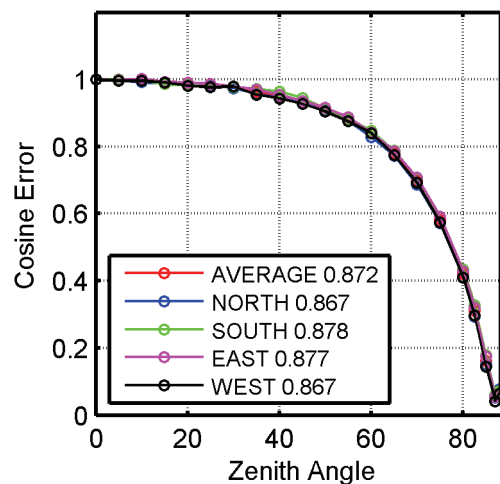


Figure 2 Cosine Error

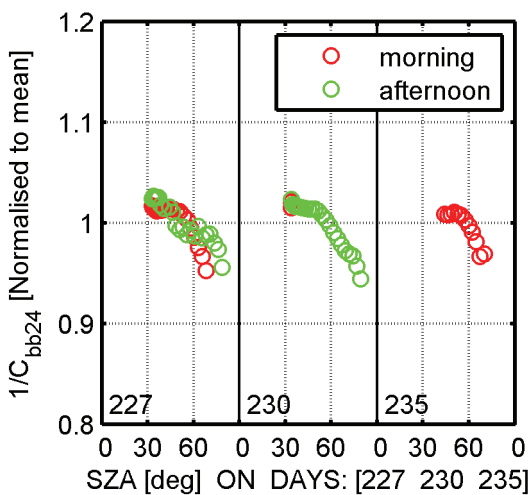


Figure 3 Calibration factor normalised to the average

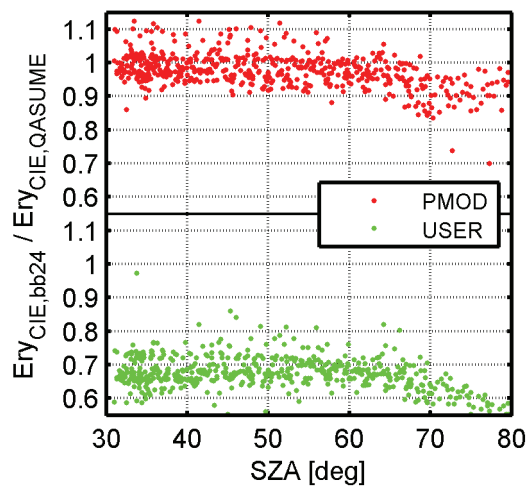


Figure 4 Erythemal weighted irradiance from Radiometer relative to QASUME

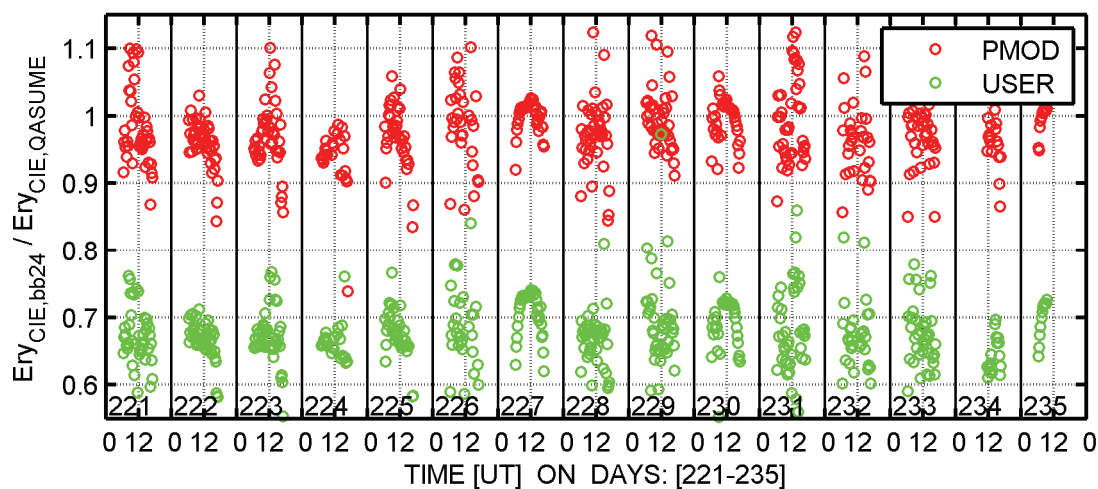


Figure 5 Erythemal weighted irradiance from Radiometer relative to QASUME spectroradiometer

### Comments on COST 726 calibration of instrument BB25

The principle issue arising from the participation of instrument BB25 in the 2006 PMOD/WRC-COST calibration and intercomparison is the relatively large calibration coefficient of 1.2567.

This coefficient indicates that the owner's radiometric calibration of the instrument is some 25% different from the radiometric calibration produced by the QASUME spectroradiometer.

The owner calibrated BB25 against a twin grating scanning spectroradiometer in June 2006. Upon examination of the spectral data used to calibrate BB25, it seems that the monochromator gratings were misaligned to produce a wavelength error of the order of 1 nm. The spectral data have insufficient resolution to allow for a more precise estimate of the wavelength error. An error of 1 nm would account for 80% of the discrepancy with QASUME.

SRMS s/n 26 (BB25)

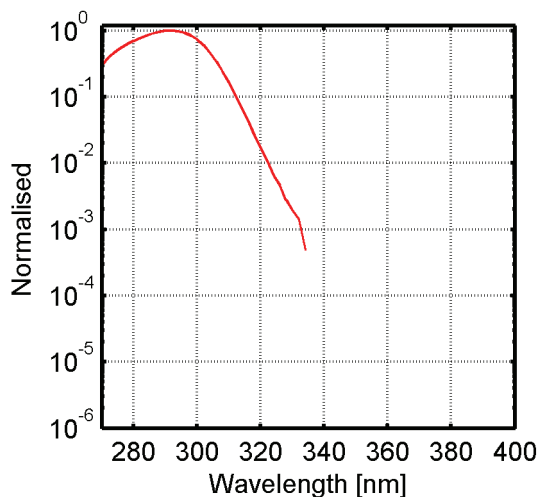


Figure 1 Relative spectral response function

(not measured)

Figure 2 Cosine Error

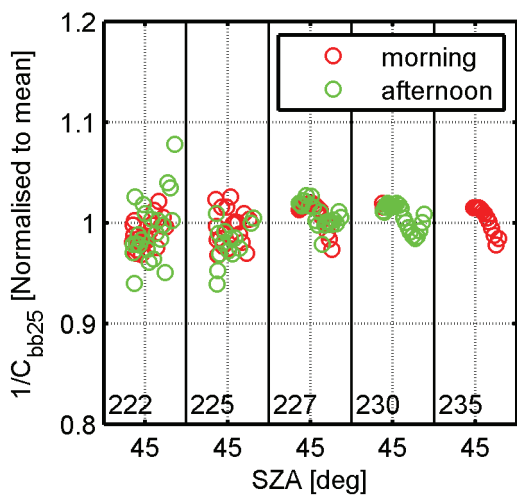


Figure 3 Calibration factor normalised to the average

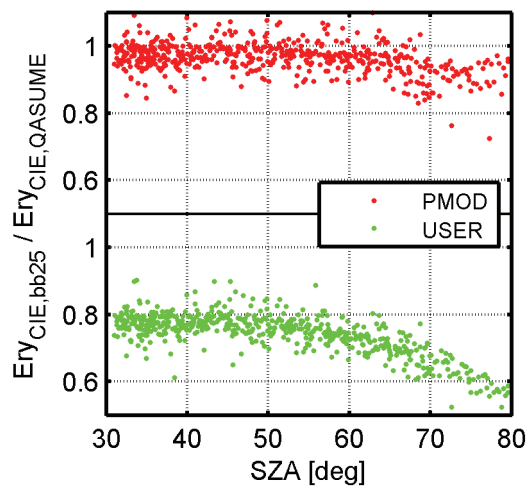


Figure 4 Erythemal weighted irradiance from Radiometer relative to QASUME

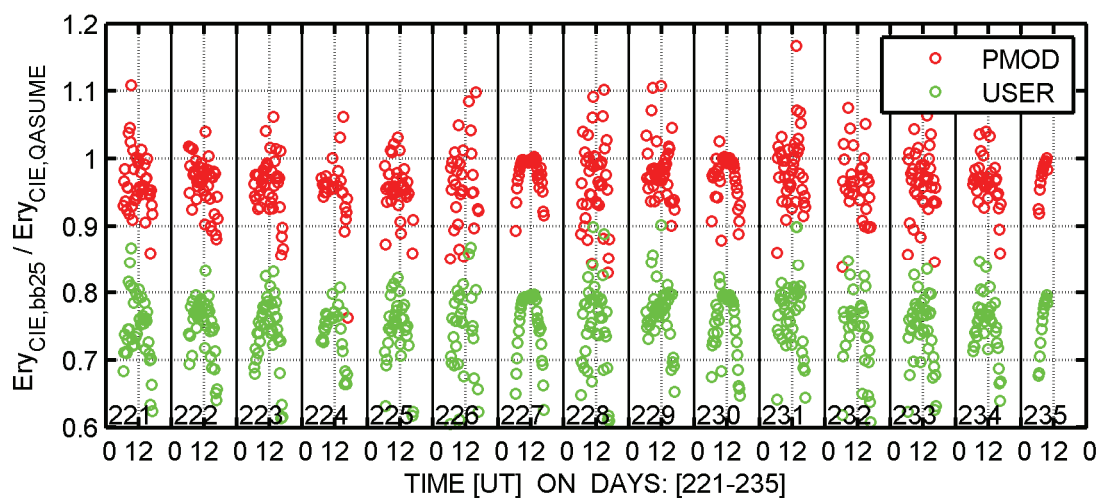


Figure 5 Erythemal weighted irradiance from Radiometer relative to QASUME spectroradiometer



YES s/n 970827 (BB26)

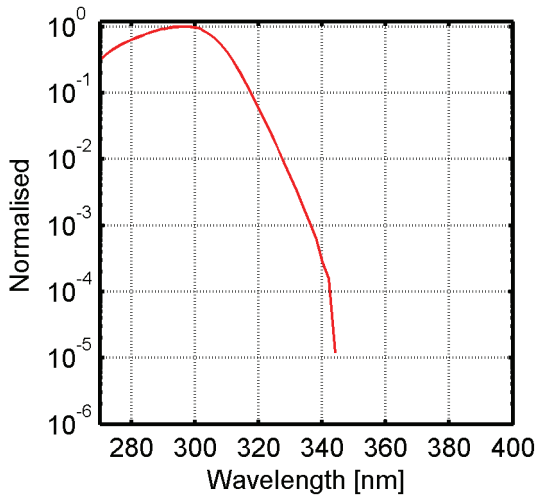


Figure 1 Relative spectral response function

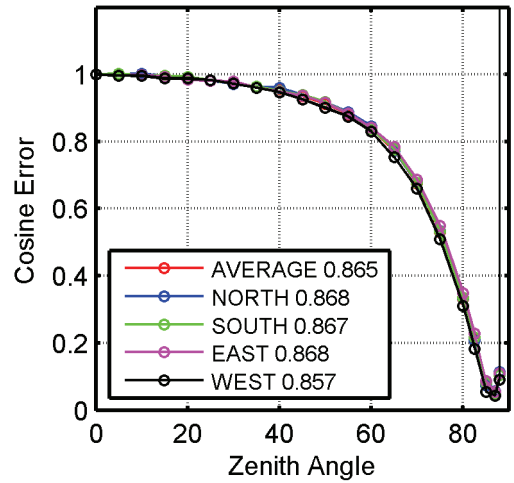


Figure 2 Cosine Error

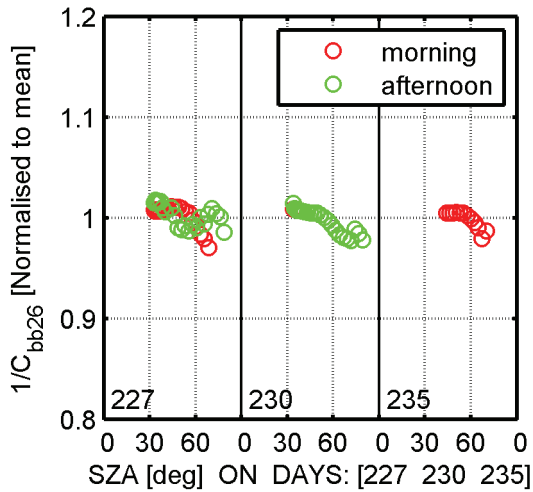


Figure 3 Calibration factor normalised to the average

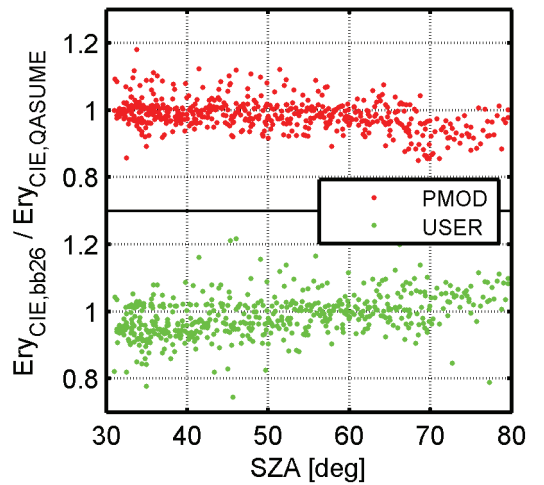


Figure 4 Erythemal weighted irradiance from Radiometer relative to QASUME

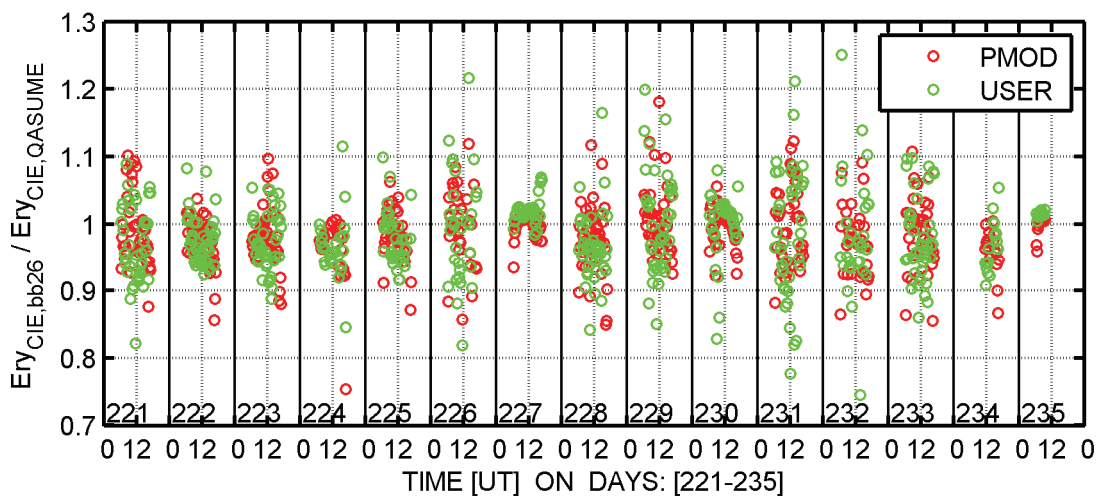


Figure 5 Erythemal weighted irradiance from Radiometer relative to QASUME spectroradiometer



Kipp & Zonen s/n 030616 (BB27)

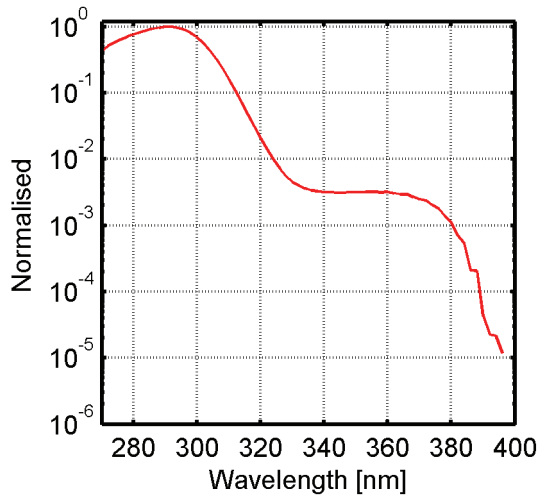


Figure 1 Relative spectral response function

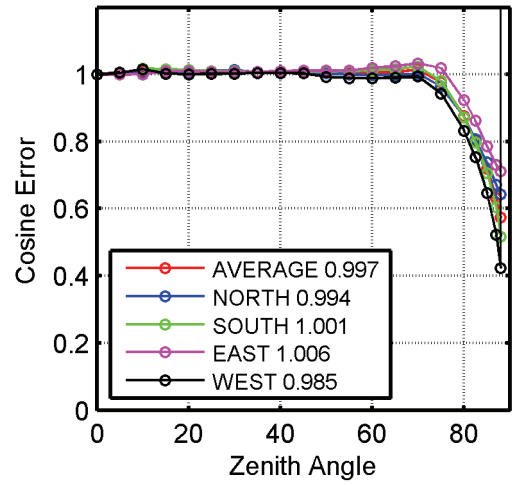


Figure 2 Cosine Error

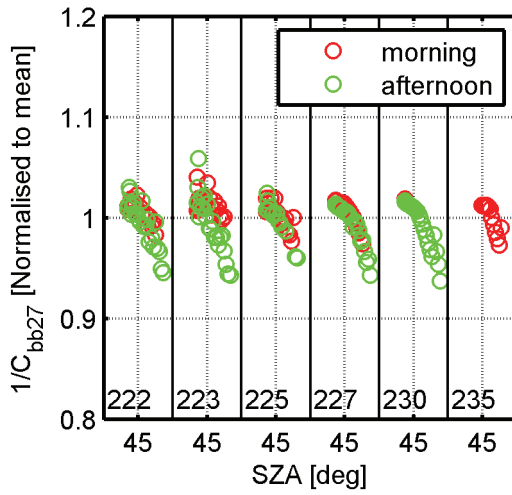


Figure 3 Calibration factor normalised to the average

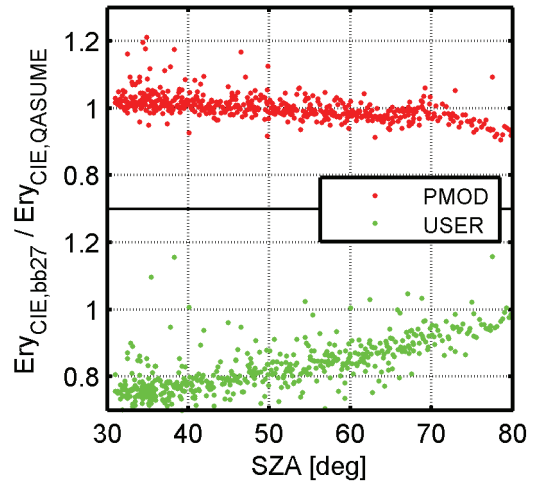


Figure 4 Erythemal weighted irradiance from Radiometer relative to QASUME

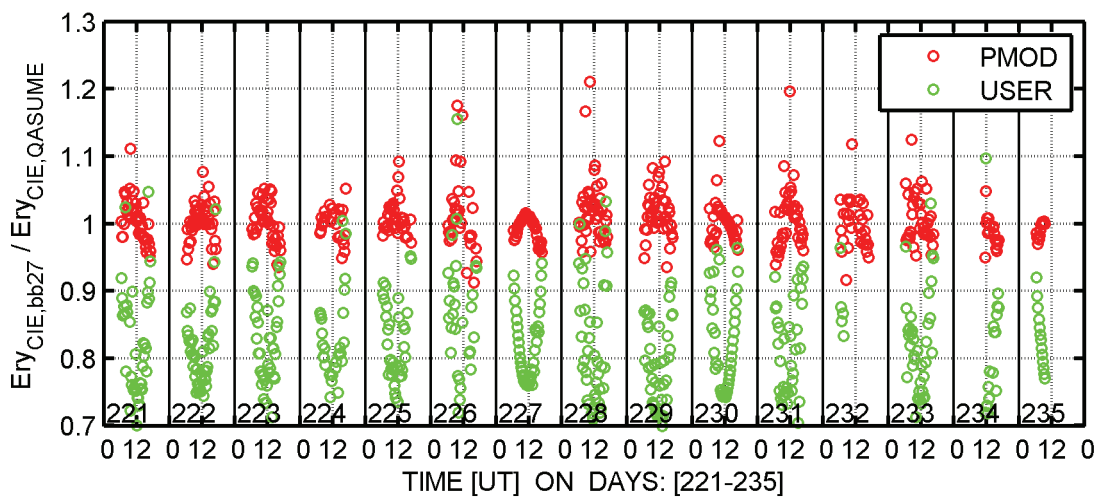


Figure 5 Erythemal weighted irradiance from Radiometer relative to QASUME spectroradiometer



Sintec s/n 010-A-00407 (BB28)

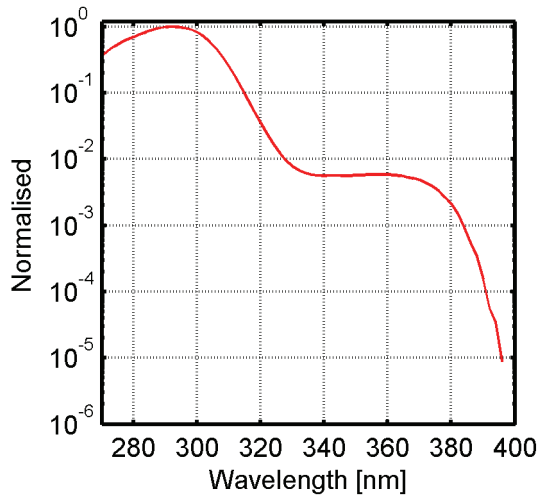


Figure 1 Relative spectral response function

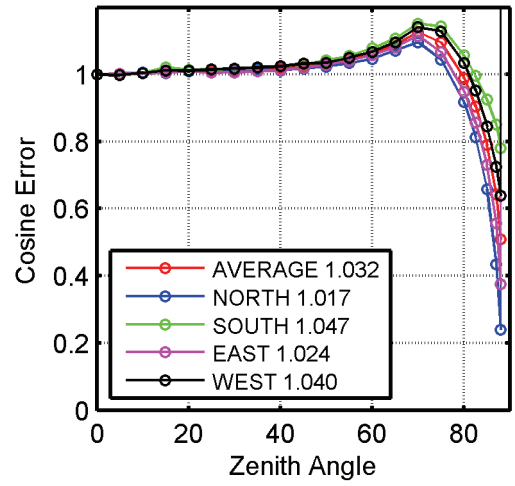


Figure 2 Cosine Error

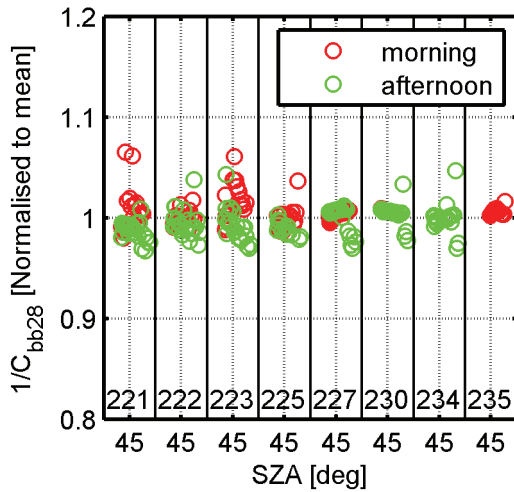


Figure 3 Calibration factor normalised to the average

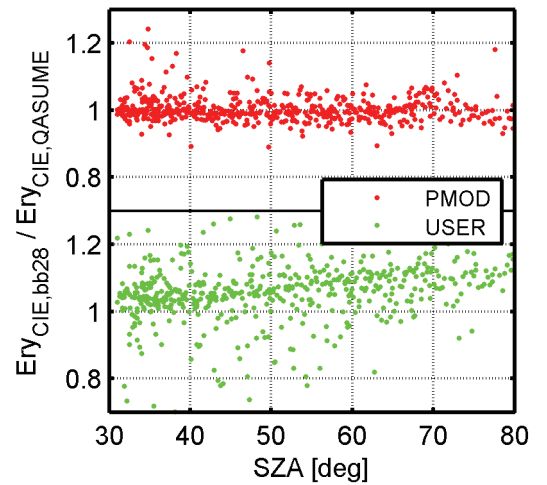


Figure 4 Erythemal weighted irradiance from Radiometer relative to QASUME

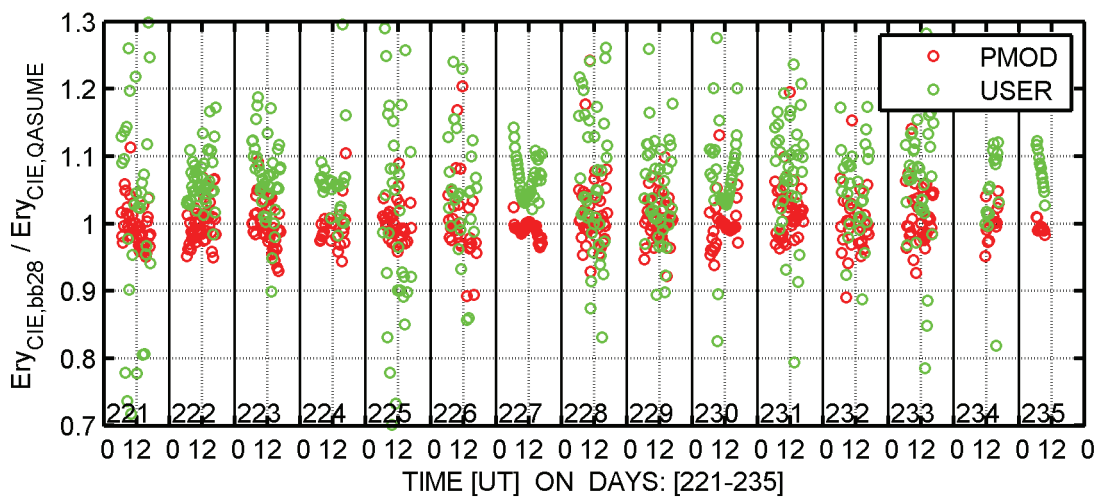


Figure 5 Erythemal weighted irradiance from Radiometer relative to QASUME spectroradiometer



YES s/n 990608 (BB29)

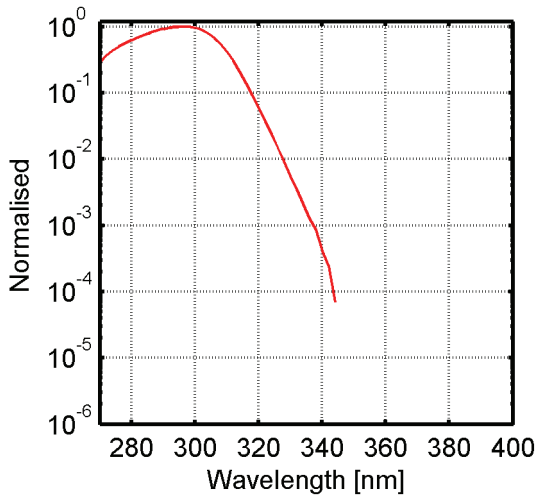


Figure 1 Relative spectral response function

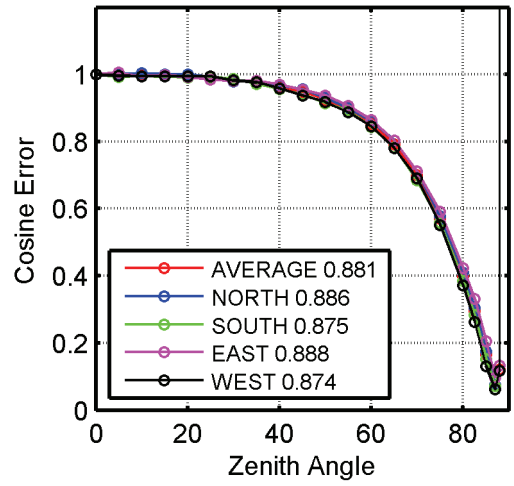


Figure 2 Cosine Error

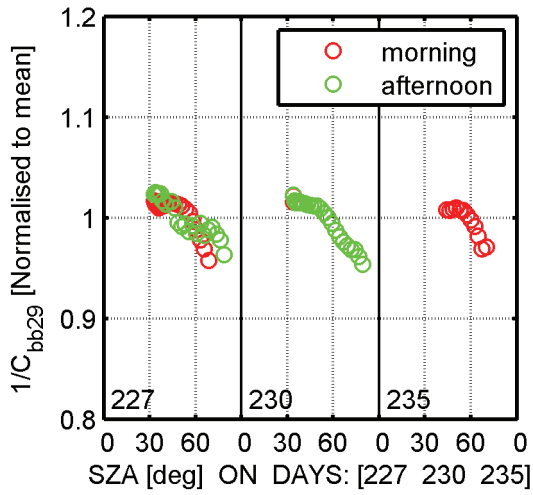


Figure 3 Calibration factor normalised to the average

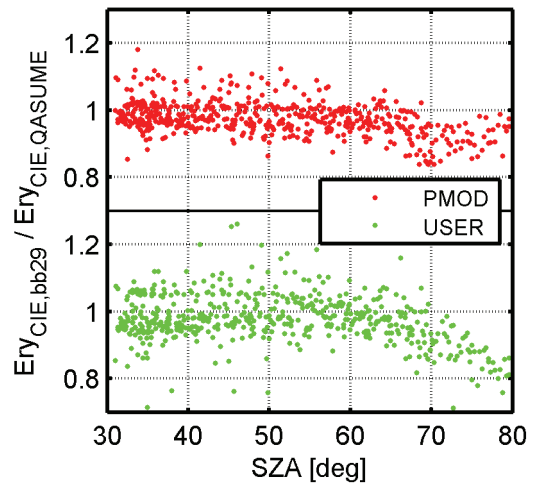


Figure 4 Erythemal weighted irradiance from Radiometer relative to QASUME

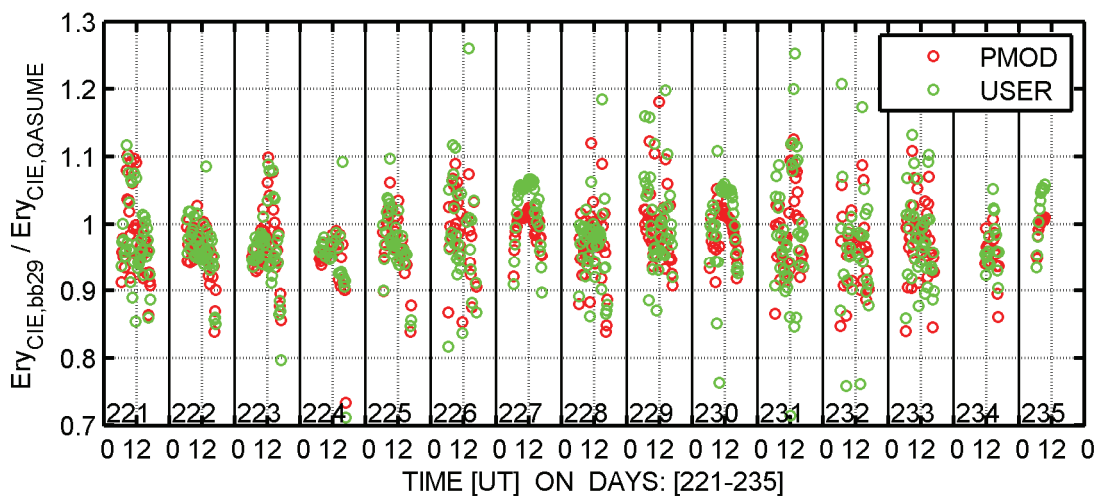


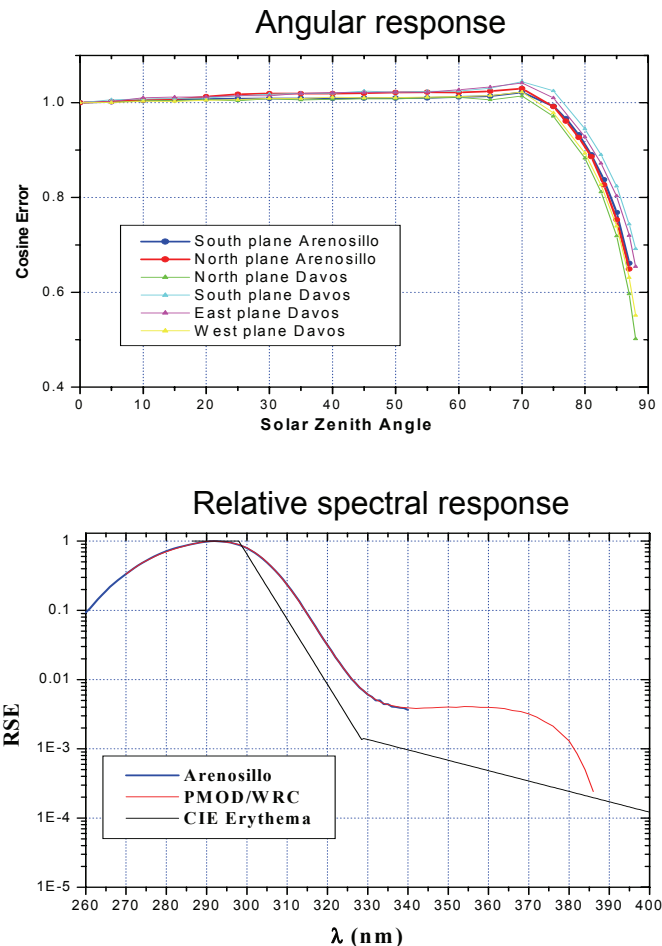
Figure 5 Erythemal weighted irradiance from Radiometer relative to QASUME spectroradiometer

## Kipp&Zonen UV-S-E-T #00518

The broadband radiometer K&Z #00518 belongs to the Department of Physics of the University of Extremadura in Spain. It was installed in the radiometric station of Plasencia (Spain) in January 2002, and it has been continuously measuring since then. Solar erythemal irradiance values are registered every one minute. This radiometer has participated in intercomparison campaigns held at “Estación de Sondeos Aerológicos – El Arenosillo” of the Instituto Nacional de Técnica Aeroespacial (ESAt/INTA) in Huelva (Spain), every two years (campaigns of 2001, 2003 and 2005). The instrument used as reference has been the spectroradiometer Brewer MK III #150. An improved one-step methodology for the calibration has been applied for obtaining the calibration coefficients (for more details see: Cancillo et al. (2005) An improved outdoor calibration procedure for broadband ultraviolet radiometers, *Photochemistry and Photobiology*, 81, 860-865). In order to account for the small drift in the calibration coefficients along the five years of measurements, a linear correction was applied.

In 2006, this instrument was characterized by two different calibration laboratories: the ESA/INTA in Spain and the PMOD/WRC (Physikalisch-Meteorologisches Observatorium Davos/World Radiation Center) in Switzerland. This characterization consisted in evaluating its angular and relative spectral responses.

The angular and relative spectral responses as evaluated by both laboratories showed a very good agreement, as shown in the two figures below. The results indicate the comparability of these two calibration laboratories.



Kipp & Zonen s/n 000518 (BB30)

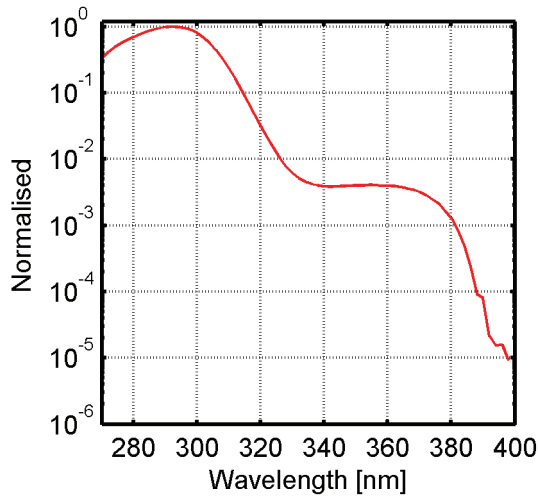


Figure 1 Relative spectral response function

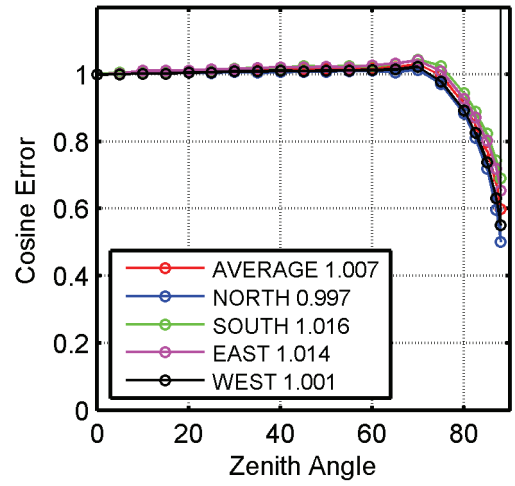


Figure 2 Cosine Error

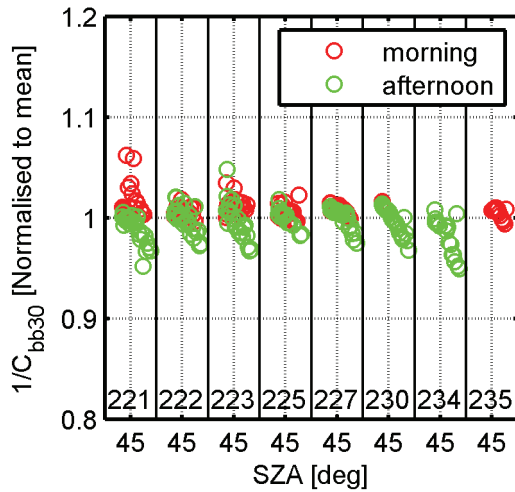


Figure 3 Calibration factor normalised to the average

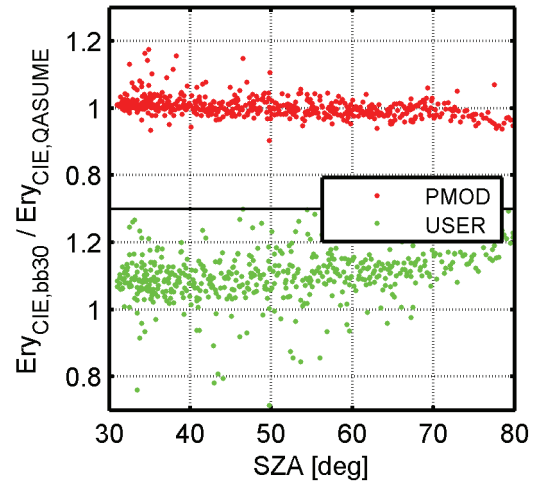


Figure 4 Erythemal weighted irradiance from Radiometer relative to QASUME

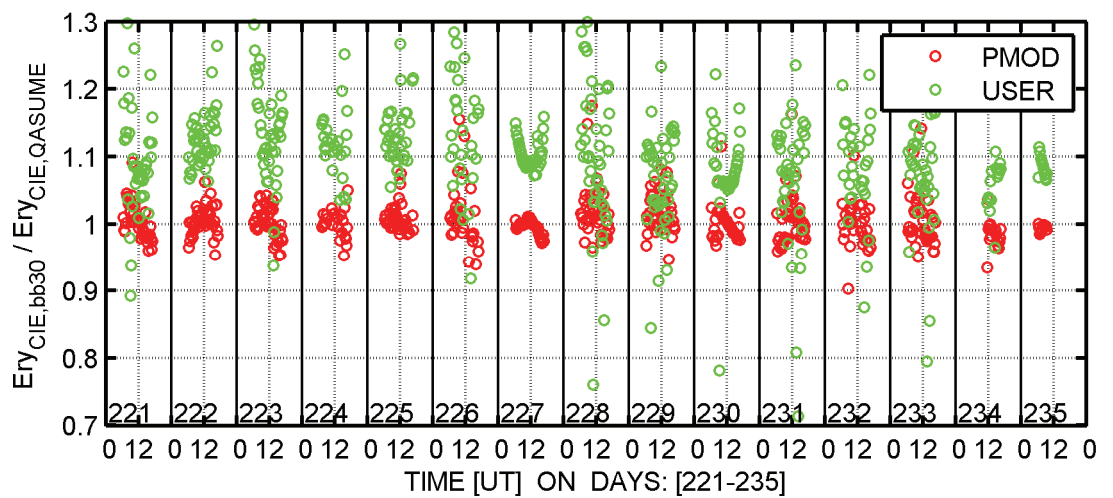


Figure 5 Erythemal weighted irradiance from Radiometer relative to QASUME spectroradiometer



YES D s/n 970839 (BB31)

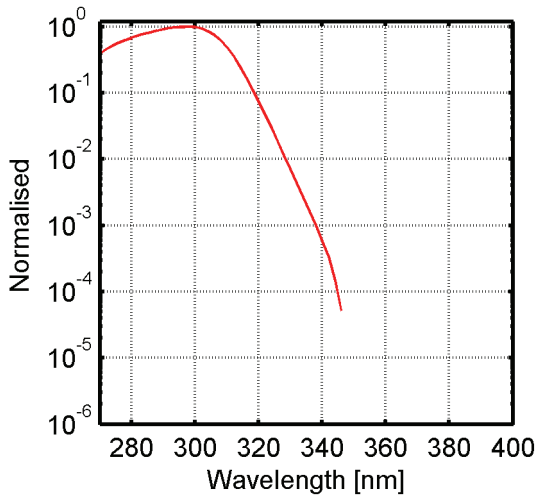


Figure 1 Relative spectral response function

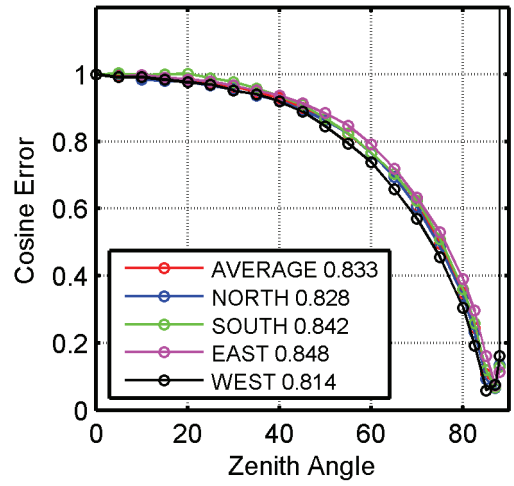


Figure 2 Cosine Error

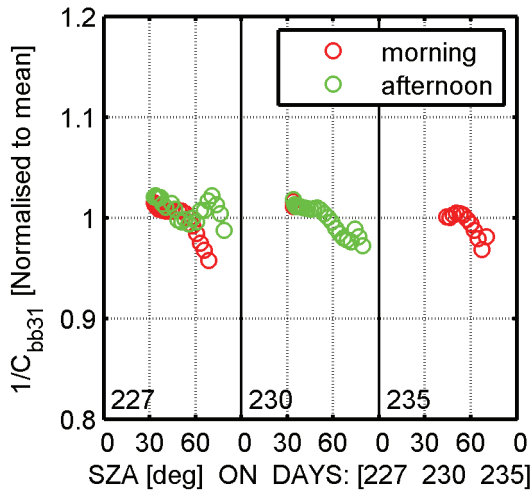


Figure 3 Calibration factor normalised to the average

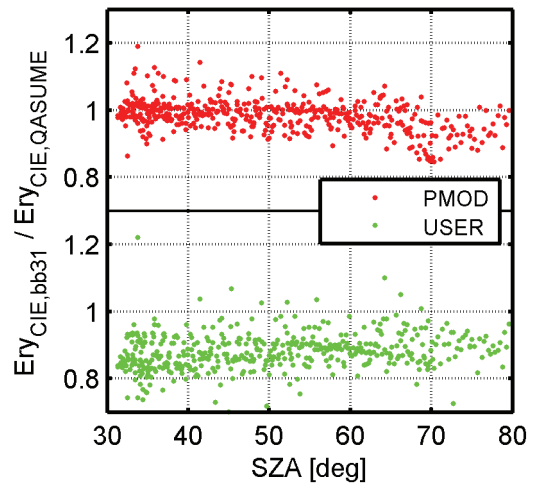


Figure 4 Erythemal weighted irradiance from Radiometer relative to QASUME

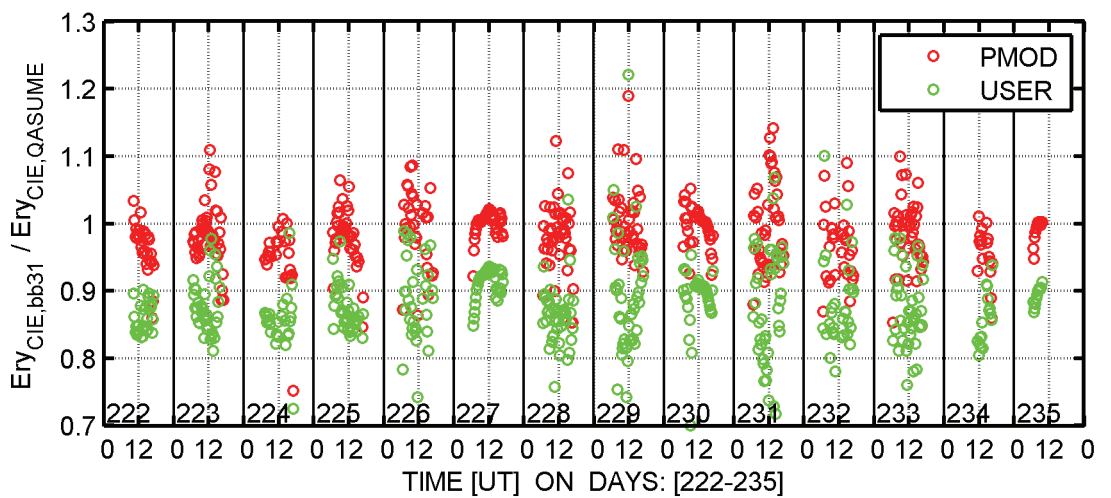


Figure 5 Erythemal weighted irradiance from Radiometer relative to QASUME spectroradiometer



Solar Light SL501 D s/n 10403 (BB32)

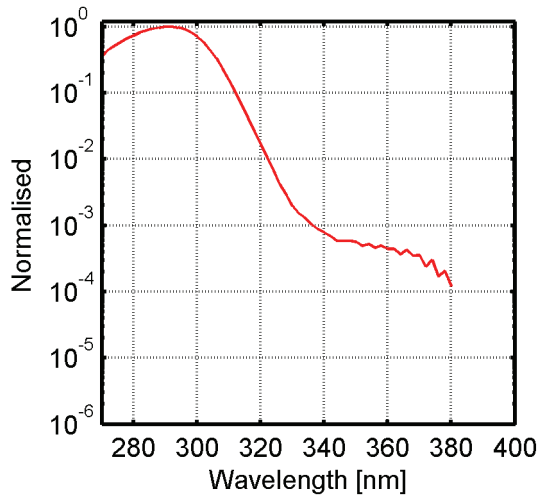


Figure 1 Relative spectral response function

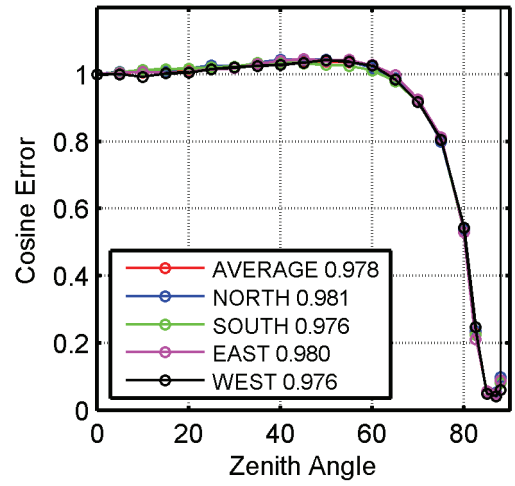


Figure 2 Cosine Error

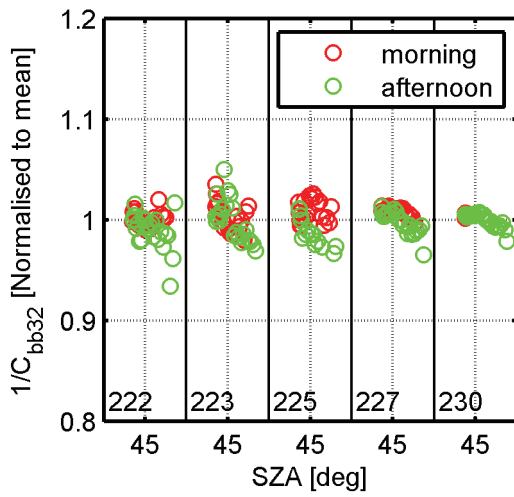


Figure 3 Calibration factor normalised to the average

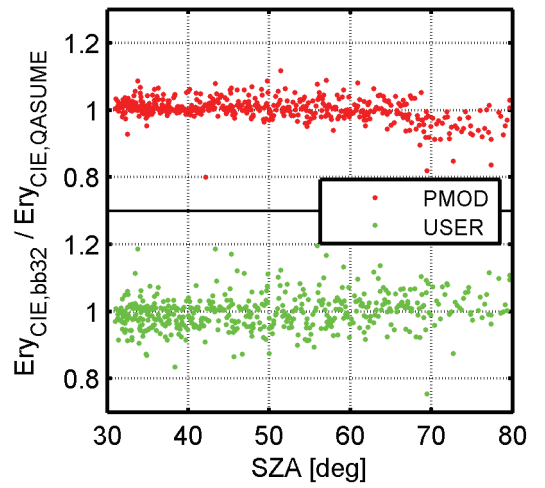


Figure 4 Erythemal weighted irradiance from Radiometer relative to QASUME

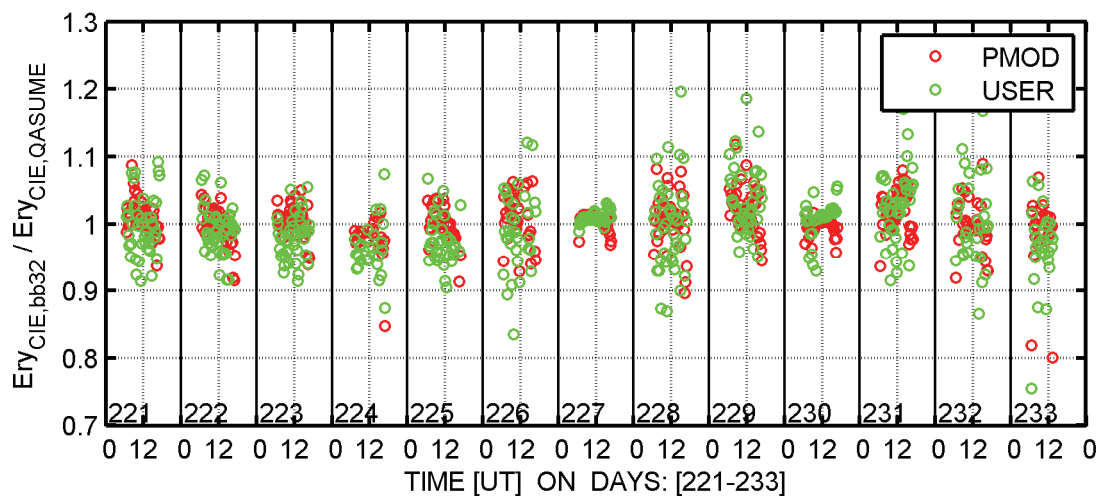


Figure 5 Erythemal weighted irradiance from Radiometer relative to QASUME spectroradiometer

IMUK is pleased by the results. We have not used an overall correction factor before. We are using our instrument mainly for campaigns. There it is mainly used for quality control purposes when measuring spectral UV irradiance.

It is presently not foreseen to use it for monitoring purposes due to lack of man power.

We thank PMOD for their professional work in organizing and evaluating this intercomparison campaign.

Solar Light SL501 D s/n 4818 (BB33)

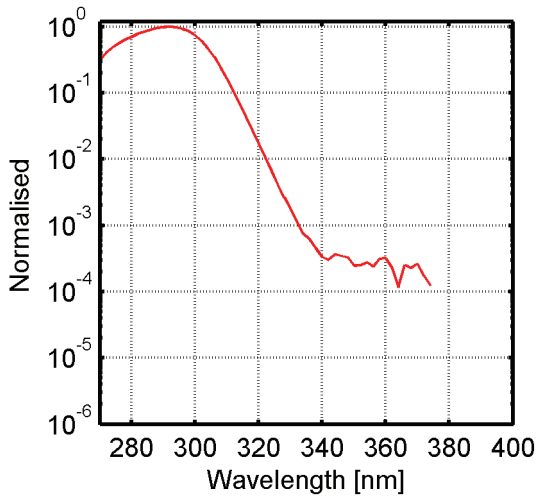


Figure 1 Relative spectral response function

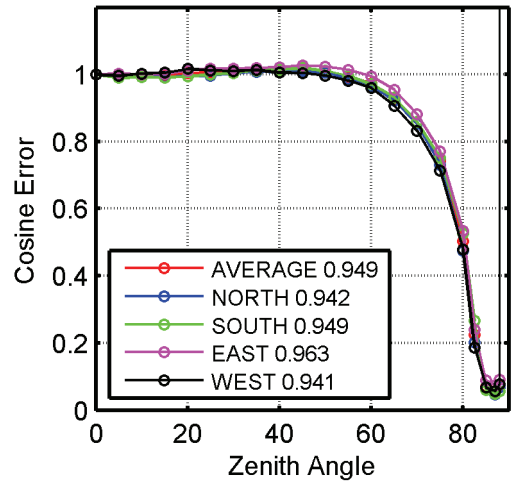


Figure 2 Cosine Error

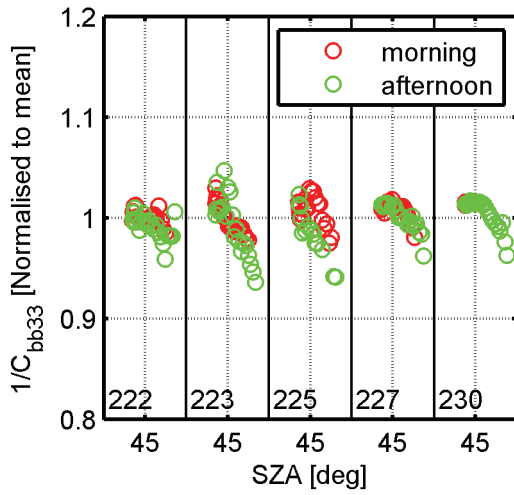


Figure 3 Calibration factor normalised to the average

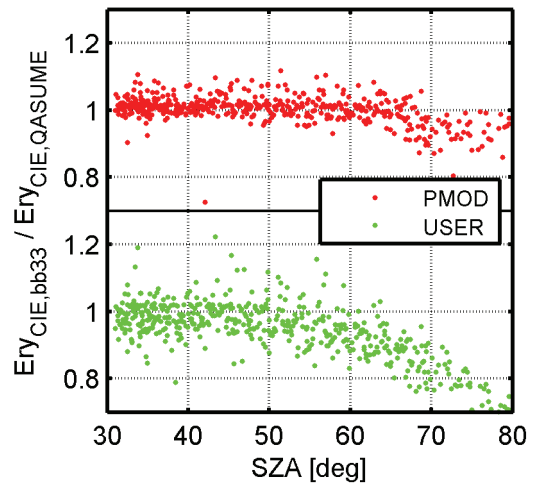


Figure 4 Erythemal weighted irradiance from Radiometer relative to QASUME

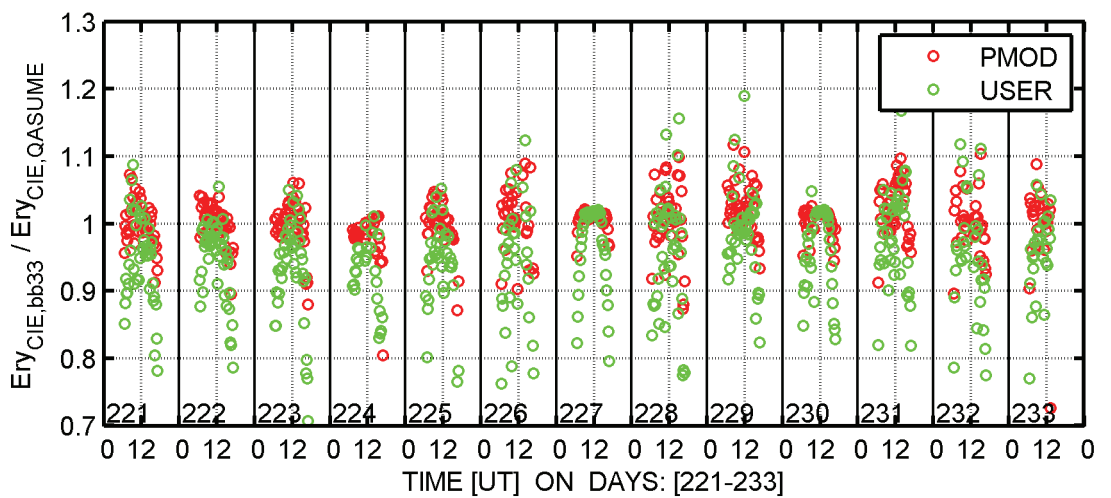


Figure 5 Erythemal weighted irradiance from Radiometer relative to QASUME spectroradiometer

## Revision of the YES UVB-1 SN-921116 data (BB34)

A. Bais, C. Meleti

Laboratory of Atmospheric Physics, Aristotle University of Thessaloniki

The monitoring of erythemal irradiance at the Laboratory of Atmospheric Physics was added to the routine daily measurements in 1991. The broadband detectors used for these measurements are of type YES UVB-1, and their output signals and the corresponding standard deviation are recorded in binary files at 1 minute intervals. Software dealing with the format of the binary files has been developed to process YES UVB-1 detectors' raw data. The algorithms of the software utilize the information of all calibrations performed (both relative spectral response and absolute calibration), and apply them to the appropriate time periods considering the solar zenith angle and the total columnar ozone during the measurements.

The calibration of the YES UVB-1 sensors consists of two parts: the determination of the instrument relative spectral response, and the calculation of the absolute factor C to convert the output signal to instrument-weighted flux (absolute calibration). The methodology applied to the LAP detectors for their absolute calibration is based on the comparison of the detector's analog output signal (in Volt) with coincident spectra from a collocated spectrophotometer, weighted with the YES UVB-1 spectral response. It utilizes clear-sky measurements taken during summer days in order to achieve small solar zenith angles and estimate the absolute factor C at SZA=15 deg. A 2<sup>nd</sup> degree polynomial is fitted on the ratios of the detector weighted integral derived from the spectroradiometer to the analog signal of the detector for SZAs smaller than 60 deg. From this fit the absolute calibration factor C corresponding to SZA=15 deg is calculated.

The traveling detector YES UVB-1 SN-921116 is calibrated for its spectral response and for its absolute calibration periodically, and its measurements are processed following the aforementioned procedure. Before shipped to Davos, both spectral response and absolute calibration were determined. The polynomial fit on the ratios R as a function of solar zenith angle was found to be:

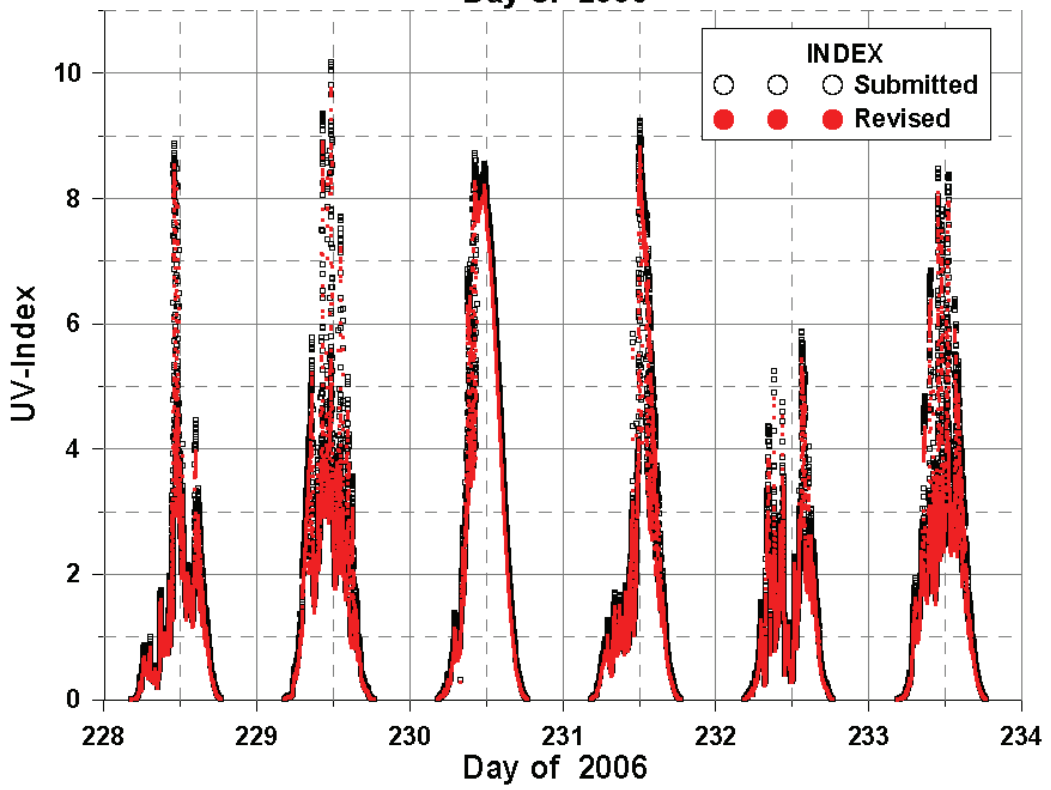
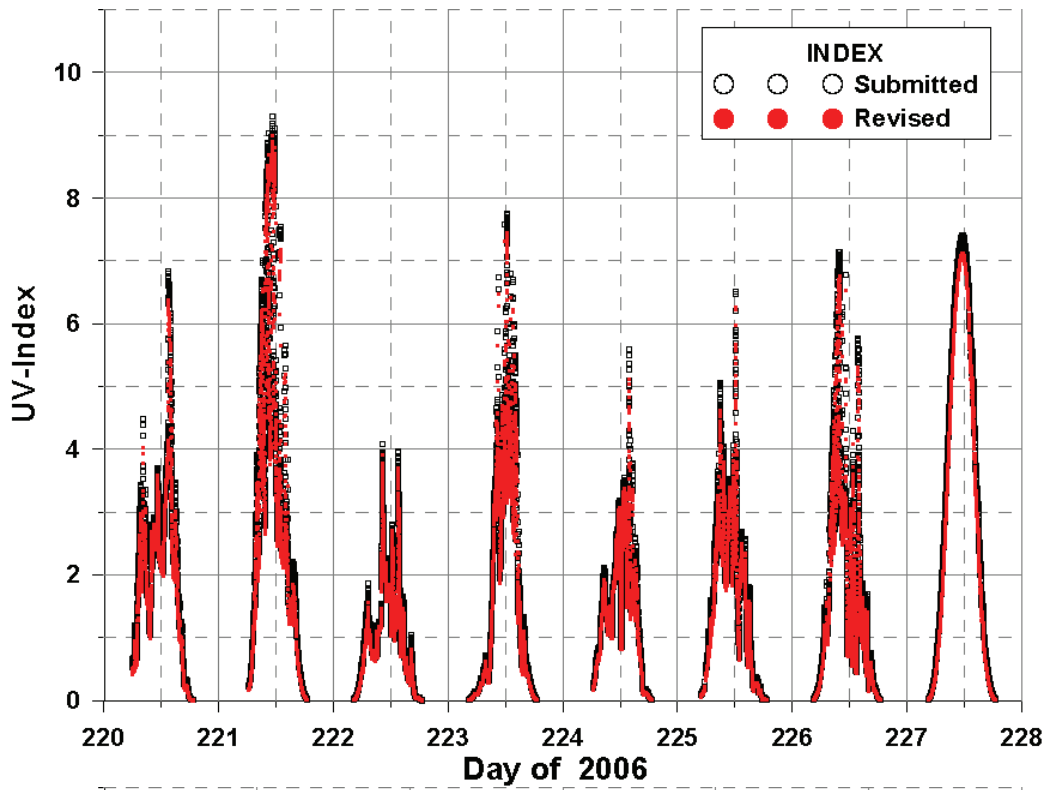
$$R(\text{SZA}) = 0.8166 - 1.3214 \cdot 10^{-3} \text{ SZA} + 6.4726 \cdot 10^{-5} \text{ SZA}^2$$

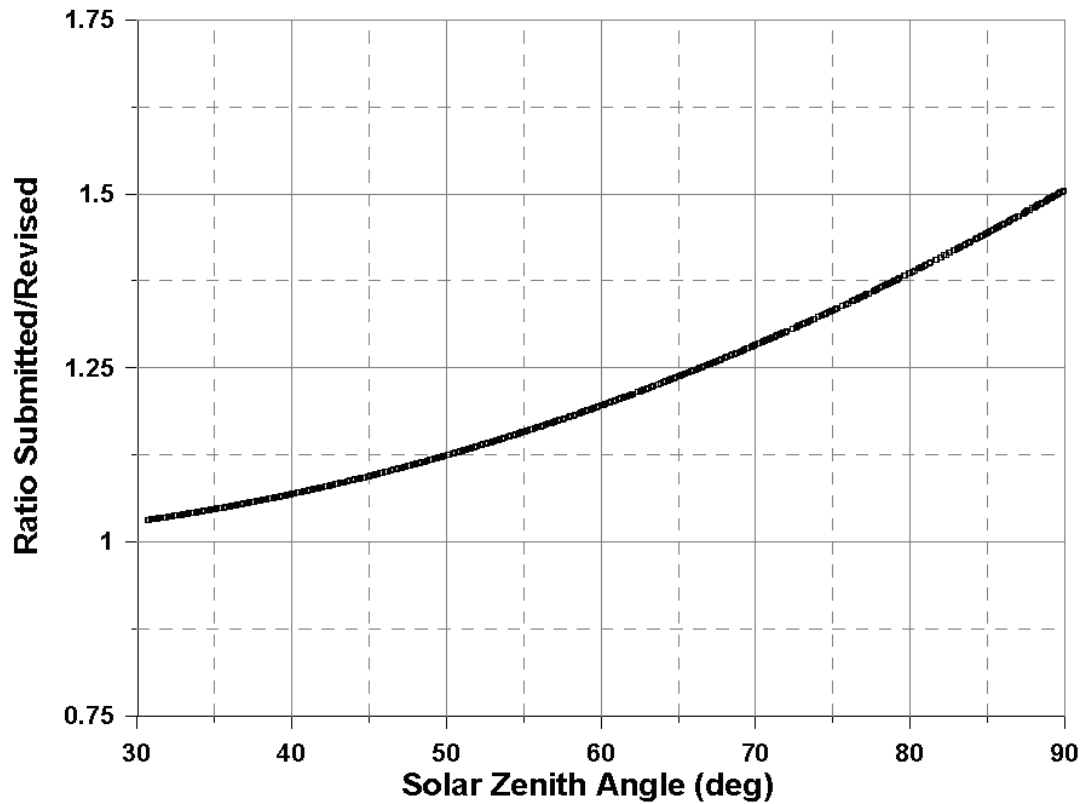
which corresponds to a value of  $C = 0.8114 \text{ W} \cdot \text{m}^{-2} / \text{V}$  at SZA=15 deg.

Because the sampling rate during the campaign in Davos was different than the usual, the data processing software was modified to be able to handle this different file format. This modification resulted in a software bug which in turn resulted in applying on each measurement a SZA-dependent absolute calibration factor C instead of the constant ( $C = 0.8114 \text{ W} \cdot \text{m}^{-2} / \text{V}$ ).

The comparison of the detector data with the QASUME spectroradiometer revealed the bug in the software, which was fixed and new revised data were submitted.

The differences between the revised and the originally submitted UV index data are demonstrated in the following graphs:





Ratios submitted to revised indexes versus solar zenith angle

As shown in the above graph, the ratio between the originally submitted and the revised UV index data versus solar zenith angle ranges from 1.03 at SZA=30 deg to 1.5 at SZA=90 deg. It is expected that the use of the revised dataset will result in better agreement with the measurements taken with the QASUME spectroradiometer.

YES D s/n 921116 (BB34) Revised data set

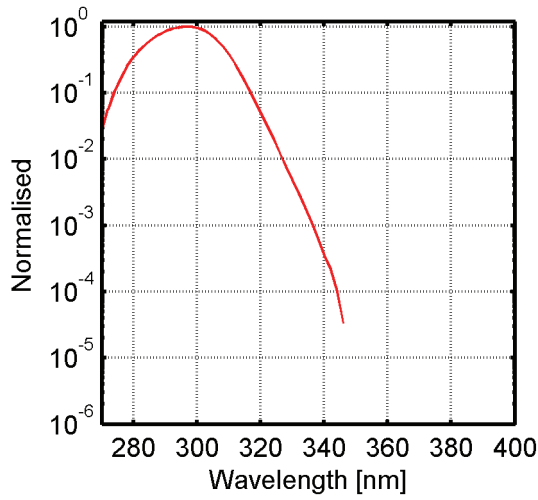


Figure 1 Relative spectral response function

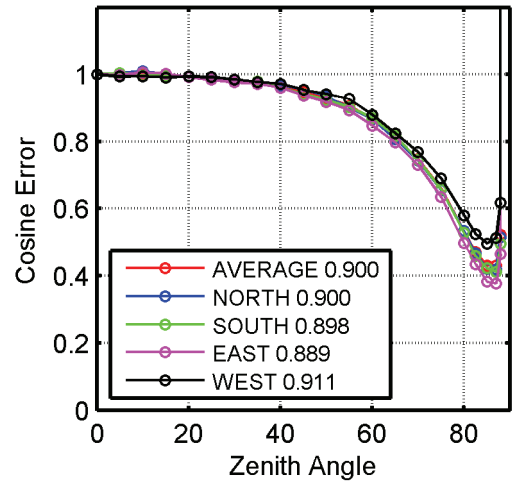


Figure 2 Cosine Error

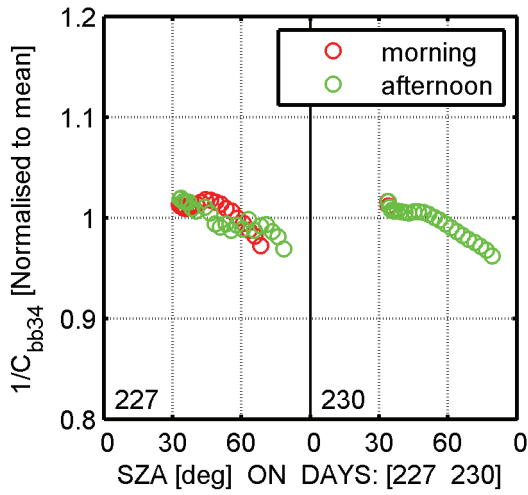


Figure 3 Calibration factor normalised to the average

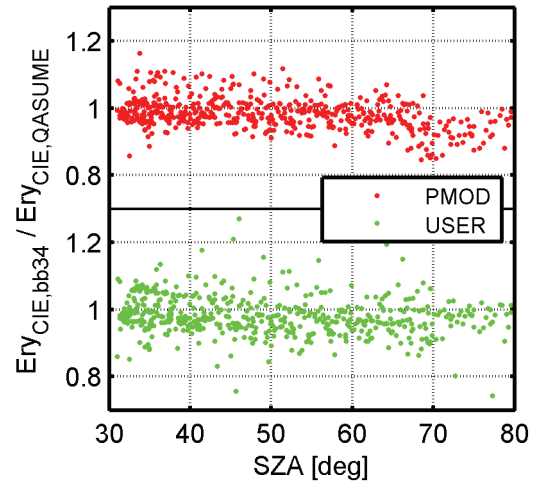


Figure 4 Erythemal weighted irradiance from Radiometer relative to QASUME

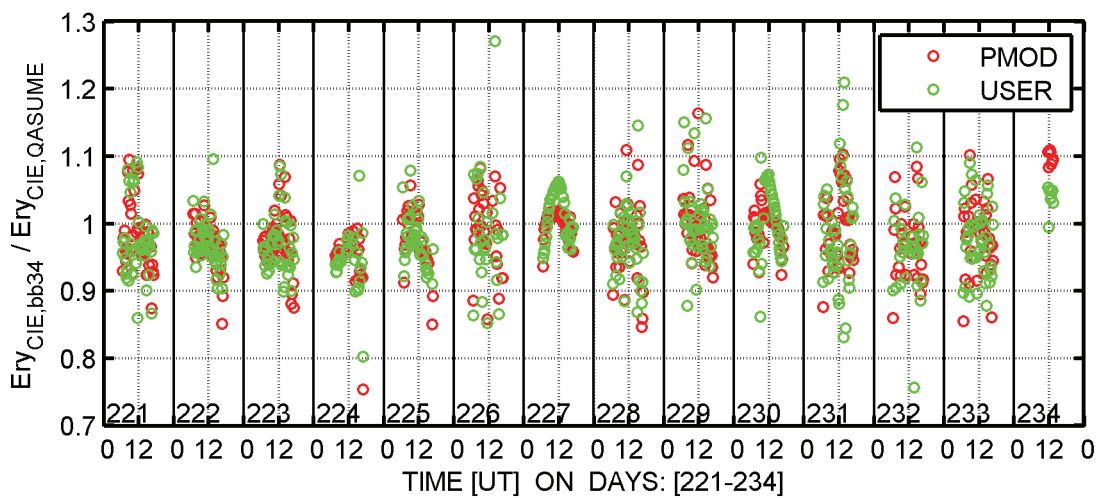


Figure 5 Erythemal weighted irradiance from Radiometer relative to QASUME spectroradiometer



Scintec 010-A-00349 (BB35)

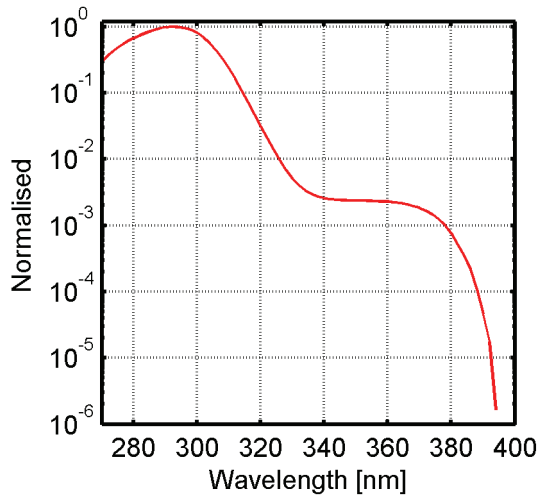


Figure 1 Relative spectral response function

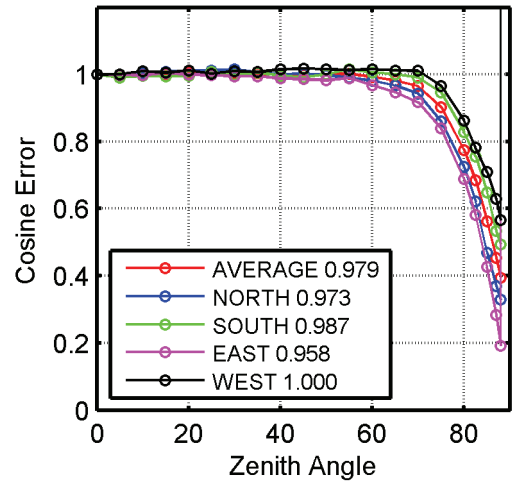


Figure 2 Cosine Error

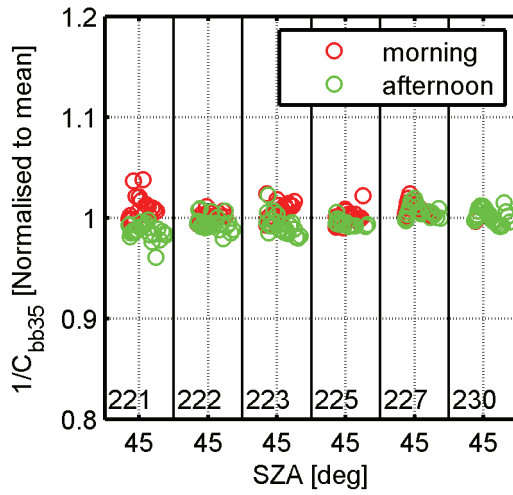


Figure 3 Calibration factor normalised to the average

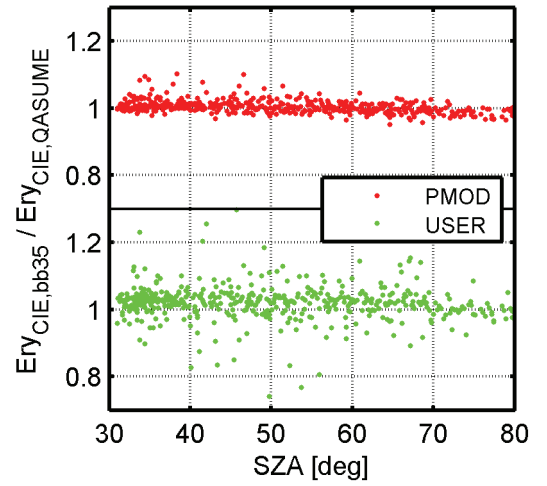


Figure 4 Erythemal weighted irradiance from Radiometer relative to QASUME

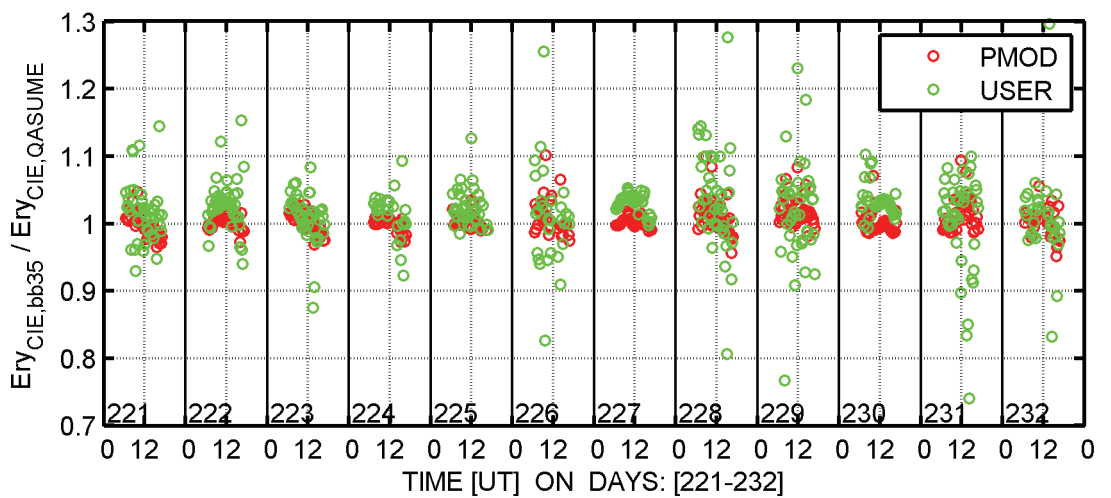


Figure 5 Erythemal weighted irradiance from Radiometer relative to QASUME spectroradiometer



Solar Light SL501 A s/n 1497 (BB36)

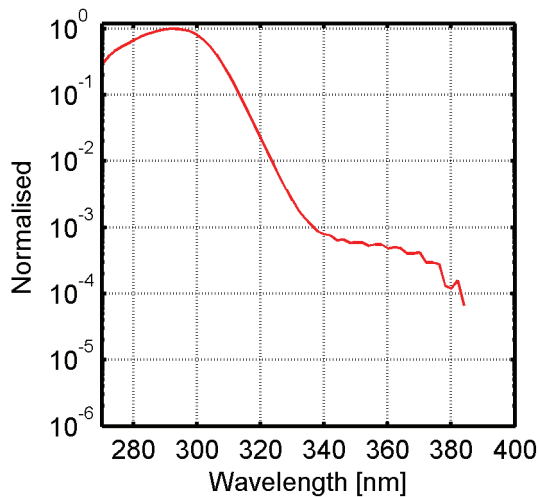


Figure 1 Relative spectral response function

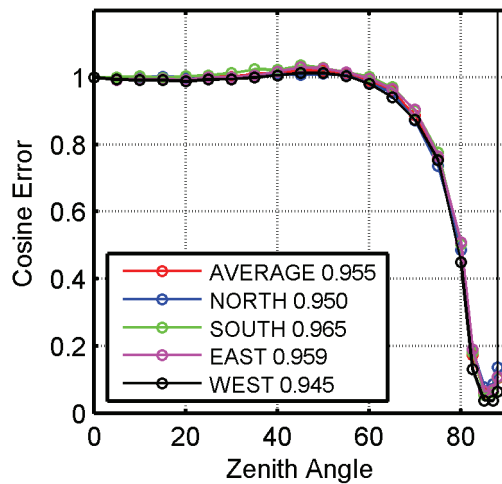


Figure 2 Cosine Error

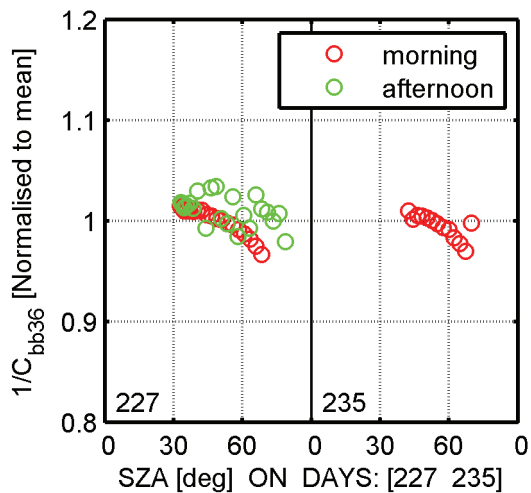


Figure 3 Calibration factor normalised to the average

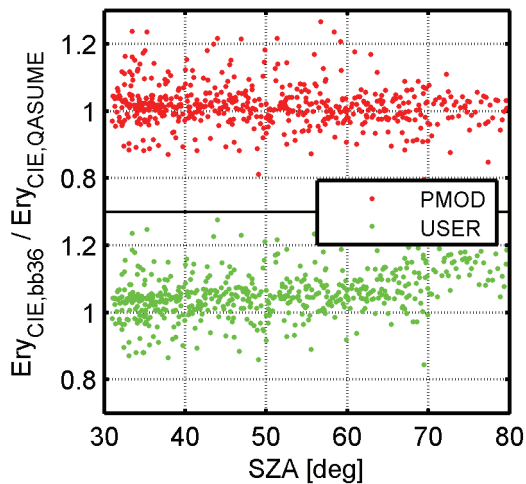


Figure 4 Erythemal weighted irradiance from Radiometer relative to QASUME

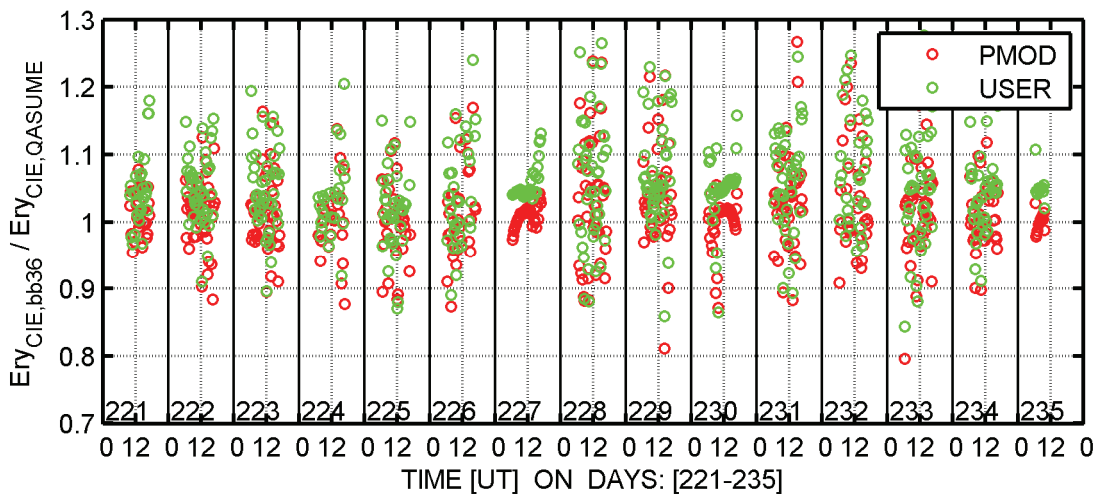


Figure 5 Erythemal weighted irradiance from Radiometer relative to QASUME spectroradiometer



Physikalisch-Meteorologisches Observatorium Davos,  
Weltstrahlungszentrum (PMOD/WRC)

**COST Action 726 – Report of the PMOD/WRC-COST Calibration  
and Intercomparison of Erythral Radiometers**

Davos Dorf, Switzerland

2009 – 110 pp. – 17.6 x 25 cm



**COST**- the acronym for European **C**ooperation in **S**cience and **T**echnology- is the oldest and widest European intergovernmental network for cooperation in research. Established by the Ministerial Conference in November 1971, COST is presently used by the scientific communities of 35 European countries to cooperate in common research projects supported by national funds.

The funds provided by COST - less than 1% of the total value of the projects - support the COST cooperation networks (COST Actions) through which, with EUR 30 million per year, more than 30 000 European scientists are involved in research having a total value which exceeds EUR 2 billion per year. This is the financial worth of the European added value which COST achieves.

A "bottom up approach" (the initiative of launching a COST Action comes from the European scientists themselves), "à la carte participation" (only countries interested in the Action participate), "equality of access" (participation is open also to the scientific communities of countries not belonging to the European Union) and "flexible structure" (easy implementation and light management of the research initiatives) are the main characteristics of COST.

As precursor of advanced multidisciplinary research COST has a very important role for the realization of the European Research Area (ERA) anticipating and complementing the activities of the Framework Programmes, constituting a "bridge" towards the scientific communities of emerging countries, increasing the mobility of researchers across Europe and fostering the establishment of "Networks of Excellence" in many key scientific domains such as: Biomedicine and Molecular Biosciences; Food and Agriculture; Forests, their Products and Services; Materials, Physical and Nanosciences; Chemistry and Molecular Sciences and Technologies; Earth System Science and Environmental Management; Information and Communication Technologies; Transport and Urban Development; Individuals, Societies, Cultures and Health. It covers basic and more applied research and also addresses issues of pre-normative nature or of societal importance.



**ESF provides the COST Office through an EC contract**



**COST is supported by the EU RTD Framework programme**